GMIT
GALWAY-MAYO INSTITUTE OF TECHNOLOGY
INSTITIÚID TEICNEOLAÍOCHTA NA GAILLIMHE-MAIGH EO

The Development, Application and Implementation of Embedded Software Algorithms for Pyroelectric Gas Level Monitors

In One Volume

Kevin McDonagh B. Eng.

September 2006

Submitted for the Degree of
Master of Engineering

Submitted to:	Galway-Mayo Institute of Technology, Galway, Ireland.
Research carried out at:	Monicon Technology Ltd. Galway, Ireland
Research Supervisor:	Dr. John Owen-Jones.

Dedicated to my Mother

Declaration

I hereby declare that the work presented in this thesis is my own and that it has not been previously used to obtain a degree in this institution or elsewhere.

_____

Kevin McDonagh.

25th September 2006.

Statement of Confidentiality

The material contained in this thesis should not be used, sold, assigned, or disclosed to any other person, organisation or corporation without the permission of:

Galway-Mayo Institute of Technology:

Contact: Dr. John Owen-Jones
Tel: +353 91 742202
Dr. John Owen-Jones email:
john.owen-jones@gmit.ie

Contact: Mr. Michael Murray
Tel: +353 91 742298
Michael Murray email:
michael.murray@gmit.ie

Monicon Technology Ltd., Galway

Contact: Mr. Pat Murphy
Tel: +353 91 752884
Pat Murphy email:
p.murphy@monicon.com

Prologue

The research described in this thesis has been carried out over a 20-month period as part of a college/industry partnership project. This project is a partnership between the Galway-Mayo Institute of Technology and Monicon Technology, a leading manufacturer of gas monitoring instruments. The aim of the project was to research and develop an infrared-based gas monitor that makes use of innovative design methodologies in order to produce a product that would place Monicon Technology to the fore of advanced gas monitoring.

Acknowledgments

There are a number of people to whom I am extremely grateful for their help and encouragement these past twenty months…

Dr. John Owen Jones and Michael Murray, my research supervisors for all your assistance, ideas, guidance and the opportunity to study at GMIT. You were always very approachable and I wish you all the best in the future.

Pat Murphy of Monicon Technology Ltd, Galway, thank you for giving your time, commitment and invaluable expertise to the project.

Dr Alan Doncaster, Clairair Ltd, Maldon, Essex, UK, for his intuitive advice.

Thanks to all of the staff in GMIT, in particular thanks to the following people: Caroline Joyce and Ann Duggan.

To Niamh for making my life a better place to be in. Without your support none of this would have been possible and I will always remember that.

Finally, and most importantly my wonderful mother Nora and all my family. Thank you for the guidance and encouragement you have given me throughout my life.

Table of Contents

Chapter 4. Implementation

Chapter 5. Testing and Validation

Chapter 6. Conclusions and Further Development

List of Figures and Tables

Figures

Chapter 4

Chapter 5

Tables

Chapter 2

Chapter 4

Chapter 5

Chapter 1

Introduction

1.1 Thesis Motivation

In recent years trends in the gas monitoring industry have suggested that the Non-Dispersive Infrared (NDIR) method of detecting gas is proving to be the most popular choice out of all the gas detection technologies. The NDIR method has many advantages over conventional methods that are sometimes deployed to detect the presence of gas. In an industrial driven world where ever increasing levels of safety are expected and demanded there is an even greater demand for high quality, reliable and well-designed instrumentation. Infrared gas monitoring is recognized as being the most likely gas detection technology that can provide the quality and reliability required in a gas detector. By tackling inherent problems evident in similar gas detectors currently on the market and by offering an attractive and competitive sale price it was envisaged that the completed instrument would boost Monicon's sales in their infrared product range.

1.2 Thesis Objectives

This thesis is based on the work done in developing the infrared gas detector. The project initially was intended to be one instrument that could be set up to detect 5% by volume CO_2 and also set up to detect a range of hydrocarbon gases in the LEL range (Lower Explosive Limit). It became clear however in the early design stages that the project has to be split into two separate instruments, a CO_2 detector and a hydrocarbon detector. The CO_2 detector was titled the IR80 and the hydrocarbon monitor was called the S500-IR. The main objective of this project is to design and develop an infrared gas detector that would place Monicon at the leading edge of gas detection instrumentation. To set the developed instrument apart from similar instruments on the market some innovative design features were to be incorporated into the development and design stages.

1.3 Research Methodology

The approach to the research is as follows:

Literature Review

- **Gas Detection Technologies**
  - Catalytic Pellistor
  - Electrochemical methods
  - Semiconductor resistive detectors
  - Paramagnetic oxygen detectors
- **Infrared Gas Monitoring**
  - Infra-Red Spectroscopy
  - Beer-Lambert Law
  - Deviations from the Beer-Lambert law
  - Pyroelectric Detector Characteristics
  - Advantages of Infrared Gas Monitoring

Requirement Analysis

- Analyze current infrared gas monitoring systems and technologies used.

- Identify shortcomings that exist in current instruments and propose a set of design methodologies that would enhance the infrared gas detector.

System Development

- Develop the IR80 CO_2 infrared gas detector and the S500-IR infrared gas detector.

Test and Validation

- Evaluate the implemented system.
- Obtain gas instrumentation expert feedback.
- Conduct a field test with the instrument.

1.4 Thesis Structure

A brief description of the structure of the thesis is given below and is illustrated in figure 1.1.

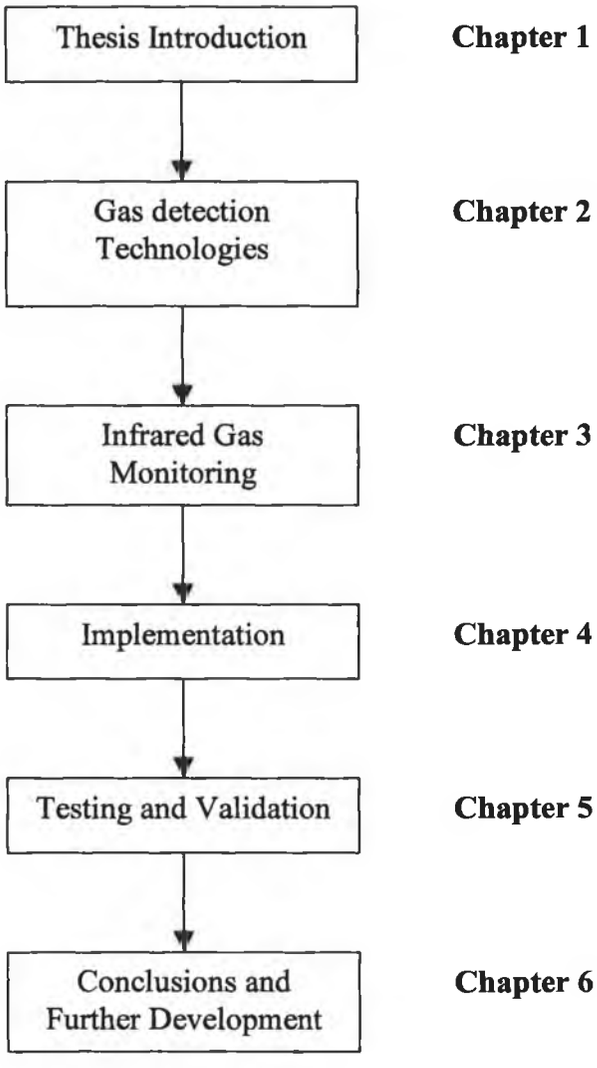

Figure 1.1 Thesis Structure

Chapter 1 presents the thesis motivation, objectives, methodology and structure.

Chapter 2 contains a literature review of the various other types of gas monitoring technology used in instrumentation. The catalytic pellistor is described in detail. Electrochemical methods deployed to detect gas are detailed. Semiconductor adsorption is explained and finally there is a section on paramagnetic gas detectors and the principles on how they operate.

Chapter 3 gives an insight into infrared gas monitoring and the theory behind it. Infrared spectroscopy is the study of how molecules absorb infrared radiation, and the theories related to this are detailed. Information is presented on the Beer-Lambert law and the deviations from the Beer-Lambert law. This law, in its basic form, relates the amount of light absorbed to the concentration of the substance absorbing it. The pyroelectric detector, which detects changes in incident radiation, is described and how it is utilized in the project design. Finally the advantages of using infrared monitoring are listed.

Chapter 4 details the implementation of the infrared gas detector. A set of functional and non-functional requirements is listed to begin with. Then all aspects of the design and implementation of the system are given.

Chapter 5 looks at the testing and validation of the infrared gas detector. The methods used to thoroughly test the implemented system are presented along with some results and feedback from instrumentation experts.

Chapter 6 concludes with a summary of the work done, the conclusions drawn from the research and recommendations for further development of the system.

Chapter 2

Gas Detection Technologies

2.1 Introduction

This chapter will introduce the most popular technologies used for the detection of gas. Most of these technologies are utilised by Monicon Technology in current production products. The advantages and disadvantages of each will be presented. Catalytic pellistor detection is discussed. Electrochemical methods to detect gas are also detailed. Another technique commercially used is semiconductor adsorption. Finally the magnetic properties of a certain gas, specifically oxygen will be described in order to explain how paramagnetic gas detectors operate.

2.2 Catalytic Pellistor

Oxidation of flammable or combustible gases on a heated catalytic pellistor is by far the most common method of detecting concentrations below the lower explosive limit (LEL) of these gases in air. The pellistor has been in production for over 40 years. Significant improvements have being made over the years in improving the overall performance of the sensor [Firth 1973].

The pellistor is basically a miniature calorimeter. A calorimeter is an apparatus for measuring the quantity of heat given off or present in a body. The pellistor is used to measure the energy liberated on oxidation of a combustible or flammable gas. It consists of a coil of small diameter platinum wire supported in a refractory bead. The coil serves two purposes. Firstly it is used to heat the bead electrically to it operating temperature of approximately 500°C. It's second purpose is to detect changes produced by the oxidation of combustible or flammable gas. As mentioned the wire is platinum. Platinum is stable, corrosion resistant and has a high temperature coefficient of resistivity, which makes it a good temperature sensor at the filament temperature. Thus the catalytic pellistor measures gas concentration by its rise in resistance, which is caused by a rise in temperature produced by the heat of combustion on the catalytic surface. However it needs a fairly high temperature for efficient combustion and for the particularly difficult case of methane detection this temperature can be up to 900°C. At this temperature the platinum wire will evaporate quite quickly giving an operating time of about 100 hours. To combat this problem the wire coil is repeatedly dipped into an aluminium nitrate, which is decomposed into alumina by heating with a current through the wire. This is repeated until the required bead size is obtained, usually 1mm in diameter. This forms a solid alumina bead around the coil that contains precious metals and catalysts. This enhanced catalytic activity resulting from the much larger surface area of catalyst available permits the much lower operating temperature of around 500°, resulting in lower power drain and a much longer device lifetime. Generally a reference bead is located beside the active bead in the sensor's housing. The reference/compensating bead does not facilitate the oxidation of a combustible or flammable gas. This reference bead can in turn be used to compensate for

environmental changes, pressure, temperature fluctuations etc. The active and reference pairs are matched together in production so they resemble each other's characteristics. The treatment of the reference bead commonly consists of boiling the bead in KOH solution, which is a strong catalyst poison [Mosley 1987]. Figure 2.1 shows the components that make up the pellistor catalytic detector.

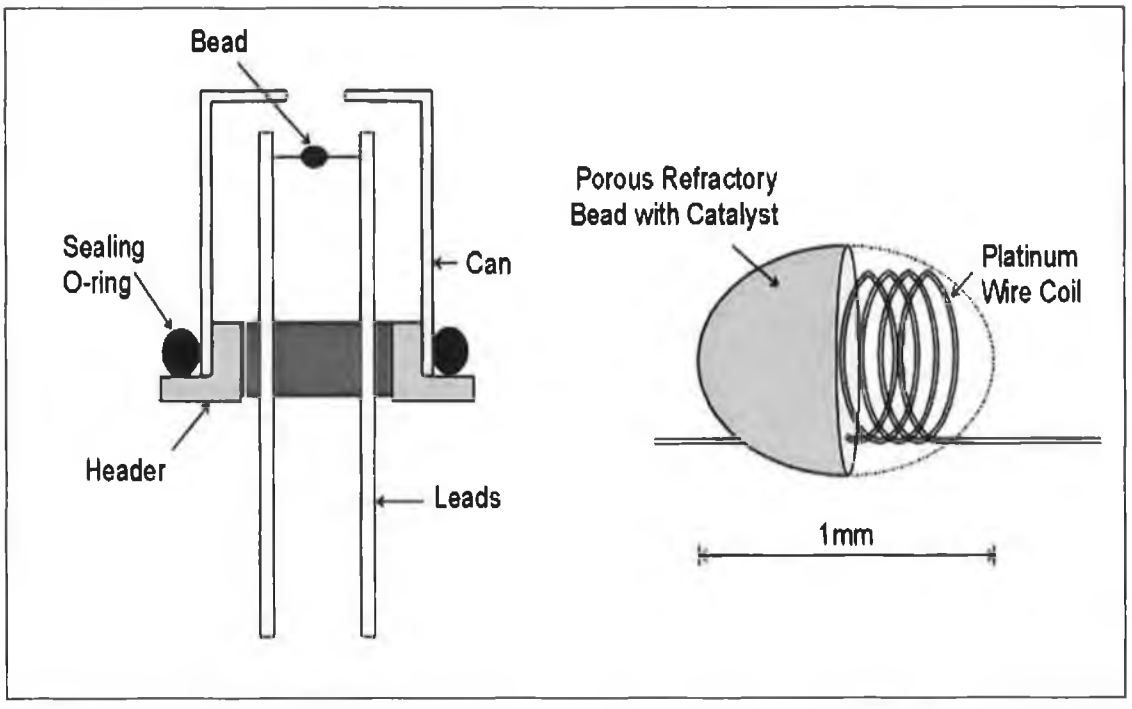

Figure 2.1 The pellistor catalytic detector

In order to integrate the pellistor into a circuit design the matched pair are connected into a wheatstone bridge circuit. A wheatstone bridge is balanced when the ratio of the resistances on the right are equal to the ratio of the resistances on the left side.

$$\frac{R1}{R2} = \frac{R3}{R4}$$

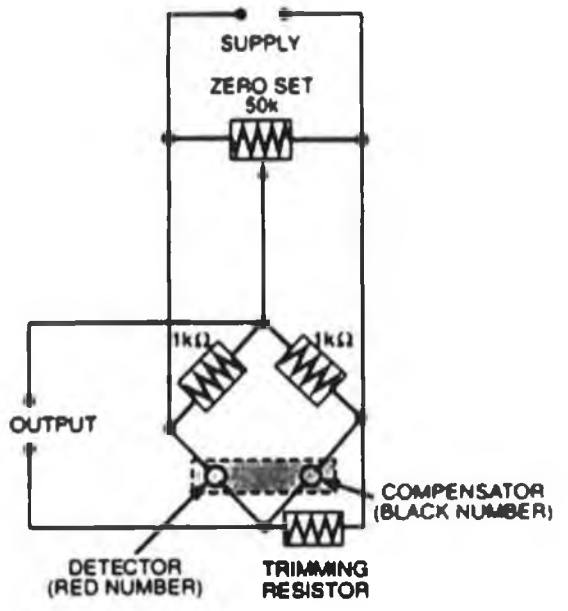

Figure 2.2 Wheatstone bridge circuit

As can be seen from the circuit diagram the active and compensating detector make up two sides of the bridge circuit. As oxidation occurs on the active element in the presence of a combustible gas the resistance increase results in an imbalance in the bridge. The bridge output rises accordingly. While in clean air the bridge can be zeroed by means of the zero potentiometer. The catalytic pellistor has a fast response time. Typically it possesses a T_{90} time of 15 seconds, T_{90} being the time it takes to reach 90% of the target gas concentration. One disadvantage of the catalytic pellistor is that if the pellistor encounters a high gas concentration, it will give an increasing output to the stoichiometric ratio, but as less oxygen is then available the output from the sensor decreases with increasing gas concentration. As in the example of methane the output is a maximum at 10% volume. To overcome this potentially disastrous situation the national standards stipulate that each catalytic pellistor based detector must operate reliably at concentrations greater than 100% LEL. The most common method for gas detector manufacturers to implement this is to over-range latch the instrument in such situations. So in the eventuality that a high concentration of gas is present it will go into alarm mode and latch.

Another disadvantage of pellistor-based detector is that they can be easily poisoned. The pellistor can be poisoned by one of three means.

- Temporary poisoning or inhibition by volatile compounds. Many halogenated compounds have this effect.
- Decomposition and deposition of relatively in-volatile substances. The most common agents are lead tetraethyl (which deposits lead) and silicones (which deposits silica). Phosphorus, sulphur, arsenic, and antimony compounds also have this effect.
- Formation of polymers that coat the surface, for example, from vinyl chloride or butadiene.

In order to make the pellistor more poison resistant a bead which had a molecular sieve construction was introduced. This molecular sieve keeps the poison molecular away as there are bigger and more "clumpy" then the molecules of a combustible or flammable gas. This however only works for some poisons. In the presence of silicones any catalytic pellistor will be irreversibly poisoned [Pallas-Areny 2001].

2.2 Electrochemical Methods

A dc electrochemical cell consists of two electrical conductors called electrodes, each immersed in a suitable electrolytic solution [Plambeck 1982]. For a current to develop in a cell, it is necessary that:

- The electrodes be connected externally by means of a metal conductor.
- The two electrolytic solutions be in contact to permit movements of ions from one to the other.
- An electron transfer reaction can occur at each of the two electrodes.

The two electrodes usually consist of one copper and one zinc.

Conduction in a cell

Three distinct processes in various parts of the cell conduct charge.

Firstly conduction can occur between the two electrodes. Electrons serve as carriers moving from the zinc through the conductor to the copper. Secondly

within the electrolytic solution ion movement towards and away from the electrodes result in conduction. Finally a third process can occur at the two electrode surfaces. Here, an oxidation or a reduction reaction provides a mechanism whereby the ionic conduction of the solution is coupled with the electron conduction of the electrode to provide a complete circuit for the flow of charge [Ewing 1975]. By definition the cathode of an electrochemical cell is the electrode at which reduction occurs while the anode is the electrode where an oxidation take place. Reduction occurs when it is the final process by which the commercially available electrochemical cell utilises in the detection of gas [Douglas 1994].

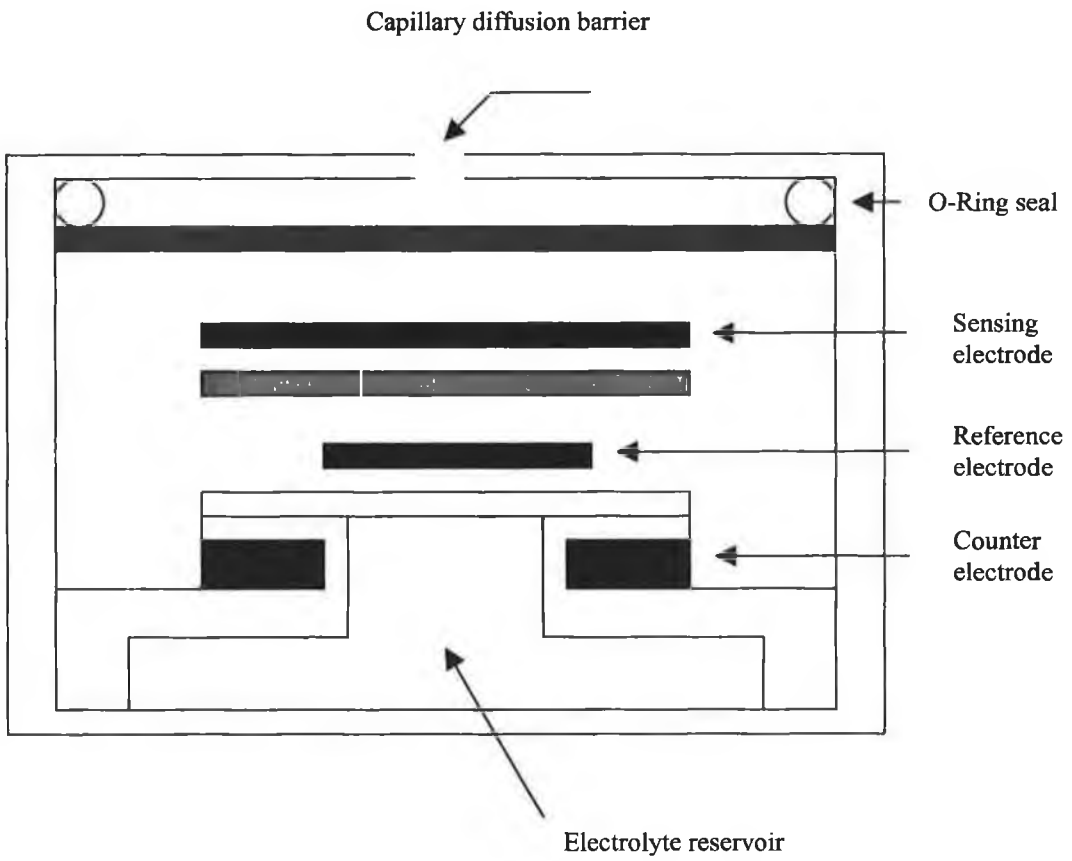

Figure 2.3 Electrochemical cell [Strobel 1975]

Oxidation and reduction

A very large class of reactions can be regarded as occurring by the transfer of electrons from one species to another. Electron gain is reduction and electron loss is oxidation [Rouessac 1998]. The joint process is called a redox reaction.

The species that supplies electrons is the reducing agent (or 'reductant') and the species that accepts electrons is the oxidizing agent (or 'oxidant'). To summarise oxidation then corresponds to the increase in oxidation number of an element and reduction corresponds to the decrease in oxidation number [Skoog 1992].

Gas diffusing into an electrochemical cell is reacted at the sensing electrode by oxidation (most gases) or reduction (e.g. nitrogen dioxide and chlorine). Each reaction can be represented in standard chemical equation form. The oxidation of carbon monoxide, for example at the sensing electrode can be represented by the equation [Fifield 1975]:

$$CO + H_2O \rightarrow CO_2 + 2H^+ + 2e^-$$

In a two-electrode electrochemical cell there is a sensing electrode where the oxidation or reduction takes places, and there is also a counter electrode, which acts to balance out the reaction at the sensing electrode. If oxidation occurs at the sensing electrode, oxygen will be reduced to form water at the counter electrode. If, however, the sensing electrode reaction is a reduction, the counter electrode reaction will be reversed (i.e. water will be oxidised). In either case current is caused to flow through the electrodes through an external circuit. This current is proportional to the concentration of gas and can be measured across a load resistor in the external circuit. As the gas concentration increases so too does the current flow, causing a change in the potential of the counter electrode (polarisation). With the electrodes connected with a simple load resistor, the sensing electrode potential follows that of the counter electrode potential [Verdin 1973].

There are however problems associated with two electrode electrochemical cells. Firstly if the gas concentration continues to rise, the sensing electrode potential will eventually move outside its permitted range. At this point the electrochemical cell will become non-linear, effectively limiting the upper concentration of gas that the two electrode sensor can be used to measure.

Secondly the potential between the two electrodes is made up of the difference between the electrode potentials of the two electrodes together with the ohmic drop (IR) due to the resistance of the electrolyte (R) between the electrodes.

$V = E(anode) - E(cathode) + IR$

Where V is the cell voltage.

The contributions of E(anode) and E(cathode) cannot be separated. If the potential of the counter electrode remains effectively constant then the value of the sensing electrode can be determined with respect to the potential of the counter electrode as a reference. This depends on the potential of the counter electrode remaining constant over a range of cell currents, which in reality is an unsatisfactory situation [Riley 1987].

The solution to the problems described in the previous section are largely overcome by the introduction of a third electrode into the cell. This third electrode is called a reference electrode and is used in conjunction with an external potentiostatic operating circuit. The function of this potentiostatic circuit is to hold the potential of the sensing electrode with respect to the reference electrode potential. The diagram below shows a typical potentiostatic circuit in conjunction with an electrochemical cell.

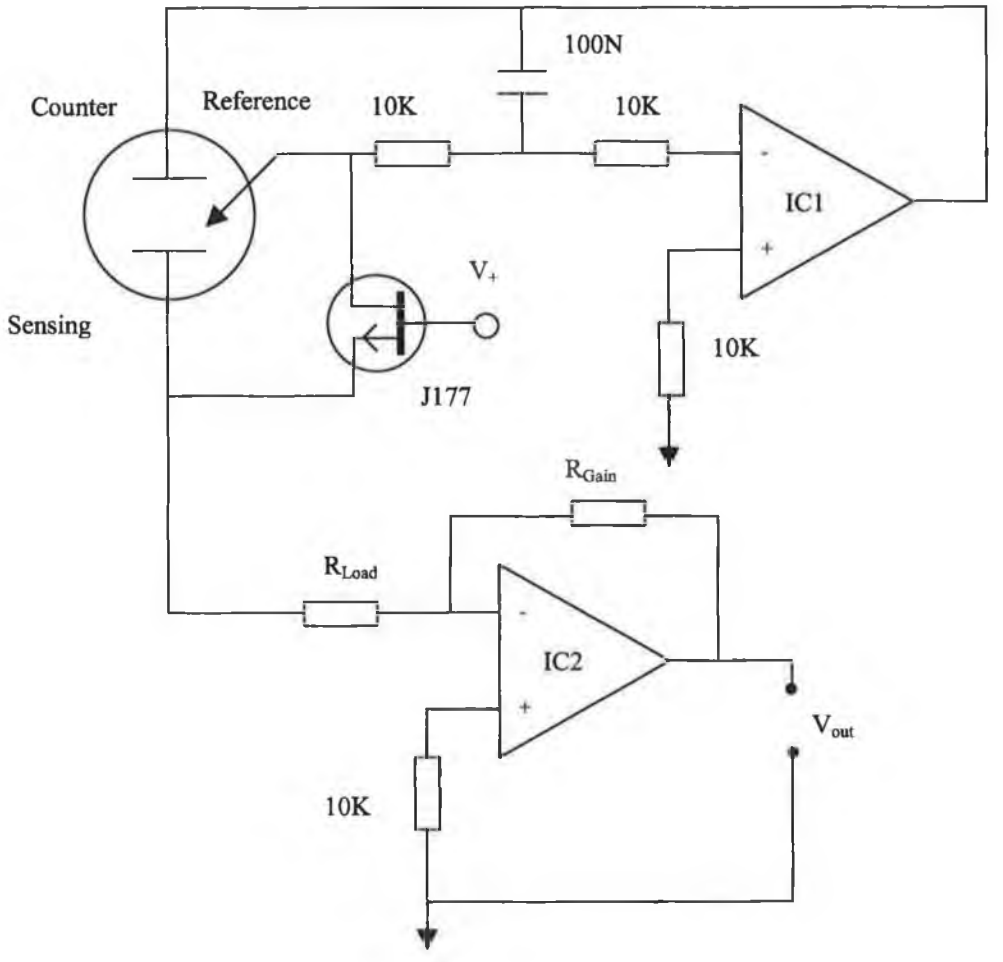

Figure 2.4 Potentiostatic circuit diagram including electrochemical cell

IC1, which is an op-amp, compares the measured value of the reference electrode to zero volts. The difference between the two is an error signal and this is fed back to the counter electrode. The sensing electrode is held at a fixed potential relative to the reference electrode. The counter electrode is still free to polarise but this has no effect on the sensing electrode and so does not limit the sensor in any way. Consequently the range of concentrations a three-electrode sensor can be used to measure is much greater.

The purpose of the junction field effect transistor (JFET) is to short the reference and sensing electrodes together when the cell is powered down. This

way the two electrodes can be at the same potential and will not take a long time to stabilize when it is powered up. When circuit voltage is applied to gate of the JFET on power up there is an effectively an open circuit between the drain and the source. It is also important to ensure that the op-amp (IC1) used in the circuit has a low offset voltage (e.g. < 100μV), or the op-amp will effectively bias the sensor.

2.3 Semiconductor resistive detectors

Semiconductor resistive gas sensors rely on the change of surface or bulk conductivity of some metal-oxide semiconductors, depending on the concentration of oxygen in the ambient atmosphere.

Crystal lattices of semiconducting oxides have defects, often oxygen-ion vacancies [Berry 1968]. These defects are also known as grain boundaries. At temperatures above about 700°C, the adsorbed and absorbed O_2 molecules from the atmosphere dissociate to form O^- by extracting electrons from the metal oxides, thus increasing its conductivity. This forms a potential barrier in the grain boundaries. This potential barrier (eV's in air) restricts the flow of electrons causing the resistance to increase. The relationship between the conductivity of the oxide and the oxygen partial pressure takes the form [Hammond 1990]:

$$\sigma = Ae^{-Ea / kT} po_2^{1/N}$$

Where, A is a constant, E_a is the activation energy for conduction, k is Boltzmann's constant, T is the absolute temperature and N is a constant determined by the dominant type of bulk defect involved in the equilibrium between the oxide and oxygen. For TiO_2, for example, $-4 < N < -6$. An increase in oxygen concentration increases the conductivity.

Metal oxides can also detect gases that react with oxygen. That is combustible gases such as carbon monoxide (CO) and hydrogen (H_2). These reactions happen at temperatures in the range from 300°C to 500°C, and they reduce the amount

of oxygen adsorbed in the surface. In an n-type oxide adsorbed oxygen acts as a trap for electrons from the bulk, hence increasing the resistance of the material. Thus, oxygen reduction by a gas decreases resistance. It does this because the potential barrier is now lowered which allows the electrons to move more easily, thereby reducing the electric resistance [Tabor 1993]. In a p-type oxide, adsorbed oxygen acts as a surface acceptor state that increases hole concentration, hence reducing the resistance of the material. Oxidizing gases such as chlorine (Cl_2) and nitrogen dioxide (NO_2) can also be detected because of their direct reaction with the oxide. The resistance of the material responds in a way opposite to that for reducing gases. Therefore if the atmosphere has a fixed O_2 concentration, as in air, minority gases increase or decrease the resistance of the material depending on whether they are reducing or oxidizing gases and on the type of material (n or p).

Over a certain range of gas concentration the relationship between sensor resistance and the concentration of the deoxidizing gas can be expressed as:

$$\mathbf{R = A[C]^{-\alpha}}$$

Where A and α are constants and [C] is the gas concentration. The sensitivity is often specified as the ratio between measured resistances at two reference gas concentrations [Putley 1970].

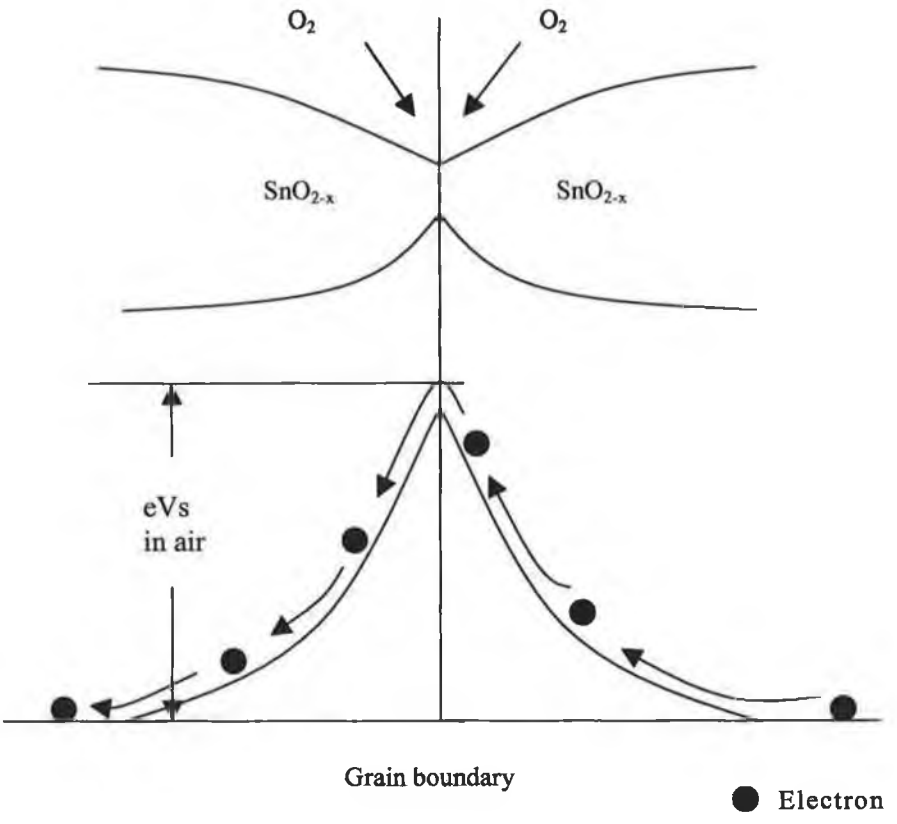

Figure 2.5 Model of inter-grain potential barrier without reducing gas present

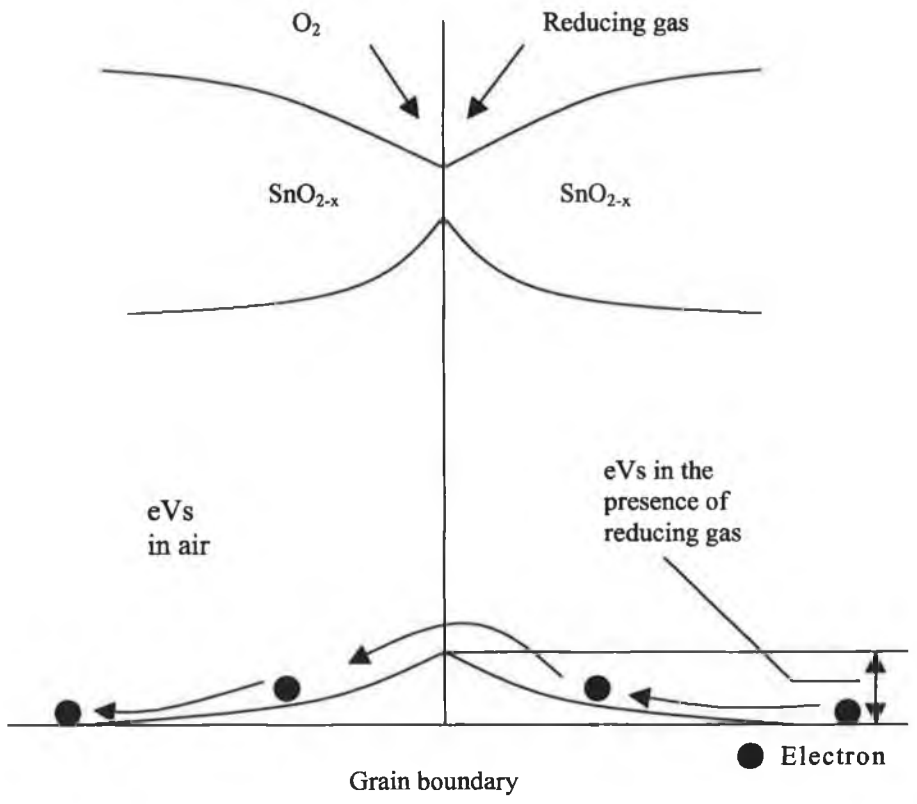

Figure 2.6 Model of inter-grain potential barrier with reducing gas present [Willard 1988]

Semiconductor metal oxide gas sensors are sensitive to temperature humidity and air pressure. These sensitivities are the major downfall in using a metal oxide sensor for gas detection. Ambient temperature will have an effect on sensitivity characteristics by changing the rate of chemical reaction. Humidity causes a decrease in the sensor resistance as water vapour adsorbs on the sensor's surface. Finally air pressure can also effect the operation of the sensor as it depends on the absorption along with the gas reaction to oxygen present in the atmosphere. Resistive gas sensors also lack selectivity (i.e. they are cross-sensitive). Their main use is in the detection of solvents, methanol, iso-butane, and combustible gases, methane, hydrogen, propane etc. Although there are carbon monoxide, ammonia and sensors for detecting CFC's available.

The most common metal oxide used in the production of semiconductor sensors is tin-oxide (SnO_2). Other sensors use Ga_2O_3, working above 950°C for oxygen detection and between 600°C and 900°C for detecting different reducing gases. Some other metal oxides tested include ZnO, WO3 and Fe_2O_3. Each sensor

contains four basic elements, as illustrated in figure 2.7. The sensing metal oxide and its support, metal contacts (electrodes) for resistance measurement and a heater to achieve the operating temperature. The sensing material can be prepared in thick films using a screen-printing method, in thin films or as sintered elements. The operating temperature of the heating element is selected to tune the sensing material for a specific set of gases. In order to reduce the humidity interference mentioned previously the heater is sometimes operated by pulsed voltage, so that it first reaches a high temperature able to remove water from the sensor and then at the operating temperature, where a sensor output reading may be taken. The Taguchi (TGS) gas sensor is a sintered n-type semiconductor bulk device and is probably the most commercially well known semiconductor resistive gas sensor. Figure 2.7 shows the construction of such a typical semiconductor device.

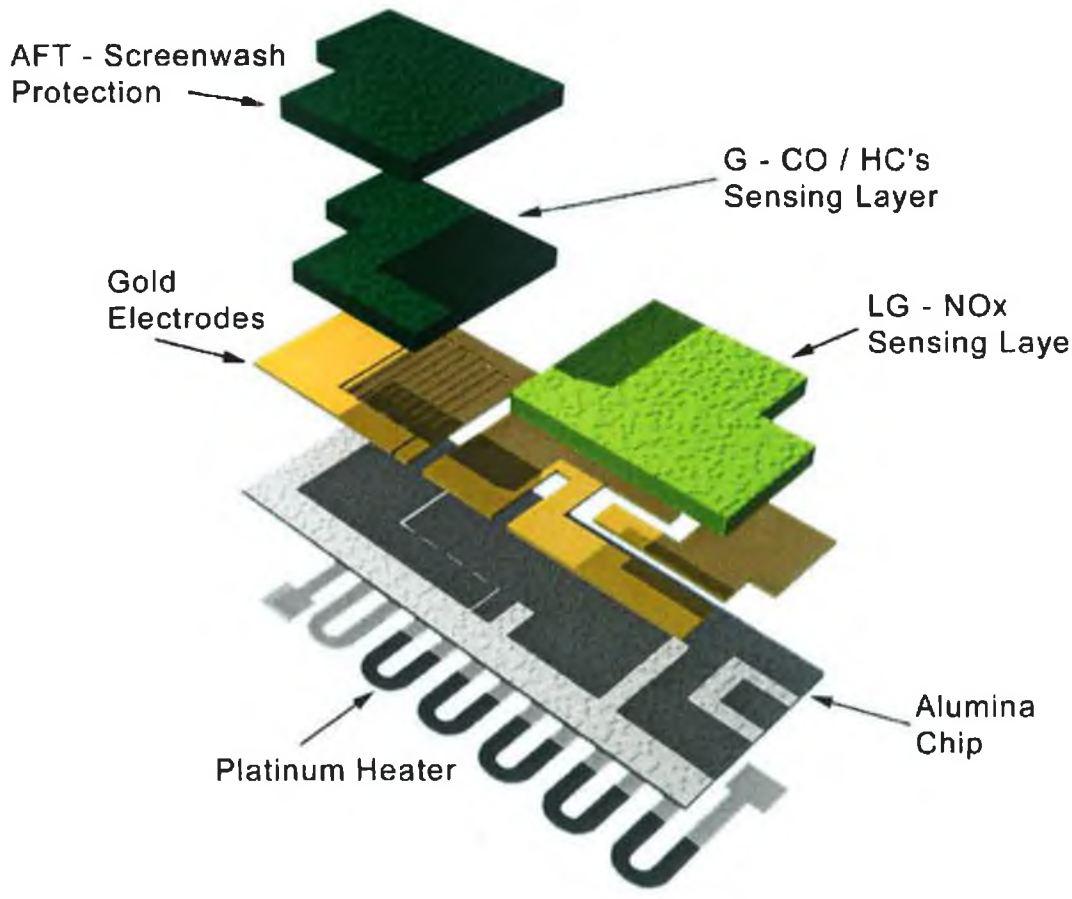

Figure 2.7 Semiconductor resistive device.

2.5 Paramagnetic Oxygen Detectors

There is a massive global demand for oxygen monitoring in all aspects of manufacturing, control and air quality. One of the most accurate methods for the detection of oxygen levels is through the use of paramagnetic analysis.

All substances possess some magnetic properties and will be either attracted to (paramagnetic and ferromagnetic) or repelled from (diamagnetic) the strongest part of a magnetic field. Each electron has a magnetic moment due to its orbit and spin. The molecules of most gases have an even number of electrons with paired spins so the individual moments cancel out and there is no permanent molecular magnetic moment. Interaction with an applied magnetic field alters the electron orbits and induces diamagnetism. Molecules with an odd number of electrons, such as NO, NO_2, ClO_2, are naturally paramagnetic. Oxygen is an unusual case as it has an even number of electrons, but when these are assigned to their molecular orbitals two are left with spins unpaired. Oxygen is therefore paramagnetic.

The influence of a magnetic field on a substance is measured by its susceptibility:

$$k = \frac{I}{H}$$

Where k is the volume susceptibility, H is the intensity of the field and I the intensity of the magnetism induced in the substance by the field. Diamagnetic gases have a negative susceptibility; parametric gases a positive susceptibility about two orders of magnitude greater. Listed below is a number of gases relative volume susceptibility.

Ammonia	-0.26
Iso-butane	-1.30
Carbon dioxide	-0.27
Carbon monoxide	+0.01
Helium	+0.30
Hydrogen	+0.24
Methane	-0.20
Nitric oxide	+43
Nitrogen dioxide	+28
Oxygen	+100

Table 2.1 Comparative susceptibilities of gases

As can be seen from table 2.1 oxygen has the greatest susceptibility making it an ideal candidate for paramagnetic analysis.

The mass susceptibility χ of a substance is inversely proportional to absolute temperature (Curie's law). Since by definition $k = \rho\chi$ where ρ is the density, also inversely proportional to temperature, the relation of volume susceptibility to absolute temperature is:

$$k \propto \frac{1}{T}$$

This relation is of fundamental importance to the thermomagnetic method, detailed shortly, and also emphasis that accurate measurements based on susceptibility need closer temperature monitoring.

The majority of paramagnetic based gas detectors combine the paramagnetic property with a heater and Wheatstone bridge detector. They are known as thermomagnetic or 'magnetic wind' instruments. In these instruments wind gas flows through a cell which contains a heated element, or zone, in a strong magnetic field. When oxygen is present the gas is paramagnetic and therefore

attracted into the magnetic field. Its magnetism decreases as it becomes hot, and it is displaced by more strongly cold gas. A continuous flow of gas or 'magnetic wind' is thus set up and cools a temperature sensitive element. The flow rate depends primarily on the temperature and the magnetic field, which are fixed, and the susceptibility of the gas, which is proportional to the oxygen concentration. Other gas properties will also affect the heat transfer and thus the temperature of the sensor that is actually measured. In a binary mixture or gas of constant background the output will be directly proportional to the oxygen concentration. In mixtures where other components vary these variations may affect the output. The extent of this effect will vary with the cell design and for many cases can be reduced to negligible proportions with careful thermal conductivity considerations.

There are two main detector designs based in the thermomagnetic method. Filament type and the ring chamber.

Filament type

The cell contains a detecting filament and a reference filament. The detecting filament is in a strong magnetic field, whilst the reference element is not. When no oxygen is present, or the magnetic field is absent, each filament is cooled to the same extent by natural convection from the gas diffusing into the cells. When oxygen is present in the sample, gas is attracted by the magnetic field into the detecting chamber where it is heated and become less magnetic. Cooler, more strongly magnetic gas is preferentially attracted, displaces the hot gas and in turn becomes heated. This magnetically induced flow adds to the cooling effect of the convection currents making the detector filament cooler and unbalancing the Wheatstone bridge. The resistance change is proportional to the oxygen concentration. This cell is very stable, simple and rugged. It is however directly affected by changes in background gas parameters, especially thermal conductivity and is not to streams where this changes markedly, for example in streams containing hydrogen.

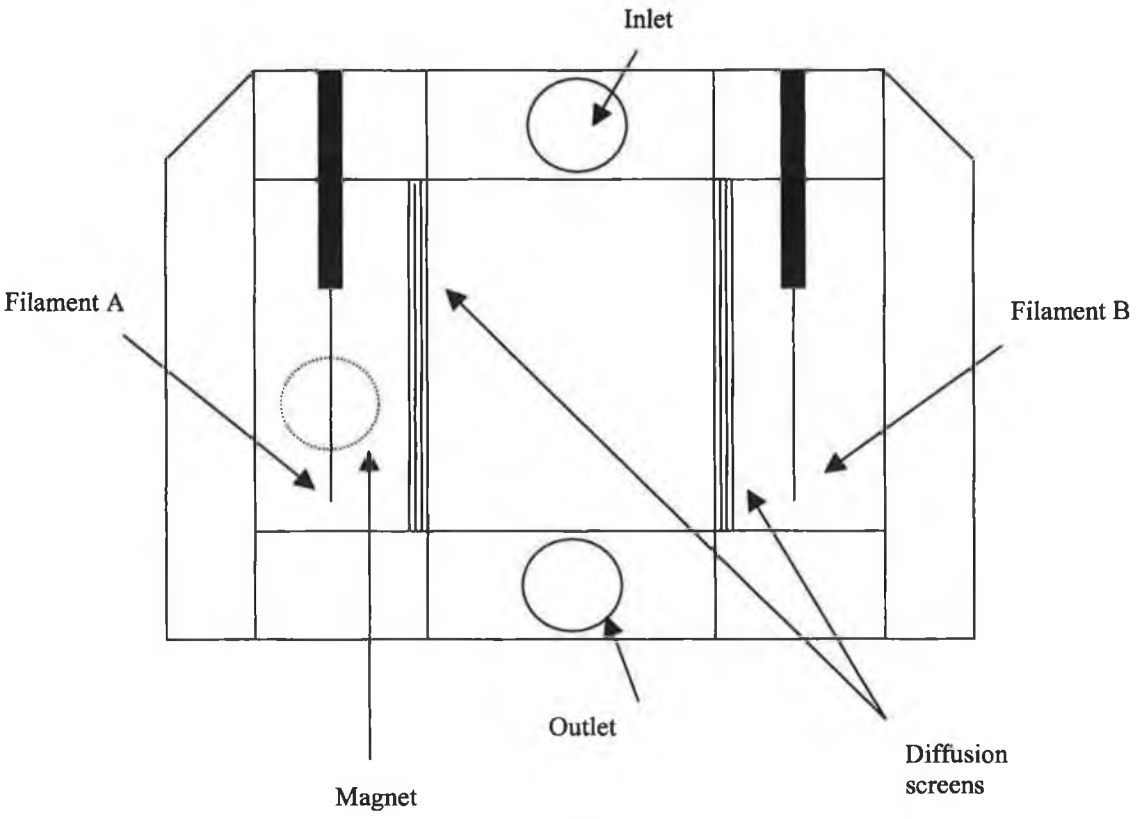

Figure 2.8 Paramagnetic oxygen cell, filament type

Ring chamber

The ring chamber is an annular cell round both sides of which gas flow. Across the centre is a horizontal glass tube connecting the two sides, with two heaters wound round it. One of the heaters is in a strong magnetic field and both are made of material such as nickel or platinum which can serves also as a temperature sensor. If the tube is accurately horizontal there will be no gas flow across it if oxygen is absent. When oxygen is present the paramagnetic gas will be attracted from the left-hand passage into the magnetic field. In the tube it will be heated, become less magnetic, and be displaced by more magnetic, cooler gas. A continuous flow from left to right will result. This flow will transfer heat from the left-hand to the right-hand winding and so unbalance the Wheatstone bridge in which they are connected. The output will be proportional to the oxygen concentration, although it is not linear over wide ranges.

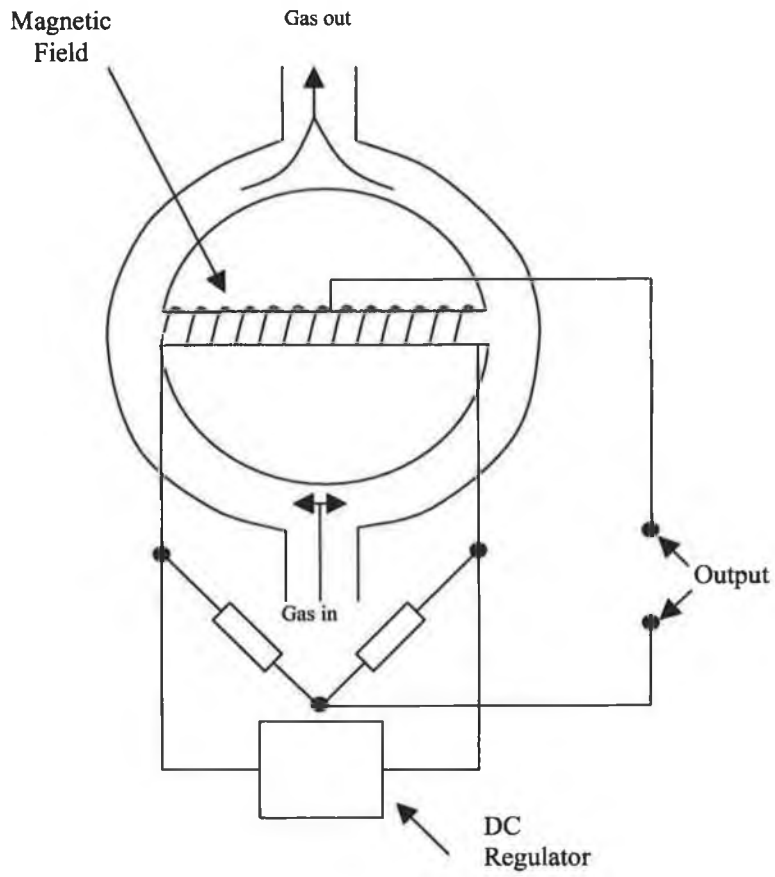

Figure 2.9 Paramagnetic oxygen cell, ring chamber

The output will also depend on the background gas. The output should be proportional to $\rho C_p/\eta$, where C_p is the constant pressure specific heat, ρ the density and η is the viscosity. The detector should be calibrated to allow for such factors. Values for $\rho C_p/\eta$ relative to nitrogen and their corresponding bridge output can be obtained for each gas.

The ring chamber detector must be mounted with the cross tube horizontal. The effect of tilting, which causes other thermal currents, is severe and also dependent on background gas composition. A 1° tilt can be equivalent to about 0.5 per cent oxygen. A zero shift can also occur through lack of thermal symmetry in the tube, which causes temperature changes as the thermal conductivity of the gas changes.

The need to heat the gas in all thermomagnetic instruments is a disadvantage in applications where combustible or reactive components are present. Although filaments are generally glass coated and heater windings are outside the tube, to avoid corrosion and catalytic action, gases may burn react or polymerise on the hot surfaces. The heat associated with these reactions will alter the output of the bridge [Verdin 1973].

Chapter 3

Infra-Red Gas Monitoring

3.1 Introduction

In this chapter the fundamentals and theories of infrared gas monitoring will be presented. Infrared spectroscopy will be discussed in order to give an insight into how molecules absorb infrared radiation. The spectra of various gases along with the carbon-hydrogen bonds of these gases will also be examined. The non-dispersive infrared technique (NDIR) for detecting the presence of certain gases utilises the Beer-Lambert equation. This equation relates the amount of light absorbed to the concentration of the absorbing substance. The equation is slightly modified to accommodate for non-absorbing wavelengths within the target gas spectrum. The NDIR method and also the theory and implementation of the Beer-Lambert equation will be detailed. The inherent characteristics of the pyroelectric detector are also described in chapter 3. The composition and behaviour of these detectors will be researched and presented. There will be an insight into the reasons for non-linearity with relation the gases spectra and finally the specific advantages of infrared gas monitoring will be listed.

3.2 Infra-Red Spectroscopy

Infrared spectroscopy is the study of how molecules absorb infrared radiation and how the infrared spectra of molecules can be interpreted to give information on molecular structure. Infrared radiation interacts with the vibration of certain chemical bonds within a molecule, namely carbon-hydrogen bonds. The wavelength of the absorbed infrared radiation is dependent on the nature of these chemical bonds [Stuart 1996].

3.2.1 The energy and bonding of a diatomic molecule

In this section a diatomic molecule is described. This form of a molecule is picked to generally describe the energy states and bonding that occur within molecules. Also the vibrational and rotational levels are explained. These same concepts apply to carbon dioxide and hydrogen molecules, the gases of interest in this infrared gas detector project.

A diatomic molecule is one that contains two atoms. When two atoms combine to form such a molecule they maybe be said to do so because of an internal electronic arrangement. Put in other words it can be viewed as a balancing of forces. Before two isolated atoms bond they possess potential energy, but as they move closer this potential energy drops off. Since energy must be conserved the corresponding kinetic energy increases as the two atoms accelerate towards each other. Each atom contains a positively charged nucleus and also a negatively charged electron 'cloud'. As the atoms moves closer together there is on one hand repulsion between the positively charged nuclei of both atoms and also between their negative electron 'clouds'. On the other hand there is an attraction between the nucleus of one atom and the electrons of the other, and vice versa. The two atoms settle at a mean inter-nuclear distance so that these forces are just balanced and the total energy of the whole system is at a minimum. The atoms effectively become trapped in a potential energy well and are therefore bonded together. These bonded atoms retain some kinetic energy and are as a result free to move about in this potential energy well. However there is insufficient kinetic energy for the atoms to separate from each other. As the diatomic molecule collides with other "third-bodies" energy is

be used to in relation to this stretching and compression. This bond, like a spring obeys hooks law.

$$f = - k(r - r_{eq})$$

Where f is the restoring force, k is the force constant and r is the inter-nuclear distance. However in the case of the diatomic bond the energy curve is parabolic so the equation takes the form.

$$E = \tfrac{1}{2} k(r - r_{eq})^2$$

This is the model of the vibrating diatomic molecule. In summary the frequency of the vibration is related to the strength of the chemical bond and the masses attached to that bond. Absorption spectra arise from transitions from each of these energy levels to the next. These transitions appear in the infrared region of the electromagnetic spectrum. The diagram below shows the vibrational energy levels and the transitions between them for the carbon-hydrogen bond in methane [Hollas 1996].

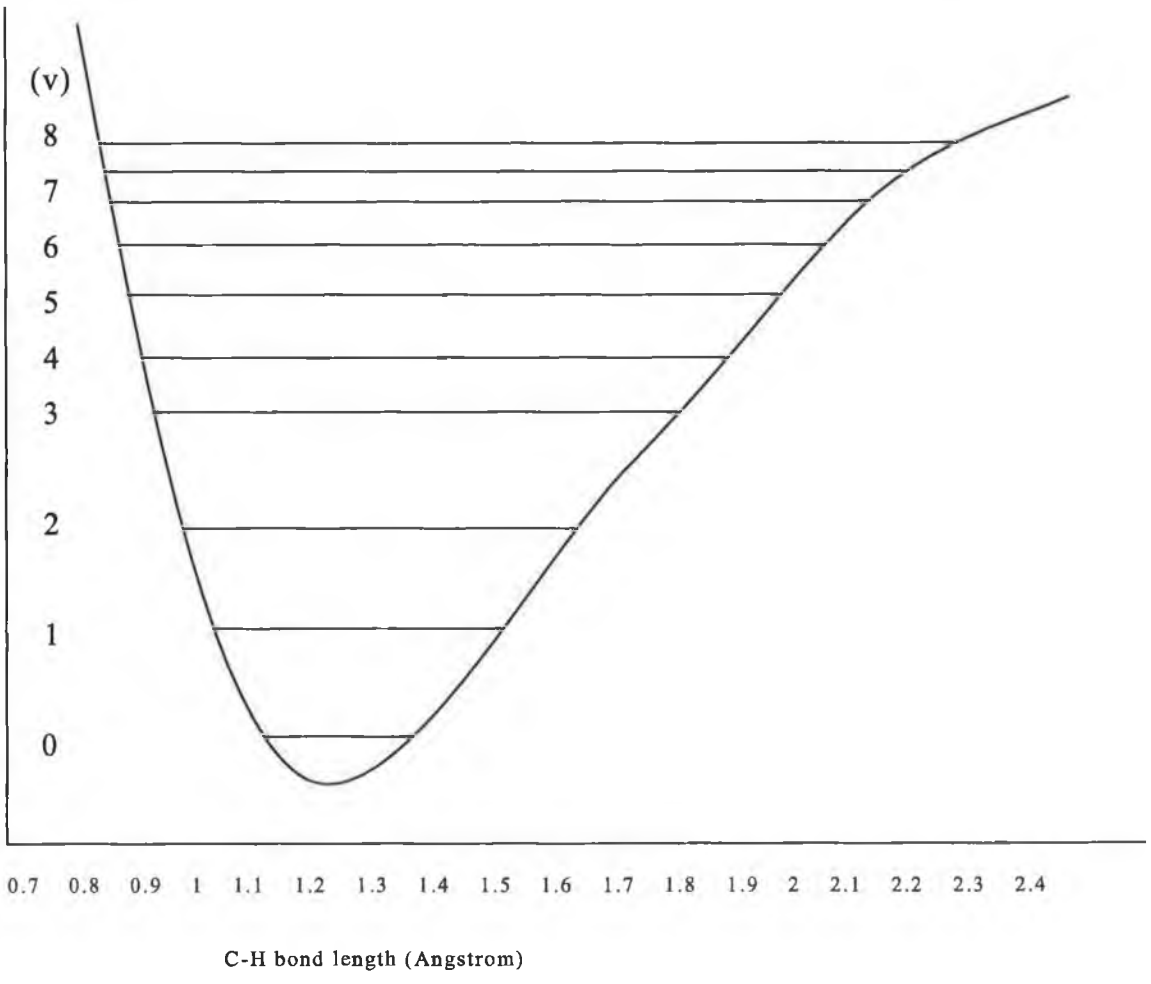

Figure 3.2 The vibrational energy level for carbon hydrogen bond in methane (CH_4)

The graph above plots the bond length, on the x-axis, with the energy levels (v) on the y-axis.

3.2.2 Rotational levels

The bond can, not only vibrate, but it can also rotate. It can be said to a good approximation that the rotational energy of a bond can be treated as independent of the vibrational energy. The rotation of a three dimensional body, a molecule, may be quite complex so it is convenient to divide it into rotational components around three mutually perpendicular directions through the centre of gravity . Thus it can be said that a molecule has its principal moments of inertia, one about each axis, usually designated I_A, I_B, I_C. Molecules can be classified into groups according to the relative values of their three principal moments of inertia. These groups are:

- Linear molecules: These, as the name implies, are molecules in which all the atoms are arranged in a straight line. Examples include hydrogen chloride (HCl), carbon oxysulphide (OCS) and carbon dioxide (CO_2).

$$H - Cl$$

$$O - C - S$$

The three directions of rotation may be taken as (a) about the bond-axis, (b) end-over-end rotation in the plane, and (c) end-over-end rotation at right angle to the plane. The plane taken as if looking down into the paper. It is self evident that the moments of (b) and (c) are the same, $I_B = I_C$, while that of (a) is very small. It can be said that $I_A = 0$.

- Symmetric tops: Consider the molecule methyl-fluoride, where there is three hydrogen atoms bonded tetrahedrally to the carbon as shown below.

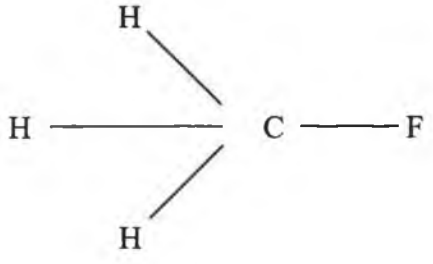

As in the case of linear molecules the end-over-end rotation in and out of the plane of the paper are still identical. Hence $I_B = I_C$. However the moment of inertia of the C-F bond axis, which is the main rotational axis, is now not negligible. This is because it now involves the rotation of three atoms of this axis. Such a rotating molecule about this axis can be imagined as a spinning top, hence the name of the class.

Symmetric tops: $I_B = I_C \neq I_A \qquad I_A \neq 0$

- Spherical tops: When a molecule has all three moments of inertia identical, it is called a spherical top. Such an example is the tetrahedral molecule methane CH_4.

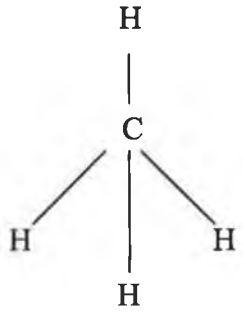

Spherical tops: $I_A = I_B = I_C$

In fact these molecules can have no dipole moment owing to their symmetry. Rotation alone can produce no dipole change and hence no rotational spectrum is observable, (dipole moment, see below for explanation).

- Asymmetric tops: These molecules, to which the majority of substances belong, have all three moments of inertia different.

$$I_A \neq I_B \neq I_C$$

Simple examples include water H_2O and vinyl chloride $CH_2 = CHCl$ [Atkins 1995].

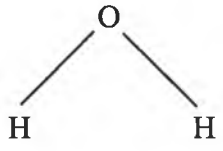

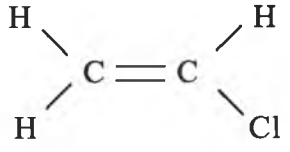

There are two requirements for the absorption of incident radiation by a substance: 1) the radiation must have precisely the correct energy to satisfy the energy requirements of the material, and 2) there must be a coupling (or

interaction) between the radiation and the substance. Radiation in the infrared region has the proper magnitude of energy to cause vibrational transitions in molecules and the first requirement for absorption is satisfied if a given frequency of infrared radiation corresponds exactly to a fundamental vibrational frequency of a given molecule. To satisfy the second requirement for absorption, the molecule must undergo a change in dipole moment when the fundamental vibration occurs. If no change in dipole moment occurs when the molecule vibrates there will be no interaction between the electromagnetic radiation and the non-electromagnetic molecule. In a situation such as this no absorption will take place regardless of the energy compatibility. Such a vibration is said to be infrared-inactive[Freiss 1961].

The dipole moment μ of two equal and opposite charges is defined as the product of the charge q and the distance r separating them.

$$\mu = qr$$

For a molecule it is the effective centre of the positive and negative charges that is important, r being the distance between those centres. Figure 3.3 below shows the linear molecule CO_2. Fig. 3.3a shows that its dipole moment is zero. More important is that the change in dipole is zero when the molecule is symmetrically stretched, (Fig. 3.3b). Thus the symmetrical stretch of CO_2 is infrared-inactive. On the other hand, as shown in Fig 3.3c, an asymmetrical stretch involves a change in dipole moment, and thus this mode of vibration is infrared-active.

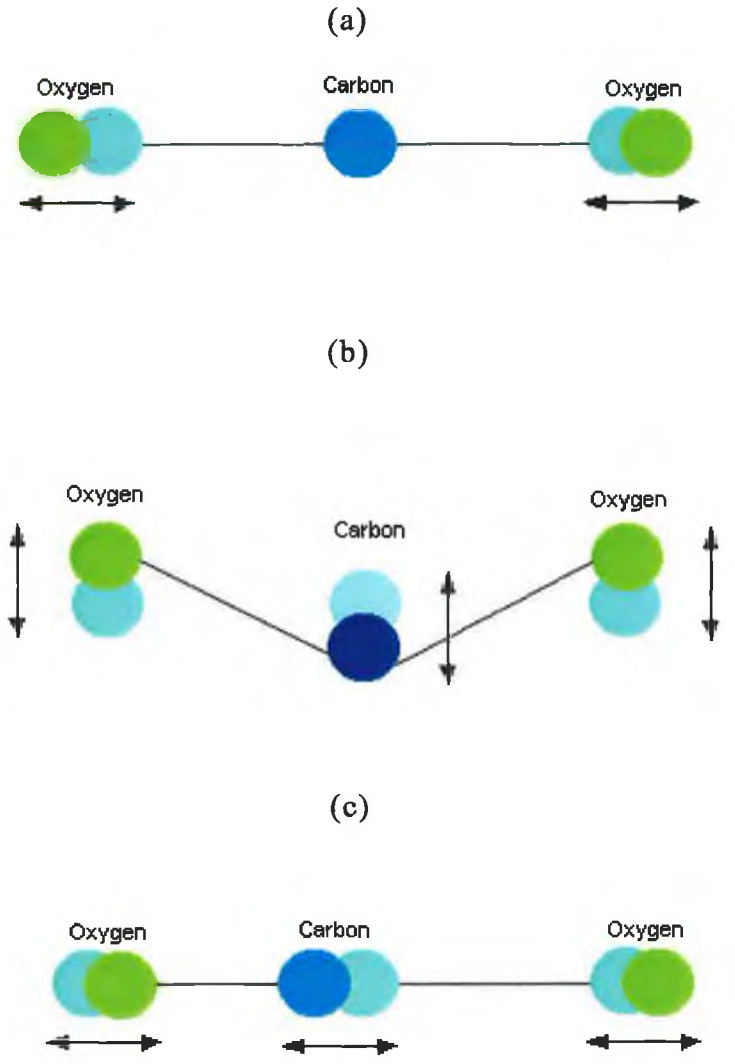

Figure 3.3 Stretching of CO_2, and it corresponding dipole moments [Maas 1972]

The rotational energy of a given molecule cannot have any arbitrary value. Its energy is limited to certain definite values, which depend on the shape and size of the molecule concerned. Taking the simplest of linear molecules, the rigid diatomic molecule, the idea of an absorption spectrum arising from increasing rotational levels will be explained in detail.

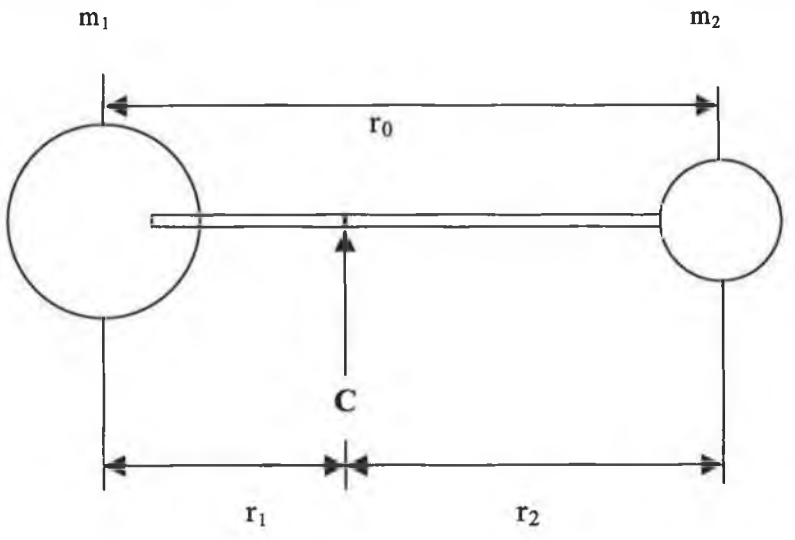

Figure 3.4 A rigid diatomic molecule treated as two masses, m_1 and m_2

Masses m_1 and m_2 are joined by a rigid bar (the bond) whose length is:

$$r_o = r_1 + r_2$$

The molecule rotates end-over-end about a point C, the centre of gravity. This is defined by the moment, or balancing equation:

$$m_1 r_1 = m_2 r_2$$

By the use of an equation used in molecular spectroscopy, called the Schrodinger equation, it can be shown that the rotational energy levels allowed to the rigid diatomic molecule are given by the expression:

$$\in_j = BJ(J + 1)\ cm^{-1}$$

B, the rotational constant given by:

$B = h / 8\pi^2 Ic\ cm^{-1}$ h is planck's constant, I is the moment of inertia for the particular molecule, c is the velocity of light. It is the differences between the energies or, more particularly in the corresponding frequency (Hz) or wavenumber (cm^{-1}), of the radiation emitted or absorbed as a consequence of changes between energy levels. In the rotational region, spectra are discussed in

terms of wavenumber, so the energies concerned are expressed in these units. This rotational constant, B, is derived from the aforementioned Schrodinger equation.

The quantity J which can takes integral values from zero upwards is called the rotational quantum number. The reason for J to take on only integral values arises directly out of the solution to the Schrodinger equation and is by no means arbitrary. It is in fact this restriction that effectively allows only certain discrete rotational energy levels to exist in the molecule.

For J = 0 it can be plainly seen that $\epsilon_j = 0$ and it can hence be stated that the molecule is not rotating at all. For J = 1, the rotational energy is $\epsilon_j = 2B$ and the rotating molecule has its lowest angular momentum. With increasing J values the rotational energy can be calculated and in principle there is no limit to this rotational energy. However in practice there comes a point when the centrifugal force of a rapidly rotating diatomic molecule is greater than the strength of the bond and the molecule is disrupted. This point is not reached at normal temperatures however [Price 1974].

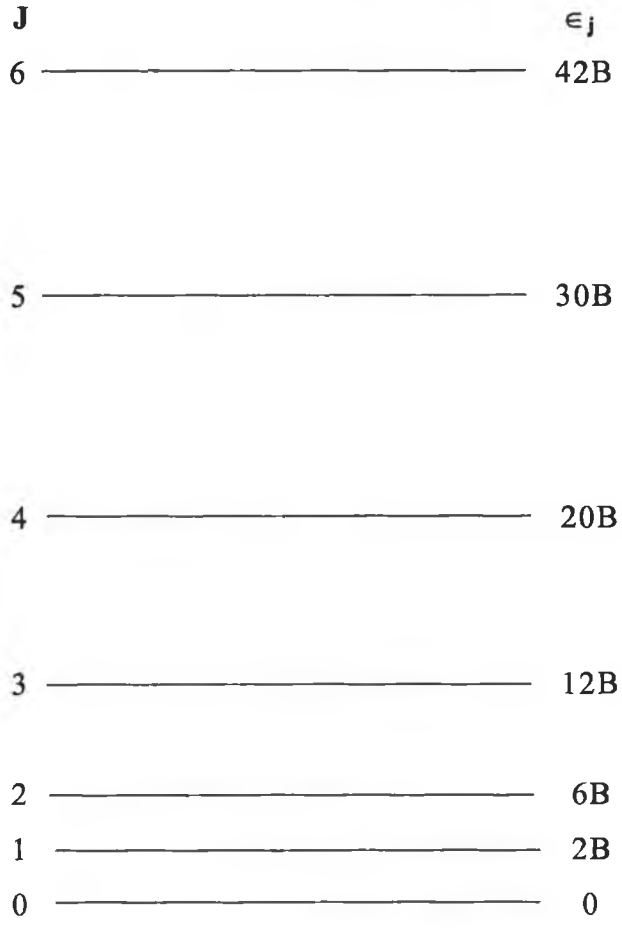

Figure 3.5 The allowed rotational energies of a rigid diatomic molecule

Taking a molecule to be in the J = 0 state (the ground rotational state, in which no rotation occurs). If incident radiation falls on the molecule it will be absorbed and it will be raised to the J = 1 state. The energy absorbed will be:

$\epsilon_{j=1} - \epsilon_{j=0}$

$$\Rightarrow \quad 2B - 0$$

$$\Rightarrow \quad 2B \text{ cm}^{-1}$$

In other words, an absorption line will appear at 2B cm $^{-1}$. If now the molecule is raised from the J = 1 to the J = 2 energy level by the absorption of more incident radiation it can be said that the required amount of energy is:

$$= 6B - 2B$$

$$= 4B \text{ cm}^{-1}$$

In general, to raise a molecule from the state J to state J + 1, we have:

$$\epsilon_{j \to j+1} = B(J + 1)(J + 2) - BJ(J + 1)$$
$$= B[J^2 + 3J + 2 - (J^2 + J)]$$
$$\epsilon_{j \to j+1} = 2B(J + 1) \text{ cm}^{-1}$$

Thus a stepwise raising of the rotational energy, through the absorption of incident radiation falling on a molecule, results in an absorption spectrum consisting of lines at 2B, 4B, 6B,..... cm^{-1}, while a similar lowering will result in an identical emission spectrum. Figure 3.6 illustrates this.

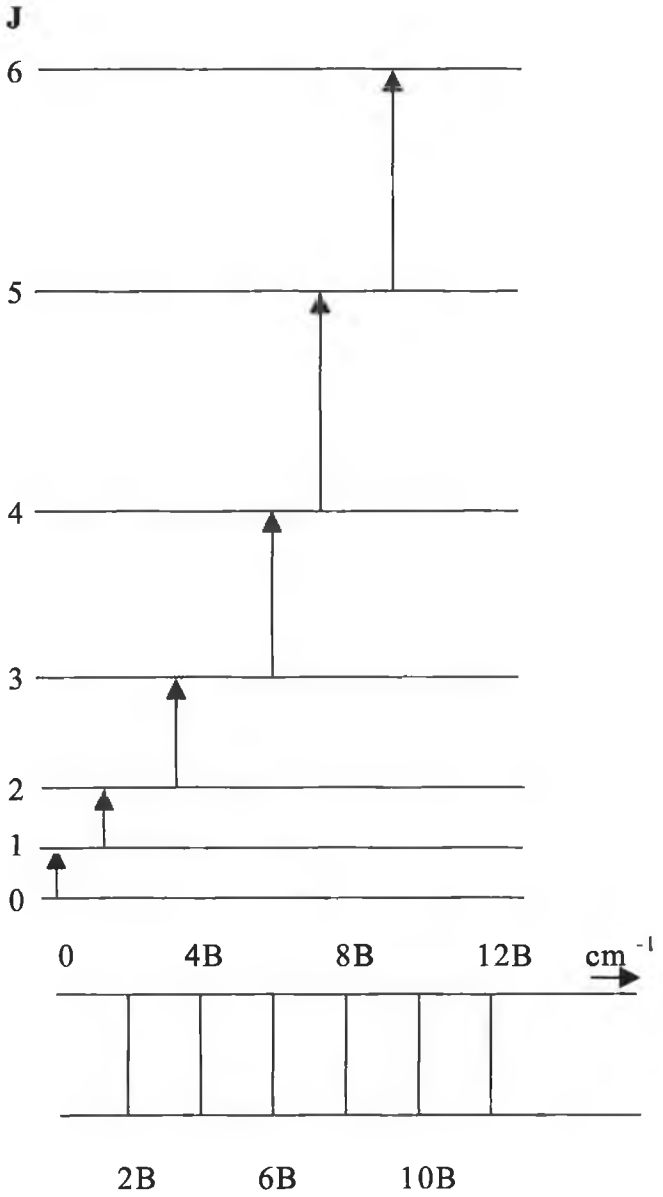

Figure 3.6 Transitions between energy levels of a rigid diatomic molecule and the spectrum which arises from them [Kemp 1975].

3.2.3 Vibration-Rotation spectra

The combination of vibrational and rotational energy levels produce what is known as the vibration-rotation spectrum. In order to observe vibration-rotation spectra a molecule must have certain properties.

- A vibrational spectrum can be observed when the vibration produces a changing dipole moment. This dipole moment changes with the inter-nuclear distance. In general, heteronuclear diatomic molecules have dipole moment changes and so they exhibit vibrational spectra. Homonuclear molecules, such as H_2 (hydrogen) and N_2 (nitrogen), have zero dipole moments for all bond length and therefore do not show vibrational spectra.
- A rotational spectrum can be observed when the rotor has a permanent dipole moment, for example HCl displays a rotational absorption spectrum in the far infrared but N2 (which is also not infrared active) does not.

The absorptions of the incident radiation falling on a molecule can be put into groups called branches of the spectra. The P branch consists of all energy transitions from the state J to the state J – 1. This branch hence consists of lines at –2B, -4B, -6B etc, with the intensity distribution reflecting both the population of the rotational levels and the $J - 1 \leftarrow J$ transition moment. The Q branch consists of all lines at J = 0, the ground state. The R branch consists of energy transitions from the energy state J to the state J + 1. This branch hence consists of lines at 2B, 4B, 6B etc. The separation between the lines in the P and R branches can be measured to calculate the bond length between the atoms [Hendrickson 1970].

3.2.4 Infrared spectrum of carbon dioxide

To explain the information presented so far in the preceding sections the infrared spectrum of carbon dioxide (CO_2) will be detailed. By looking at this relatively simple spectrum the ideas and concepts presented thus far will become clear.

CO_2 is a linear molecule with no permanent dipole. There are 4 normal modes of vibration. The symmetrical stretching vibration v_1 cannot cause a changing dipole moment, and therefore this mode of vibration is said to be inactive in the infrared. The molecules vibrate along the inter-nuclear axis in a symmetric manner. The twofold degenerate bending vibration v_2 causes a changing dipole moment, and is therefore active on the infrared, giving rise to a fundamental absorption band at 667 cm^{-1}. In this mode of vibration the atoms vibrate perpendicular to the inter-nuclear axis. This mode is doubly degenerate as there is a similar bending vibration normal to the plane of the paper. The anti-symmetric stretching mode v_3 also causes a changing dipole moment and is observed in the fundamental absorption band at 2348 cm^{-1}. The atoms vibrate along the inter-nuclear axis in an asymmetric manner. The stretch frequency is much higher than the bending one. This is a general result, because it is easier to distort a molecule by bending than by stretching, and the force constant is hence lower for a bending mode. The vibrational state of the molecule is described by three quantum numbers, v_1, v_2 and v_3, where v_1 denotes the number of vibrational quanta in the symmetric stretching mode, v_2 the number of vibrational quanta in the bending mode and v_3 the umber of vibrational quanta in the asymmetric stretching mode.

In addition to the fundamental absorption bands many combination and overtone bands occur in the infrared spectrum of CO_2. These however have lower intensities than the fundamental [Rubeska 1971].

Symmetric stretch

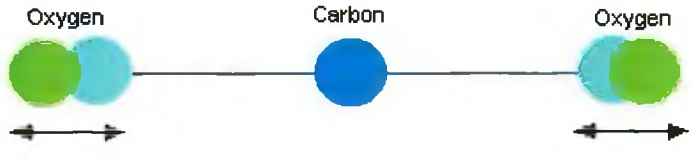

The atoms vibrate along the internuclear axis in a symmetric manner. Since this does not produce a changing dipole moment this vibration is said to be inactive in the infrared.

Bending mode

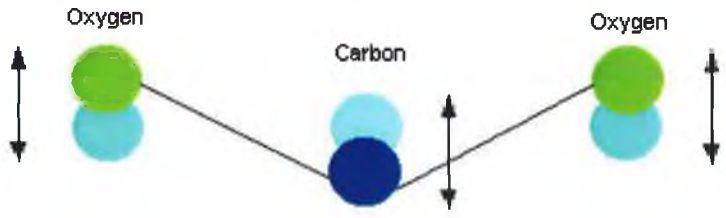

The vibration of the atoms is perpendicular to the internuclear axis creating a changing dipole moment. This mode is doubly degenerate and there is a similar bending vibration normal to the page. The fundamental absorption for this vibration occurs at 14.986 microns.

Asymmetric stretch

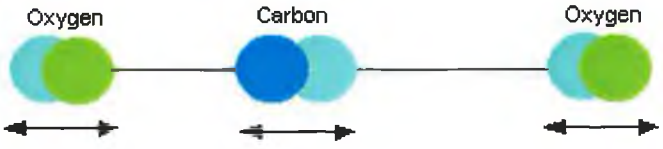

The atoms vibrate along the internuclear axis in an asymmetric manner creating a changing dipole moment. The fundamental absorption for this vibration occurs at 4.25 microns and is the target absorption band for the carbon dioxide sensors. Note that the stretch wavelength is much shorter than the bending wavelength; this is because it is easier to distort a molecule by bending than by stretching and the force constant and subsequent energy requirement for the bending mode is much lower.

The presence of the P and R branches caused by rotational level changes is clearly illustrated in the asymmetric stretch region of the infrared spectrum, figure 3.7

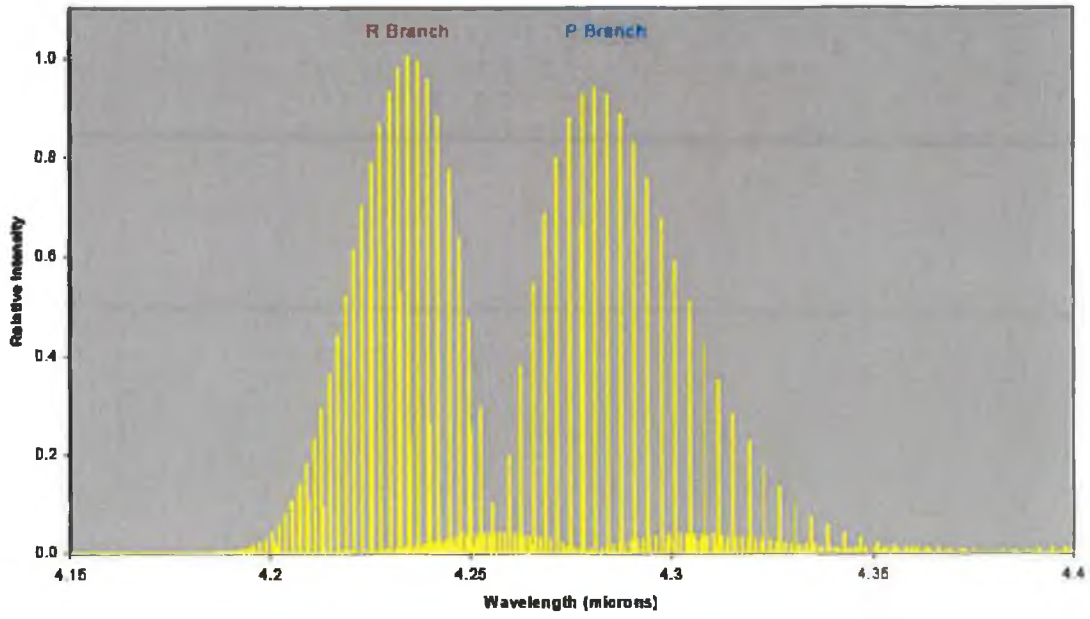

Figure 3.7 Carbon Dioxide Spectrum showing P and R branches

Below is shown the infrared spectrum for a variety of hydrocarbon type gases.

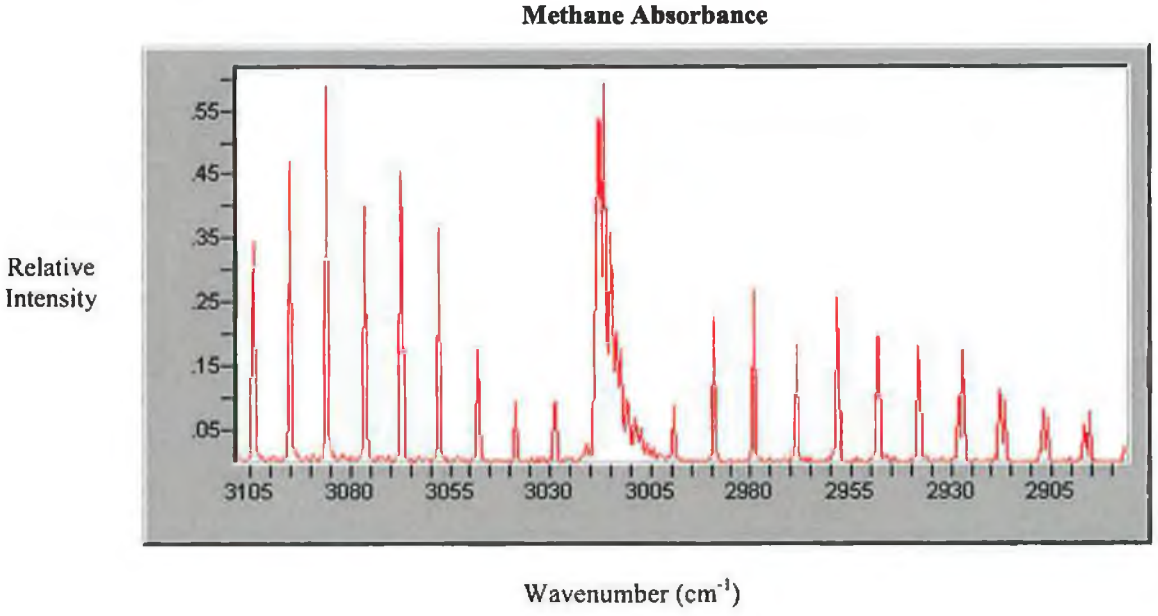

Propane Absorbance

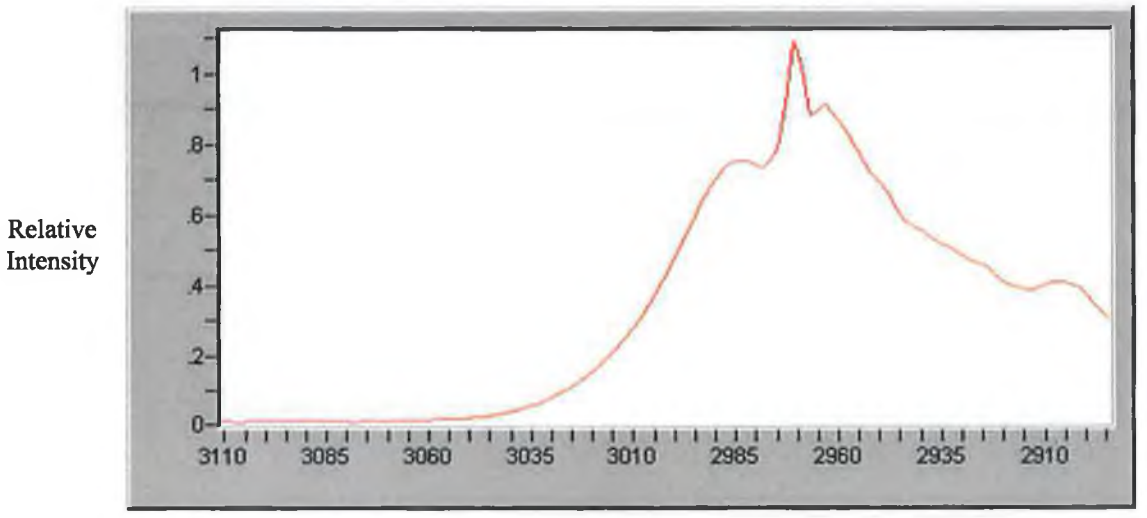

Ethane Absorbance

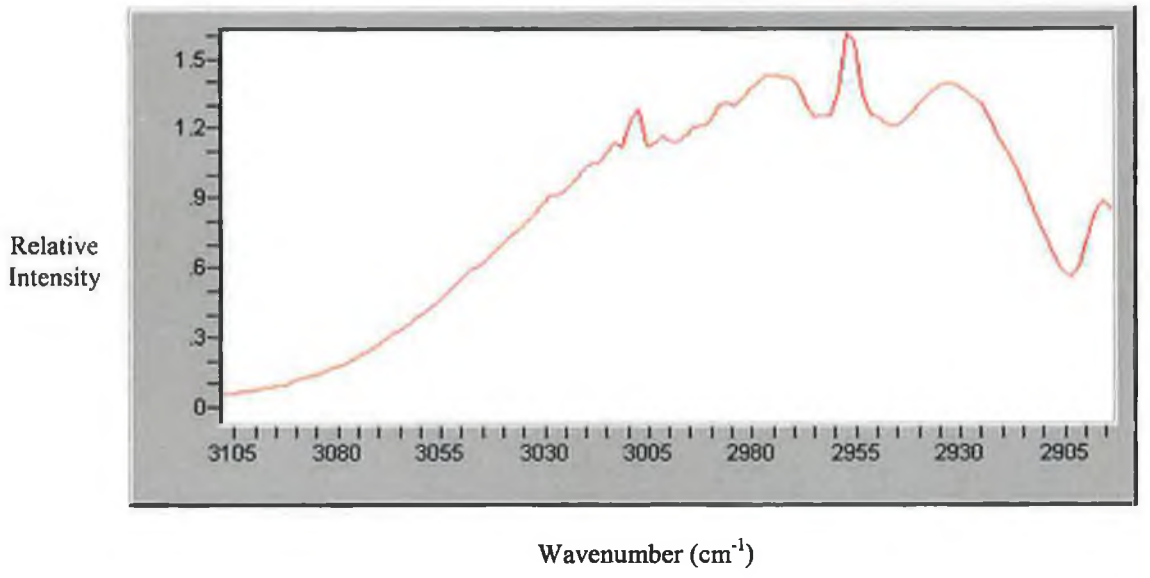

The optical filter fitted on the hydrocarbon pyroelectric has a passband of 3.0 to 3.5 micron. This is optimally chosen to detect the hydrocarbon gases that absorb in this region.

3.3 Beer-Lambert Law

Light incident upon a macroscopic system can be reflected, transmitted, refracted, scattered or absorbed. The fraction of incident light absorbed depends on the thickness of the medium that is traversed. The law of absorption,

originally stated in 1729 in a memoir by P. Bouguer, was later rediscovered by Lambert. It can be expressed by [Olsen 1975]:

$$-dI = \frac{bdx}{I}$$

Where I is the intensity of the light at a distance x from its entry into the medium, and b is called the absorption coefficient. On integration with the boundary condition $I = I_0$ at $x = 0$, we obtain:

$$I = I_0 e^{-bx}$$

Thus

$$\ln I = \ln \tau = \frac{-bx}{I_0}$$

Where τ is the internal transmittance.
Using decadic logarithms this can also be defined.

$$\log \frac{I}{I_0} = \log \tau = -ax$$

Where 'a' is the absorption coefficient.

In 1852, Beer showed, that for many solutions of absorbing compounds in practically transparent solvents, that the coefficient a is proportional to the concentration of solute c. Thus the Beer-Lambert law is:

$$\log \frac{I}{I_0} = -\varepsilon cx$$

Where c is the molar concentration and ε is called the molar absorption coefficient. The molar absorption coefficient is defined as the absorbance of a 1M solution in a 1cm cell. Absorbance is thus seen to be directly proportional

both to the concentration of the absorbing species and to the thickness of the absorbing medium. This however is only obeyed strictly for monochromatic light [Allen 1968].

According to the Beer-Lambert law, absorbance is linearly related to the concentration of the absorbing species, c, and the path length, b, of the radiation in the absorbing medium. That is:

$$A = \log(P_o/P) = abc$$

Where a is a proportionality constant called the absorptivity

All of the above is however only obeyed for strictly monochromatic light. In practice it is not only monochromatic radiation which is measured but all the radiation in a definite frequency interval ("spectral bandwidth") isolated by the application of a monochromator or filter. In the case of the pyroelectric used in this project a filter is utilised to create a frequency passband which is specifically tuned for the target gas. Therefore some wavelengths within the passband may not be absorbed. This are referred to as non-absorbing wavelengths and they have two main sources.

- Spectra where there are non absorbing wavelengths interspersed with absorbing wavelengths (eg: carbon dioxide or methane)
- Where the passband of the optical filter is wider than the absorption peak of the target molecule. This allows non-absorbing wavelengths, each side of the absorption peak, to contribute to the overall signal.

Rearranging the intensity law described above leaves:

$$\mathbf{I = I_0 e^{-\epsilon cl}}$$

Taking into consideration the effect of the non-absorbing wavelengths modifies the intensity law to the form:

$$\mathbf{I = I_0 * ((1-S) * e^{-\epsilon cl} + S)}$$

Where S is the contribution to the signal intensity caused by the effect of the non-absorbing wavelengths. The (1 – S) factor constitutes the range of the absorbing wavelength contribution. This (1 – S) factor now constitutes a span level. This span control can be tuned to detect for a range of concentration levels. By increasing the span figure it, in a sense, it has the effect that there is more absorbance occurring then there physically is. In other words the absorbance of infrared radiation by the target gas can be attenuated or amplified to achieve the desired gas concentration in the presence of the target gas. These span factors are calculated by inserting various span figures into the intensity law until the desired output from the equation is achieved. For the carbon dioxide instrument, which is set up to detect a range of 0 – 5%, it is 0.2, and for the hydrocarbon infrared detector, which is set up to detect a range of 0 – 100% LEL, it is 0.386.

The exponential factor is also modified by a power factor. Since the passband used in the detector observes a range of wavelengths there is a summation of the product $-\epsilon cl$. This product in inseparable for each individual wavelength. The exponent of the summation is converted into a usable form via the relationship:

$$\exp\left(-\sum [\epsilon cl]\right) = \exp\left(-\alpha x^{\beta}\right)$$

β is a spectrum related constant specific to the target gas.

3.3.1 Determining the gas concentration

The above discussion leads to the following modification to the intensity law:

$$I = I_0 * ((1-S) * \exp(-\alpha x^{\beta}) + S)$$

So in order to use this relationship the individual components are defined as follows:

I = Intensity of the detector signal. This is the peak to peak value of the detector output which is modified by the presence of the target gas.

I_o = Intensity of the detector signal in absence of the target gas. This can be determined from the peak to peak value of the reference output *Ir* and the peak to peak value of both the detector and reference outputs in the absence of target gas. This should be continuously monitored using the correlation $I_o = I_r * (I / I_r)_0$ where $(I / I_r)_0$ is the ratio of detector output to reference output in the absence of target gas and can be denoted by the symbol Z, which constitutes a zero level.

S = Non absorbing wavelength contribution to the signal. The range of the absorbing contribution is defined by (1 – S) which constitutes a span level.

x = Target gas concentration in units defined by the units of α.

α = Exponential constants that also defines the units of the target concentration.

β = Power constant dependent on the spectrum of the target gas.

Therefore in terms of terms of the signals from the detector, I and I_r (in a dual pyroelectric detector system, with an active detector and a reference detector), this results in the relationship:

$$(I / (Z * I_r) . S) / (1- S) = \exp(-\alpha x^{\beta})$$

The gas concentration can now be found by the rearrangement of the above formula:

$$x = (-\ln \{ (I / (Z * I_r) . S) / (a * (1 - S)) \})^{1/\beta}$$

Where x is the gas concentration, Z is the zero factor equal to (I / I_r), S is the span factor equal to the asymptote of the ratio change with increasing gas concentration, a is a constant and β is a constant.

The intensity law can be rearranged to produce the equivalent relationship in terms of absorbance, where absorbance is defined as $(1 – I / (Z*I_r))$:

$$(1 – I / (Z*I_r)) = (1 – S) (1 - * \exp(-\alpha x^{\beta}))$$

The gas concentration, x, can therefore be found from the rearrangement:

$$x = (-\ln \{ (1 - (1 - I / (Z^{*} I_r)) / (1 - S) \} / \alpha)^{1/\beta}$$

In this case the span is equal to (1 – S) and all other factors and constants are as described above [Stroud 1993].

3.4 Deviations from the Beer-Lambert Law

The linear relationship between absorbance and pathlength at a fixed concentration is a generalization for which there are few if any exceptions. On the other hand, deviations from the direct proportionality between absorbance and concentration (when the pathlength is constant) are frequently observed. Some of these deviations are fundamental and represent a real limitation to the law. Other occur as a consequence of the manner in which the absorbance measurements are made (instrumental deviations) or as a result of chemical changes associated with concentration changes (chemical deviations) [Shriver 1999].

3.4.1 Real limitations to the Beer-Lambert law

The Beer-Lambert law is successful in describing the absorption behaviour of dilute solutions only and in this sense it is a limiting law. At high concentrations the average distances between ions or molecules of the absorbing species are diminished to the point where that each particle affects the charge distribution of its neighbours. This interaction can alter their ability to absorb a given wavelength of radiation. Because the extent of interaction depends on concentration, the occurrence of this phenomenon causes deviations from the linear relationship between absorbance and concentration. In general the Beer-Lambert law is used for detecting concentration below 10^{-2} M. The two infrared detectors designed through the course of this project detected low concentrations, 5% CO_2 and 100% LEL CH_4. When the two detectors are exposed to over 70% and 10% by volume respectively the response of the

detector becomes noticeably flatter, as a result of the reasons outlined previously.

3.4.2 Instrumental limitations

Indeterminate instrumental variations which cause apparent deviations include

- Stray radiations reaching the detector (reflected within the instrument)
- Sensitivity changes in the detector
- Power fluctuations of the radiations source and detector amplification system
- Instrumental deviations which occur from the use of polychromatic radiation

The dual pyroelectric detector used in this project eliminates the occurrence, to an acceptable level, of the second and the third deviation cause. The problem of stray radiation is a more unavoidable instrumental cause of deviation.

As mentioned previously the Beer-Lambert only stays true to absorbance measurement with monochromatic radiation. Truly monochromatic sources, such as lasers, are not practical for routine analytical measurements due to the high costs associated with producing such sources. In most cases a polychromatic continuous source is employed in conjunction with a filter that isolates a band of wavelengths around the particular wavelength of interest. Unless the molar absorptivity is invariant within the wavelength band used, the absorbance measured is an "average" absorbance over the band. Due to the logarithmic nature of absorbance, this is not a true average. The greater the slope of the absorption curve through the wavelength band, the greater the deviation.

Figure 3.8 demonstrate that the shape of the calibration curve often depends on the bandwidth.

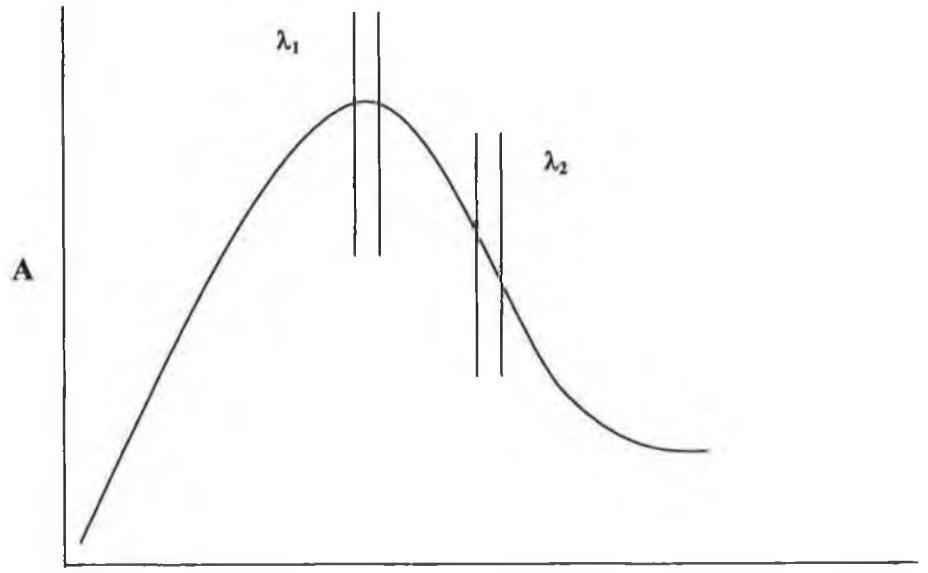

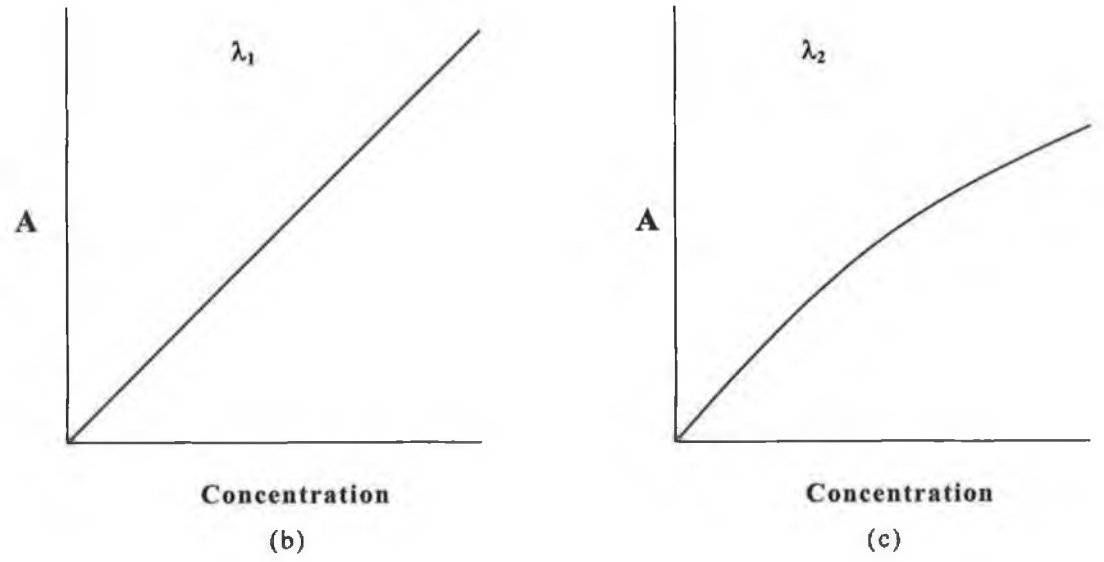

Figure 3.8 Effects of finite bandwidth [Hart 1995]

Two filters with wavelength ranges of equal width are designated λ_1 and λ_2. The best wavelength for quantitative analysis is λ_1, for two reasons. First, at the absorption maximum the change in absorbance with concentration is at a maximum, this yields greater sensitivity and higher accuracy. Secondly, within this band the molar absorptivity is relatively constant and a linear calibration curve is obtained as shown in figure 3.8 (b). However if a wavelength is selected on the side of an absorption peak, e.g. λ_2 in figure 3.8a), the molar absorptivity varies across the band. At this wavelength the system does not follow the Beer-Lambert law and a curved calibration plot is obtained, as in figure 3.8 (c). Narrow band widths are hence desirable for best accuracy, but as the band is decreased less energy reaches the detector. Consequently there is always a trade off between accuracy, sensitivity and detector requirements. In the case of the filter used in the pyroelectric for the infrared gas detector a broad pass band was deployed for the S500-IR hydrocarbon instrument. A filter of centre frequency 3.3μM with 200nM each side of this centre frequency was used for the active pyroelectric. For the reference pyroelectric a filter of centre frequency 3.95μM with 90nM each side was used to create the band-pass. This was because a variety of hydrocarbon gases were required to be detected. In the case of the IR80 CO_2 detector a filter with a much tighter pass band was used on the active pyroelectric. 4.24μM centre frequency with 140nM pass band in total, 70nM each side. The same reference filter as the S500-IR was used.

These deviations are overcome in the infrared gas detector through the use of the linearization constants in the modified Beer-Lambert equation, which is used in calculating the gas concentration. The span constant in the formula can be tweaked to give the desired concentration. Also the power constant takes into account the range of wavelengths that the passband on the pyroelectric detector incorporates. If the target gas has a spectrum whose continuum completely envelopes the optical bandwidth of the sensor (3.1 - 3.5 microns) then the power term would be equal to unity. In reality however the spectrum of most gases is made up of absorbing wavelengths and non-absorbing wavelengths as explained previously. The mean value of the molar absorptivity multiplied by the pathlength, (el), is adjusted by the power of this constant.

3.5 Pyroelectric Detector Characteristics

The Pyroelectric Effect

A pyroelectric detector contains a noncentrosymmetrical crystal, which below its curie temperature, exhibits an internal electric field (or polarization) along the polar axis. This electric field results from the alignment of electric dipole moments. Heat resulting from radiation absorption produces thermal alteration of the crystal lattice spacing, which in turn changes the value of the electric polarization. The surface of the crystal normal to the polarization axis then develops a polarization charge. If electrodes are applied to these surfaces (one of the electrodes must be infrared-transparent) and connected through an external circuit, free charge will be brought to the electrodes to balance the polarization charge, thus generating a current in the external circuit. The detector comprises of a thin plate of pyroelectric material between two electrodes, forming a capacitor. The high impedance is reduced, by mounting the subassembly in an enclosure that contains a field effect transistor connected as a simple source follower and a matched load resistor [Cima 1993].

When the change in temperature ΔT is uniform throughout the pyroelectric material in question the pyroelectric effect can be described by means of the pyroelectric coefficient, which is a vector **p** with the equation

$$\Delta \mathbf{P} = \mathbf{p}\Delta T$$

where **P** is the spontaneous polarization.

For the purposes of the infrared gas detector project this effect is used to detect changes in incident radiation. When the detector absorbs radiation its temperature and hence its polarization changes resulting in a surface charge on the capacitor plates.

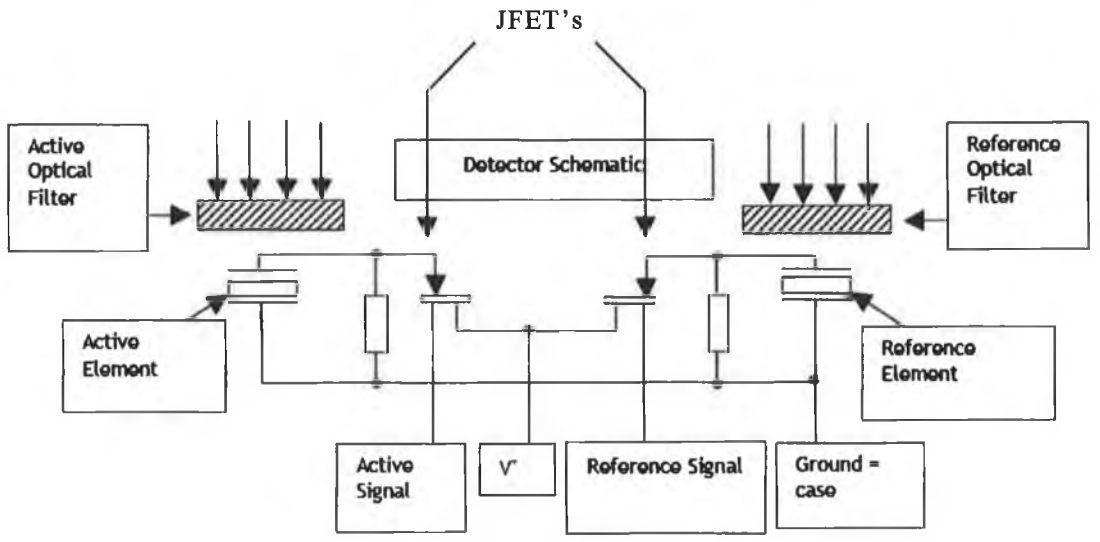

Figure 3.9 Pyroelectric detector

If A_d is the area of incident radiation and the detector thickness *b* is small enough so that the temperature gradient in it is negligible, then the charge induced will be

$$\Delta Q = A_d \Delta P$$
$$= pA_d \Delta T$$

where ΔT is the increment in temperature of the detector. The resulting voltage on the capacitor will be

$$v_o = R_v P_i$$

P_i is the power the incident radiation when it is pulsating.
R_v is the responsivity or voltage sensitivity that is given by:

$$R_v = \frac{\alpha p}{C_E \varepsilon A} \quad \frac{\tau}{v1 + (\omega\tau)^2}$$

α = the fraction incident power converted into heat

p = the pyroelectric coefficient for the material

τ = the thermal time constant

C_E = the volumetric specific heat capacity

ε = the dielectric constant

ω = the pulsating frequency for the incident radiation

As with other radiation detectors, pyroelectric sensors are also sensitive to thermal noise. Thermal noise comes from the random motion of free electrons within the pyroelectric sensors itself. The energy for this electron motion comes from the thermal energy of the surrounding air. The noise equivalent power (NEP) is the equivalent input power yielding an output response that in a given bandwidth equals that of thermal fluctuations in the detector. The detectivity is D = 1/NEP. This NEP depends on wavelength, operating frequency, temperature and noise bandwidth. For an ideal detector with area A_d cm^2, at ambient temperature the NEP is about $5.5 * 10^{-11}$ v A_d (W/vHz). The D^* (D-star) parameter normalizes the NEP to a given constant area.

$$D^* = \frac{v\ A_d}{NEP}$$

Where thermal noise becomes an issue is when the ambient temperature surrounding the pyroelectric rises. Temperature compensation techniques are required to negate such effects and these compensation techniques are discussed in detail in chapter 4 (4.4.6 Temperature Compensation). The other factors previously mentioned which affect the NEP are negligible with regard to integration into the infrared gas detector [Liu 1978].

Figure 3.7 illustrates the expected output of the pyroelectric detector when exposed to incident radiation.

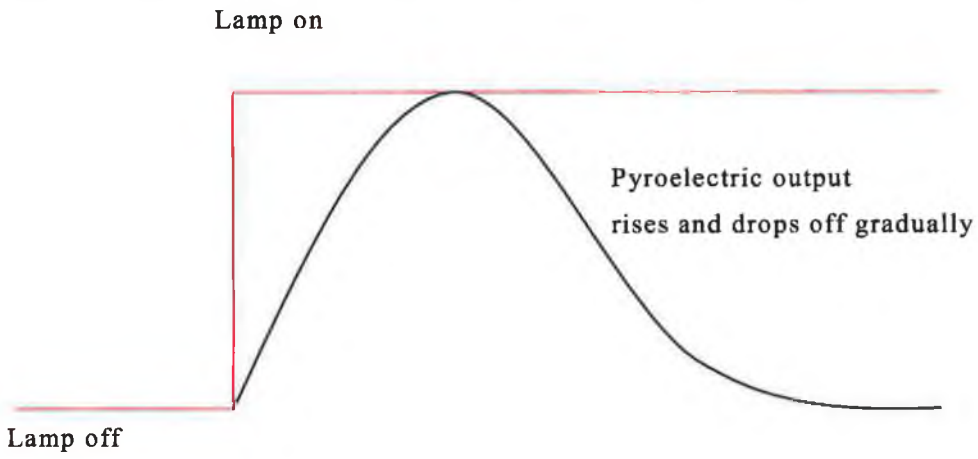

Figure 3.10 Pyroelectric output when exposed to incident radiation.

A pyroelectric detector responds to a change in incident radiation, which induces a change in temperature. If the pyroelectric is subjected to a single pulse of incident radiation the output reaches a maximum and then decays off at a rate determined by the thermal and electrical time constants of the detector. When the incident radiation is subsequently removed the signal follows the same characteristics but in the negative direction. This reverse in polarity of the signal is a result of the cooling of the pyroelectric surface during the dark phase. As it cools the charge on the pyroelectric element becomes negative. In order to obtain a usable signal, i.e. sinusoid signal, from the pyroelectric the incident radiation needs to be pulsed on/off. The frequency of the pulsating radiation and the output signals obtained are described in chapter 4 (4.4.3 Infrared Lamp Driving).

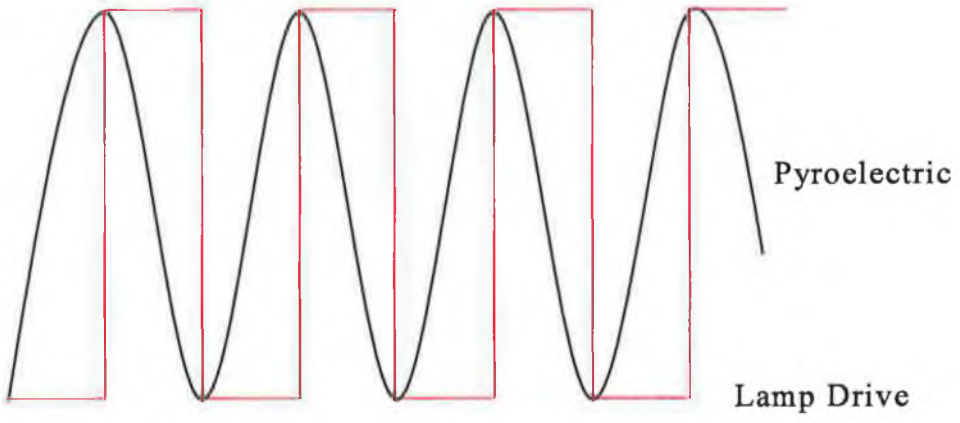

Figure 3.11 Pyroelectric output with pulsating incident radiation

Pyroelectric materials include triglycine sulpate (TGS), deuterated triglycine sulphate (DTGS), $LiTaO_3$, $LiNbO_3$ and some polymers. Generally TGS and DTGS show superior features but have limited use because of their hydroscopic nature and low Curie points (approximately 49°C). For ease in handling and higher Curie points $LiTaO_3$ or $LiNbO_3$ is frequently used. With a 100MΩ load resistor the response time is 1msec and responsivity (ratio of detector output to incident radiation) is about 100. Unlike other thermal detectors, the pyroelectric effect depends on the rate of change of the detector temperature rather than on the detector itself. This allows the pyroelectric detector to operate with a much faster response time than other detectors would allow. Its also means that this type of detector responds only to changing radiation that is chopped, pulsed or otherwise modulated. So this means that it ignores steady background radiation.

3.6 Advantages of Infrared Gas Monitoring

The main advantages of infrared gas monitoring are listed below:

- Technique is highly selective for the target gas, no fear of interference from other gases.
- NDIR detectors do not suffer from any known poisoning effects, not damaged by silicones, lead compounds, etc
- Ability to operate in the absence of oxygen or in enriched oxygen, unlike catalytic based detectors.
- Ability to operate in continuous presence of gas, unlike electrochemical methods.

Chapter 4

Implementation

4.1 Introduction

Chapter 3 provided a look at the history of the Non-dispersive infrared technique for monitoring gas. A review of the chemistry involved was provided to give an insight into the specifics of the Beer-Lambert equation. In chapter 2 we discussed the various technologies used in gas detection. This chapter identifies the functional and non-functional requirements of the project. These requirements are proposed improvements on the existing infrared gas sensing technology currently available. The technologies used in the development of the system will be discussed. Then the design of the instrument will be detailed covering both mechanical, hardware and software aspects. Finally a summary about the implemetation of the detector will be presented.

4.2 Requirements

The requirements of the infrared gas monitor can be broken up into two sections: functional and non-functional requirements. The functional requirements outline the characteristics and behaviour of the proposed system. The non-functional requirements are constraints that need to be imposed on the project. These constraints will be imposed for a number of reasons. The main ones being: compatibility with existing Monicon Technology products currently in the field, budgetary considerations for the overall project, industry standards that must be adhered to, customer feedback relating to the overall operation of the instrument and also the rules imposed by national standards in the certification requirements of gas detection instruments.

Given the nature of the project the infrared unit must supply an industry standard 4-20mA analogue output and have alarm relays rated for mains operation. In addition the instrument must have full serial communication capability. Various protocols have being investigated to isolate the most suitable one for this project, and are detailed towards the end of the chapter.
The peak to peak calculation of the sine wave outputs from the pyroelectric detectors needs to be highly reliable and accurate. One interactive way is to phase lock the time that the analogue to digital converter (ADC) readings are taken to the high and low points of the sine wave. Another solution to the problem may be to time slice the sine wave into a number of slices, which could be used to accurately monitor the waves and detect anomalies and spurious spikes with a view to negating such effects.

In order for the instrument to be reliable and accurate it must not deviate too much from the ideal linear response. Each gas has unique deviations in linearity. Hence software techniques must be implemented to compensate for such deviations. Manipulation of the Beer-Lambert law will probably be the optimum solution to the linearity problem in conjunction with careful and precise design of the optical cavity. The optical cavity houses the pyroelectric detector and the infrared lamp source The infrared lamp source is a thin walled tungsten halogen source.

Temperature effects on the sensor can cause undesirable effects and it is a requirement of this project to provide temperature monitoring of the pyroelectric and associated components of the sensor, and to compensate for any changes in signal integrity. This is especially important as the instrument will be certified EExd IIC T6, and it must operate as normal in a temperature range of -20°C to +50°C.

Zero drift is an inherent problem in some commercial gas detection monitors. The problem, which will never be totally eliminated, will however need to be addressed and looked into.

4.2.1 Functional Requirements

The proposed infrared gas monitoring instrument should meet the following requirements:

- The infrared gas monitor should be a fully functioning commercially viable gas detector. It must contain two mains rated alarm relays, a 4-20mA analogue output, a user configurable menu and full serial communications capability.
- The sensor head must include a thermistor at the pyroelectric detector for the monitoring of temperature transients. Temperature compensation must be incorporated in the firmware.
- The instrument must maintain full compatibility with existing Monicon Technology gas detectors currently in the field and in production.
- A linear response, with minimal deviations from the ideal response, right through to full scale is an essential requirement for the instrument.
- False alarms as a result of noise or spurious response patterns must be eliminated.
- The instrument must provide full diagnostics for the following conditions. Sensor failure, thermistor failure, low supply voltage, EEPROM write or read failure, excessively negative zero drift and a gas concentration over range situation.
- Peak to peak calculation of the pyroelectric output wave signal must be extremely accurate and reliable.

- The instrument should have a relatively quick T90 (length of time the detector takes to detect 90% of the target gas concentration). T90 of less than 30 seconds must be achieved.
- An 8-digit alphanumeric LED dot matrix display must be used to display instrument status, menu: etc.
- The electronics are required to be housed in a rugged yet aesthetically pleasing enclosure that is IP65 rated.

4.2.2 Non Functional Requirements

In addition to the functional requirements, there are several non-functional requirements that must be adhered to. These are as follows:

- The instrument should run on a 18-30V dc supply. Reverse polarity protection should be included.
- The target firmware must be written in C and developed using the IAR compiler/linker.
- The microcontroller used in the system should be an 8-bit flash microcontroller.
- The infrared gas detector should be relatively low cost and comparable with competitor's infrared detectors on the market.
- Design for manufacture should be a key constituent in the design process.
- The instrument should be protected from any RF interference and should comply with the standard EN 50082-1: 1992.
- The firmware should be initially developed using the Ashling C51 emulator.
- The target gas used in the development of the detector must be mixed using Mass Flow Controllers (MFC's). They must have a divide ratio of 100:1 when mixed with the diluent.

4.3 Technologies

The overall architecture for the infrared gas detector is given in figure 4.1 and a description of each module is provided below. The technologies used to design and develop the instrument are also given.

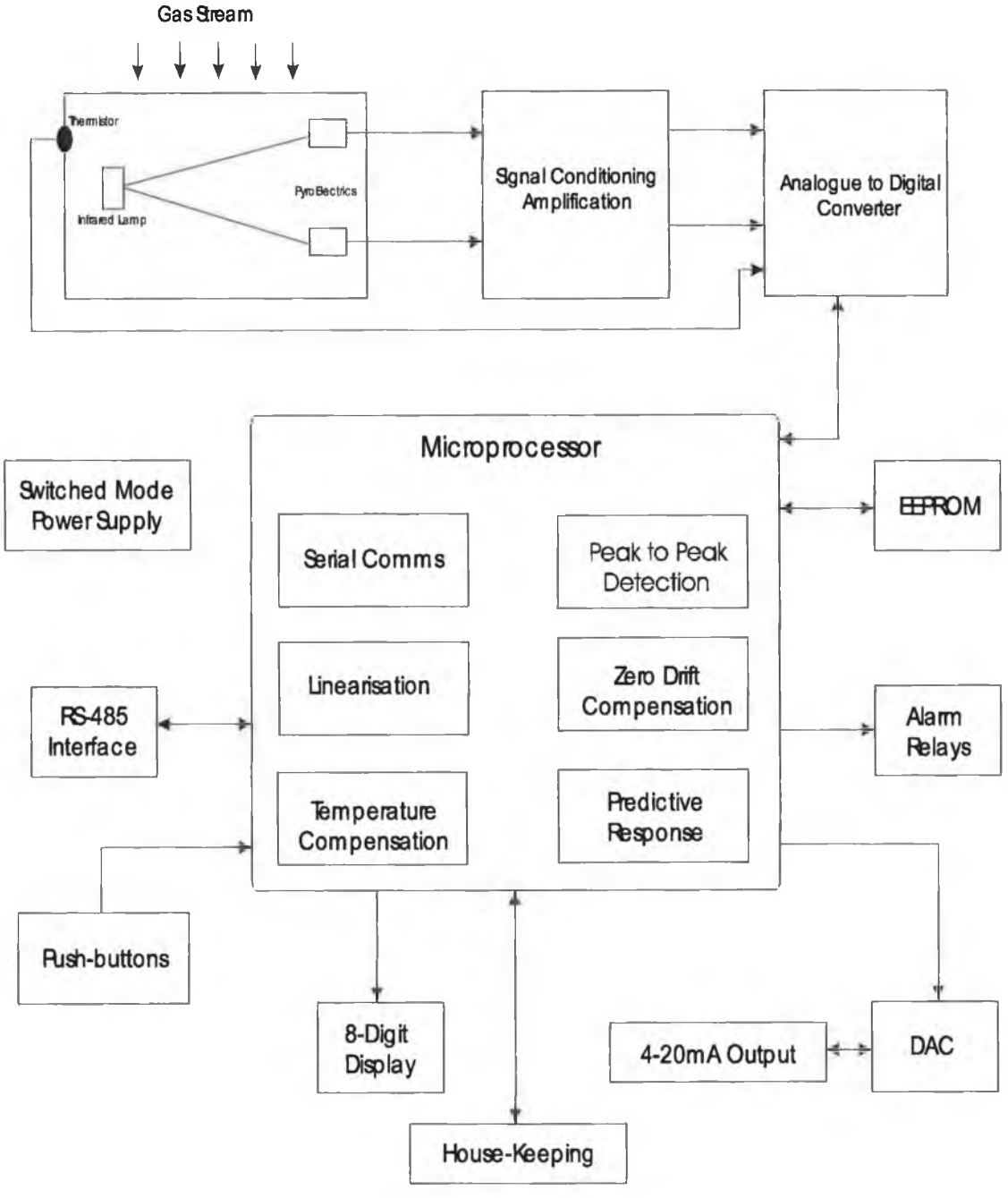

Figure 4.1 Infrared detector system architecture

The optical cavity used to collect the gas sample will need to precisely designed and engineered. This cavity will house the infrared light source, the reference and active pyroelectric detector and the thermistor used for temperature monitoring. The infrared light source is controlled through an interrupt driven square wave from the processor and its frequency needs to be extremely stable and consistent to achieve good signal stability and integrity. Signal conditioning and amplification is applied to the low level signals (mV) from the pyroelectrics. The analogue to digital converter (ADC) digitises the analogue signals bringing them into the microcontroller for analysis and processing. An EEPROM is included to save user set variables to non-volatile RAM, e.g.: alarm set points, alarm latch/non-latch, serial communication unit address etc. Two switched mode power supplies (SMPS) are required, one to provide 12V drive to the relays, op-amp gain circuitry and 4-20mA analogue output circuitry. The other SMPS provides a 5V output to drive all the CMOS digital ICs. The 4-20mA analogue output is controlled by the digital to analogue converter which receives its commands from the microcontroller. The 4-20mA output signal has a load capability of 500 ohms. An 8-digit dot matrix LED alphanumeric display is used to display the instrument current status. The instrument has 4 pushbutton switches. They are named CAL, SET, ACCEPT and RESET. On power up the instrument goes into normal operational mode. Pressing CAL will put the unit into calibration mode. In this mode the menu can be scrolled through by repeatedly pressing the SET button. Fig 4.2 shows the layout of the software menu.

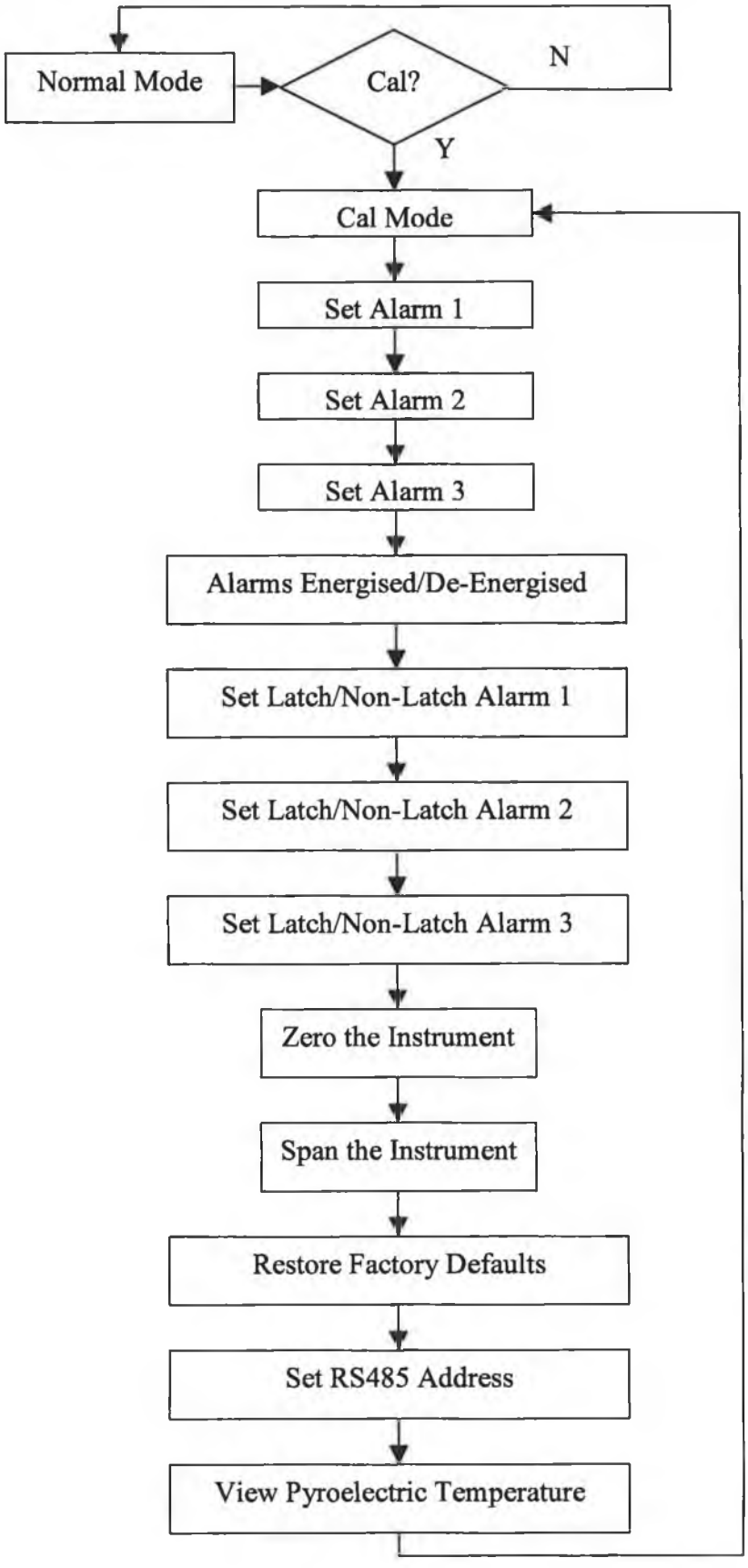

Figure 4.2 Menu Layout

Alarm 3 is a software alarm. There is no physical relay available for the alarm. This was included for a possible future extension to the firmware, in which the level of alarm 3 could be monitored over the serial port. The ACCEPT and RESET pushbuttons each have a dual function. When the instrument is in normal operational mode the RESET switch resets a latched alarm, when the gas concentration has dropped below the alarm setting. A little bit of hystersis is added to the alarm setting so it actually comes out of alarm when it drops below the alarm setting minus 5% of the full scale. In normal mode the ACCEPT button accepts an alarm condition and can be used to switch in annuciators, beacons, etc that may be attached to the open collector output. When the instrument is in calibration mode the function of the ACCEPT and RESET switches is to adjust the user configurable settings in the menu, alarm set points etc. When in calibration mode pressing the CAL switch again will save the adjust variables to non-volatile RAM (EEPROM) displaying a message on the display as it does so.

All embedded systems use either a microprocessor or microcontroller for the computation and transfer of data between devices. A microcontroller is a chip with a microprocessor and a set of peripherals such as serial ports, timers, RAM and ROM. Since most embedded systems usually require the device to be as compact and cheap as possible, a microcontroller is the logical choice. The microcontroller used for the infrared gas monitor is the Atmel AT89C51RD2. The AT89C51RD2 is a high performance 8-bit microcontroller. Its main on-board peripherals include a clock doubling facility, up to 2048 bytes of RAM, internal watchdog timer, serial communication port and multiple timers [Atmel 1999].

The IAR tool chain provides compilers, assembler, librarian and linker for a wide range of processors. For the infrared gas monitor the IAR Embedded Workbench for 8051 will be used. Used in conjunction with this is the IAR C-SPY high level language debugger and also the Ashling C51 emulator.
The firmware is broken down into seven distinctive units integral to the instrument. The serial communication module deals with interrogations from a master unit. The module is set up as an interrupt driven process in which the

code vectors to a serial port handler when it detects data on the serial port. However the square wave drive to the infrared lamp source is set up as a timer interrupt process. Hence the serial port handler is given a lower priority then the timer interrupt process. The reason being that the accuracy of the drive frequency to the infrared lamp is crucial to ensure the pyroelectric output is stable and of good integrity. The linearization section takes care of the non-linear problems that are associated with the gas fractional absorbance. An ideal response, or as close as, is desired here and techniques into achieving these results is presented in chapter 3. Temperature compensation is also addressed with the aid of the thermistor located in the optical cavity. The thermistor will be fed into an ADC and a temperature calculated from the reading. Fast falling temperature increases or decreases as well as slow gradual changes can have serious effects on the pyroelectric and software as well as hardware techniques will be deployed to negate the effects of such phenomena. The peak to peak detection will include a rolling 16-way buffer with advanced true peak detection firmware. Through the use of this rolling buffer signal spikes and transients can be observed and analysed to determine their true nature and hence discarded if they prove to be spurious noise. Zero drift and full span drift compensation will make up another of the software modules. The analysis of lamp intensity and the condition of the optics will be factored in when compensating these drift characteristics. Source ageing is also a factor in zero drift and this phenomena will be investigated. Successful implementation of this module will result in a far more stable and accurate instrument and also will increase the time between re-calibration by the service engineer. Predictive response will be addressed with the aim of providing a fast T90. A high level gas response will be extrapolated by monitoring low level response rates and patterns. DSP (digital signal processing) algorithms will be used in this analysis. Finally the normal house keeping duties of the microprocessor make up the final software module. Duties such as the watchdog timer, menu facility, instrument error detection and 4-20mA analogue output all take place in the background.

4.4 Design of the Solution

The design of the solution can be broken up into two parts: hardware and software. These are discussed in the following sections.

4.4.1 Hardware

Through prototyping the solutions using different technologies the hardware specification for the infrared gas monitor was finalized as follows:

- Atmel AT89C51RD2 microprocessor
- 1Kbit EEPROM
- 12-bit Analogue to Digital converter
- 2 * SPST Relays rated @ 240V AC 3A
- 4-20mA current output
- Microprocessor monitor (brown-out detection)
- 2 * switched mode power supplies (buck regulator type)
- High precision op-amp amplifier circuitry
- 8-digit alphanumeric LCD display

After the design was finalized a Printed Circuit Board (PCB) was required. A software package called Power Logic was used to draft out the circuit diagram and this was then exported into another software package called Power PCB to layout and route the board. Both packages are by Mentor Graphics. For initial prototyping and verification of the completed layout a prototype board was created using a micro-milling machine, which milled and drilled out the design. Input information gathered from the gerber files of the layout files was used to achieve this and the machine used was the LPKF Protomat C30. Careful layout of the board was essential for proper operation. The high frequency tracks of the switched mode power supplies needed to be routed as short as possible in order to minimise the pickup of noise. Care also needed to be taken to route the high voltage tracks from the relay contacts at an appropriate distance from neighbouring tracks. As well as the main CPU printed circuit board a small board was required to accommodate the pyroelectric detectors and the infrared lamp. This board consisted of three low pass (resistor, inductor) filters and an 8-

way 2mm pitch ribbon cable to transfer the signals and power to and from the board. The idea of the low pass filters was to eliminate any radio frequency interference (RFI) interfering with the pyroelectric sine wave output, keeping in mind that the output is a low level signal, approximately 6-7mV. Values of 1uF and 47mH were picked to give a cut off frequency of about 734Hz, enough to let the 3.1Hz pyroelectric outputs through but block higher frequencies that could be detrimental to the signals. When the two boards were fully prototyped they were built, populated with all the components and electrically tested by Monicon Technology's in house manufacturing facility.

4.4.2 Optical Cavity Design

The design of the optical cavity to house the pyroelectric detectors and the infrared lamp source was imperative to the success of the project. In order to achieve quality output signals of good integrity careful engineering of the cavity was required. In order to keep in compliance and have compatibility with Monicon's existing accessories the optical cavity was going to be located inside a cylindrical shaped enclosure made from stainless steel 303. The diameter of the enclosure is 42mm. A CAD drawing of the enclosure can be observed in the appendix.

From the outset one of the most critical components of the cavity's design was the path length. As discussed in chapter 3 the longer the path length through which the target gas has to travel, the more infrared radiation that will be absorbed by the target gas. The more infrared that is absorbed by the target gas results in a greater reduction in the output signal. This is due to the lower amount of light reaching the pyroelectric detector.

The optical cavity hence needed to have the longest path length achievable within the confines of the sensor body enclosure. Prototyping of the cavity was carried out in Monicon Technology. The availability of a CNC vertical mill and a CNC lathe aided this process tremendously. Initially the cavity was made from aluminium. The reflective surface of the aluminium provided an excellent medium in which the infrared light could travel. Also the aluminium did not absorb or "soak" any of the light, which in turn fully illuminated the chamber providing a high intensity of light to the pyroelectric detector. The formation of

condensation droplets in the interior of the optical cavity was avoided by the heating effect of the filament light source. The formation of droplets on the interior of the cavity will produce a lensing effect which will alter the pathlength of the cavity. The cavity was always approximately 10 degrees celsius higher then the ambient temperature due to this effect. Extensive temperature cycling tests with simulated humidity conditions were carried out to validate this, and the results proved positive. Droplets of moisture forming inside the cavity would be detrimental to the transmission of infrared through the cavity and hence affect the sensors performance. The notion that a heating element, which was adopted in the early design stages, might be needed to prevent condensation was duly dropped and shelved.

However as the aluminium optical cavity was subjected to accelerated ageing techniques, in Monicon Technology's research and development lab, it was found that the aluminium cavity was prone to corrosion and degradation through natural environmental means. The result of which has an adverse affect on the operation of the infrared gas detector. Signal output from the pyroelectric detectors decreased as less intensity of infrared radiation reached the pyroelectrics. This in turn reduced the sensitivity of the instrument. Hence other materials were investigated which would provide a non-corrosive yet highly reflective surface to aid the transmission of the infrared radiation through the cavity. After researching numerous materials including platinum, silver and alloys types, it was decided that the most suitable would be gold. The optical cavity was to be constructed out of polycarbonate material with gold plating on the external walls of the cavity. This gold plating provided excellent properties for the transmission of the infrared radiation through the chamber. Gold's resistance to corrosion made it an ideal candidate for the rugged and punishing environments that the detector may be placed in. The gold plating process was carried out by a third party metallurgy company.

As mentioned earlier the optical cavity was to be located inside a cylindrical shaped enclosure made from stainless steel 303. The diameter of the enclosure is 42mm. The design of the cavity was to take into consideration that the longest possible path length for the infrared transmission was desirable. In the end a

45mm path length was achieved and this proved sufficient for the detection of carbon dioxide and the hydrocarbons to a minimum level of 5% and 100%LEL repectively. As described in chapter 3, it was with the hydrocarbons that the path length really needed the maximum length possible due to the lower absorption characteristics of the hydrocarbon gases. A drawing of the optical cavity can be observed in the attached appendix.

The optical cavity was positioned on top of a PCB which contained the pyroelectrics, infrared lamp source, RC filters for RFI immunity and an 8-way ribbon cable to transfer the signals in and out of the detector. A negative temperature coefficient (NTC) thermistor, whose resistance decreases with increasing temperature, was attached to the pyroelectric detector with the aid of potting compound. This provided accurate temperature sensing at the pyroelectric. The cavity was held in place with two small retaining clips and the whole assembly was fixed in the stainless steel enclosure through the use of Robnor PX314ZG potting compound. This compound has extremely low conductivity and is ideally suited for the potting of electronic components. The whole cavity assembly is designed to be a disposable unit so in the event of a component failure a replacement is issued. It is also worth noting that in order to comply with the rules imposed by national standards in the certification requirements of gas detection instruments the assembly has to be potted to contain potential explosions or sparks within the detector.

4.4.3 Infrared Lamp Driving

The infrared light source is a thin walled tungsten filament lamp that is rated at 5V and 65mA. The mean time between failures (MTBF) of the lamp is approximately 100,000 hours. It was sourced from a third party company called Gilway. The thin wall of the lamp greatly increases the emission of the infrared wavelengths, particularly in the 1-5 micron range which is the range required for the particular gases being detected. In effect the wall absorbs the longer wavelengths. By keeping a residual amount of current in the filament during the off cycle the life of the lamp was increased. This technique reduced the inrush current at the start of the on cycle and was achieved by placing a 150 ohm resistor from the output of the transistor drive to ground. This maintained the

small residual current required. Another way to increase the life of the lamp is to apply less than 5V during the on cycle. Doing this however results in less intensity of infrared reaching the pyroelectrics that subsequently resulted in a diminished output AC sinusoid. Due to the reduced path length available it was decided to drive at max voltage to achieve as much signal as possible out of the sensor. Another intuitive technique to drive the lamp source on/off would be to connect a linear voltage regulator to the lamp and switch the regulator on and off by means of a shutdown pin located on the chip. This could be controlled from a port pin on the microcontroller. However the transistor technique was favoured over the regulator idea in order to keep the chip count and hence the board costs down. Shown below in figure 4.3 is the transistor circuit used for driving the lamp source. As explained earlier the 150Ω resistor is added to allow some residual current to remain in the lamp

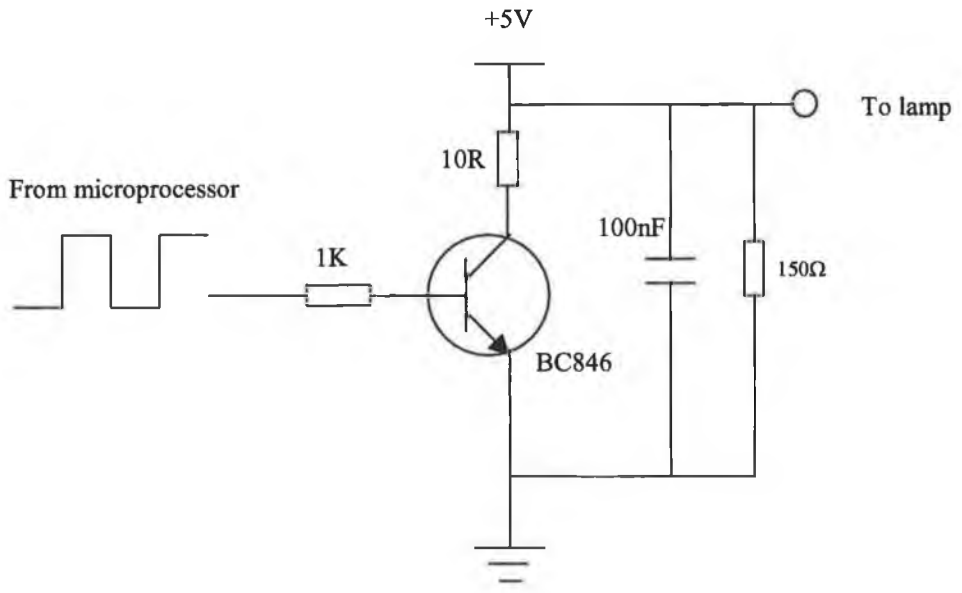

Figure 4.3 Lamp drive circuit

As explained in section 3.5 pyroelectric detectors only respond to a change in incident radiation. This is the fundamental reason why there is a need to pulse the lamp on and off, to provide both light and dark states. The following section details the characteristics of the pyroelectric signal versus the frequency of incident infrared radiation reaching the surface of the detector. If the

pyroelectric is subjected to a single pulse of incident radiation (lamp switched from 0V to 5V) the output reaches a maximum and then decays off at a rate determined by the thermal and electrical time constants of the detector. When the incident radiation is subsequently removed the signal follows the same characteristics but in the negative direction. This reverse in polarity of the signal is a result of the cooling of the pyroelectric surface during the dark phase. As it cools the charge on the pyroelectric element becomes negative. Figure 4.4 shows the expected signal output in such a situation.

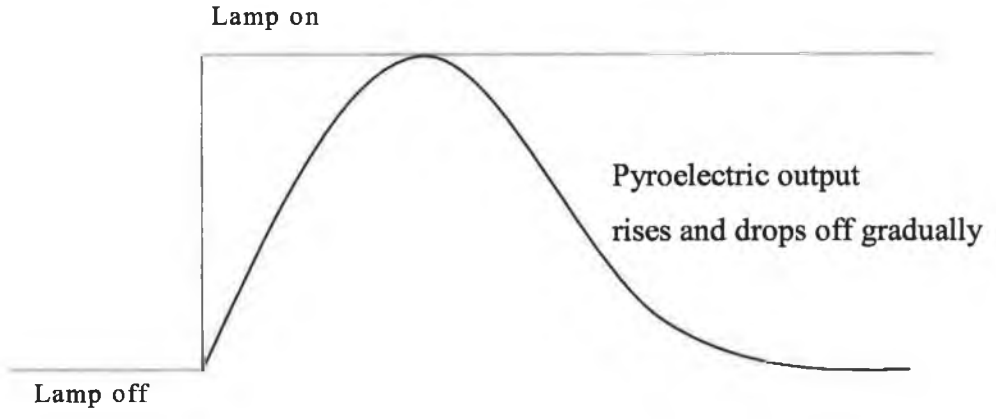

Figure 4.4 Single incident radiation pulse output

In the next situation the on/off cycle to the lamp is continuous. If the frequency of the source is of a slow rate of change, say less than 2Hz, then as before the signal reaches a maximum value during the on value. However the signal becomes distorted and begins to fold over as heat at the pyroelectric element starts to leak into the actual housing element enclosing the detector. This reduces the net temperature drop across the element that causes the aforementioned distortion. During the off cycle the process causes a similar signal in the negative direction. As can been seen from figure 4.5 the peak to peak intensity is lower than that achieved with a single pulse of radiation since a repetitive cycle is maintained.

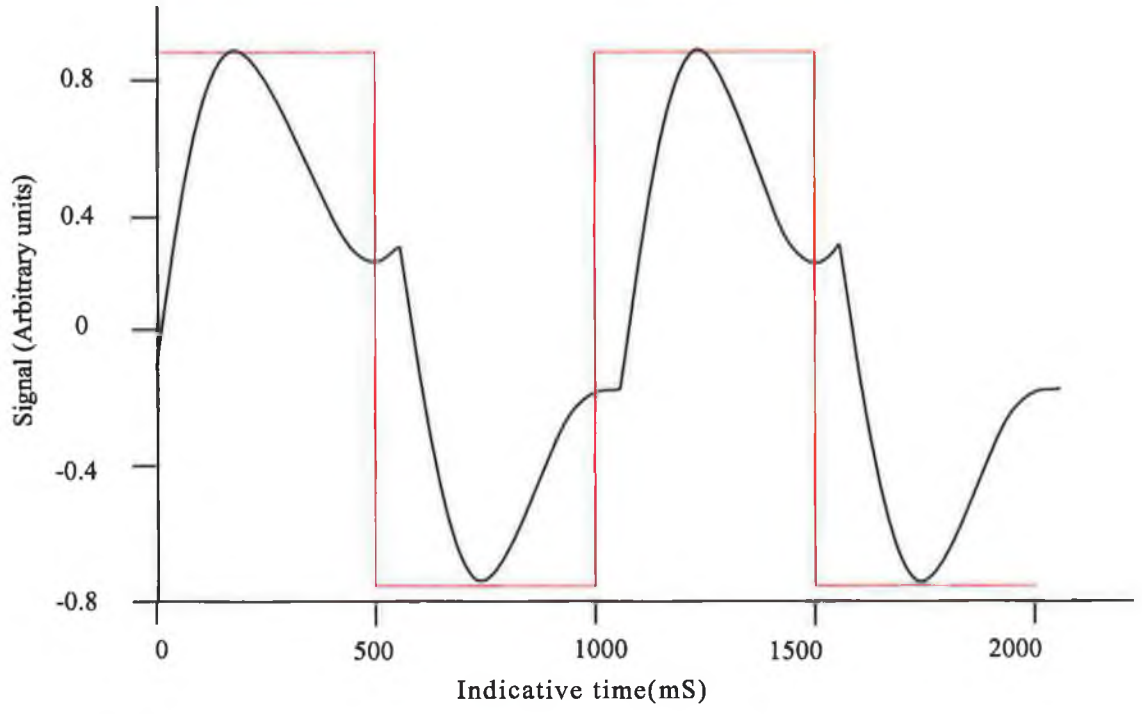

Figure 4.5 1Hz frequency waveform

By increasing the frequency of incident radiation reaching the detector saturation is prevented. The frequency of the on/off cycle used in the project is 3.1Hz. A sinusoid type waveform is produced from the pyroelectric when such a frequency is used. The peak to peak amplitude decreases with increasing drive frequency. This happens because the heating and cooling effects on the pyroelectric elements occur in shorter time frames. Hence it can be said that the meaningful signal from the pyroelectric elements is related to the total charge generated during the light and dark states. This simplifies to a measure of the peak to peak amplitude if the drive frequency is kept fixed. Fixed frequency is extremely important for stable and accurate output signal. Hence the timer interrupt source used to supply the drive frequency is given highest priority. This is achieved by setting the T1 bit located the Interrupt Priority register (IP) of the microcontroller. Giving the timer interrupt highest priority prevents the serial port, which is also interrupt driven, from disrupting the drive frequency timer. Shown below in figure 4.6 is the pyroelectric output expected for a drive frequency of 3.1Hz.

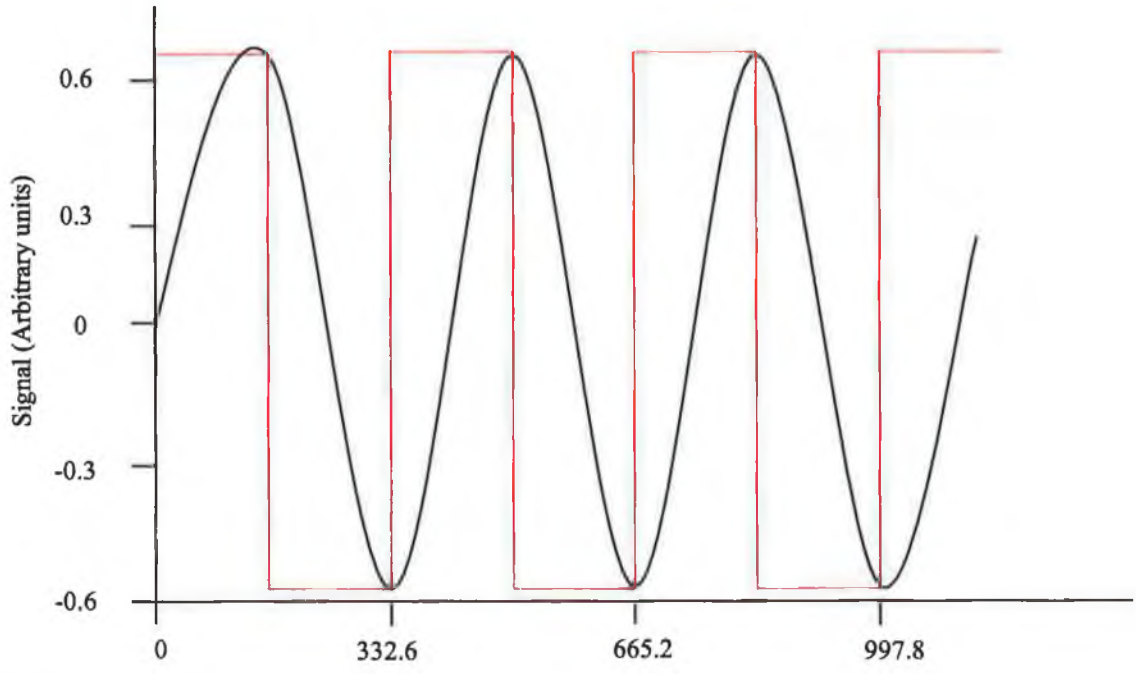

Figure 4.6 Pyroelectric output at drive frequency of 3.1Hz

4.4.4 Gas Concentration Calculations

Section 3.4 detailed in depth the Beer Lambert equation, which relates the amount of light absorbed to the concentration of the substance absorbing it. This law derived the equation:

$$\log(I / I_0) = -\epsilon cl$$

Where:

I = intensity of light

I_0 = (I_0 = I) when distance of lights entry into medium = 0

ϵ = molar absorption coefficient

c = molar concentration

l = pathlength

To extract the target gas concentration the active and reference peak to peak values are firstly used to calculate the ratio

Ratio = ((Active peak to peak) / (Reference peak to peak)) / Zero)

It is the ratio of the active to reference signal that is used. This compensates for effects such as temperature fluctuations, pressure changes etc. As the two pyroelectrics are on the one substrate they should theoretically change by the same amount in such situations. To monitor a change in signal output the intensity of the active signal needs to be recorded in the absence of the target gas. This is the Zero value in the above equation. The ratio can be now be stored and saved to EEPROM through a menu setting on the instrument. For the carbon dioxide version of the detector this ratio value has to recorded in the presence of nitrogen. This is because in ambient air there is CO_2, approximately 400 ppm (parts per million). Also humans expel CO_2 so the true zero value would not be recorded in ambient air. The live readings of the active and reference are continuously monitored. These readings are calculated and stored in the microprocessor's Random Access Memory (RAM). The fractional absorbance, which is directly related to the amount of incident radiation absorbed by the target gas, can now be calculated.

Fractional Absorbance = (1 – Ratio)

However the standard Beer's law formula needs to be deviated from slightly. The law above is obeyed strictly only for monochromatic light. The NDIR method observes the intensity of a range of wavelengths that is contained in the passband of the particular optical filter utilised in the detector. Chapter 3, section 3.4 Beer-Lambert Equation, details the interaction of the non absorbing wavelengths and how they combine to modify the Beer-Lambert equation to take into account non-monochromatic radiation.

The now modified and deviated formula, as derived in section 3.4, is as follows:

$$\textbf{Gas Concentration}^{pwr} = \ln((1 - \textbf{fractional absorbance}) / \textbf{SPAN})) / \epsilon l$$

pwr = power term

ϵl = constant dependent on target gas and pathlength

SPAN = (1 – S), where S is the contribution to the signal intensity caused by the effect of the non-absorbing wavelengths.

4.4.5 Peak To Peak Detection Techniques

One of the most important and integral part of the software design for the infrared gas detector was the peak-to-peak detection of the pyroelectric output sinusoid. Truly accurate and reliable results were needed to maintain the instrument's integrity, as a fully functioning infrared based gas detector. The techniques researched and investigated will be discussed in the following sections.

In the early design stages a hardware approach was adopted to detect the peak of the sinusoids. A peak detector was designed using an op-amp diode and capacitor and some resistors. A circuit diagram of this simple circuit can be observed in fig 4.8

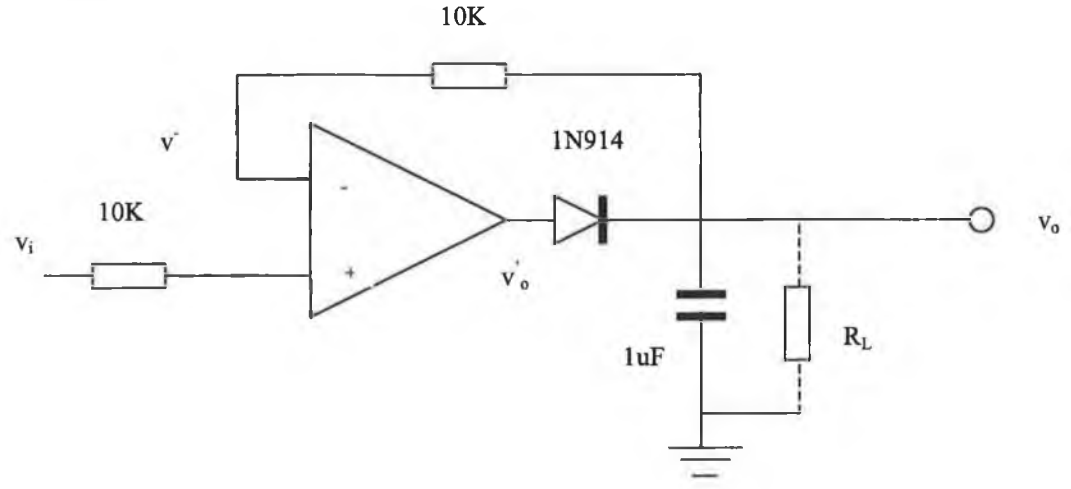

Figure 4.7 Peak Detector Circuit [Malvino 1999]

Initially, when $v_i > 0$ the op-amp will be positive and the diode will be forward biased. Operation in the linear active region requires that $v^- = v^+$, forcing the circuit output voltage v_o to reach to the peak value of the input:

$$v_o = v_i(peak)$$

The capacitor charges quickly to this value through the low-resistance path consisting of the op-amp output resistance and the diode forward resistance. Feedback forces the op-amp output v'_o at this point in the circuit to be:

$$v'_o = v_o + 0.7$$

After the capacitor is charged to the peak input voltage, and the input value drops below this value, the differential input voltage $v^+ - v^-$ becomes negative and the op-amp output voltage in turn becomes negative. The diode then becomes reverse biased, and the loop is broken. The op-amp output voltage then swings down to negative saturation. The voltage across the capacitor remains close to the peak value of the input voltage, although the effect of any load will result in the depletion during the remainder of the input cycle. During the next cycle the op-amp will move back into the linear region for the interval in which the input voltage exceeds the capacitor voltage. During that interval the capacitor is charged back to the peak input voltage [Stanley 1984].

This approach did not work too well for two reasons. First the peak detector circuit was not accurate enough for this application. The time constant changed as the temperature changed resulting in inaccurate results. Secondly this technique could not measure the trough of the sinusoid. Since the gas concentration is related to the ratio of the detector peak to peak against the reference peak to peak this method did not prove adequate. It was decided to try and monitor the peak to peak purely through software in an algorithmic fashion. Two software based design solutions were drawn up to achieve true peak to peak detection, the second one really being an extension and improvement of the first solution.

As described in section 4.4.3 (Infrared Lamp Driving) the source lamp is driven by an interrupt based timer in the AT89C51RD2. It has a frequency of 3.1Hz and a duty cycle of 50%. When an interrupt occurs, once every 161.3 milliseconds, the lamp state is toggled. The characteristics of a pyroelectric have already being detailed in chapter 3. As light energy is incident on it's surface the output rises in a sinusoidal fashion. If the light energy is pulsed on and off the output of the pyroelectric rises and falls continuously resulting in a sine wave output. Hence it can be safely assumed that at the precise moment before the infrared lamp source is switched off, the sinusoid is at its highest peak. It can also be assumed that at the precise moment before the lamp is switched on, the sinusoid is at its lowest trough.

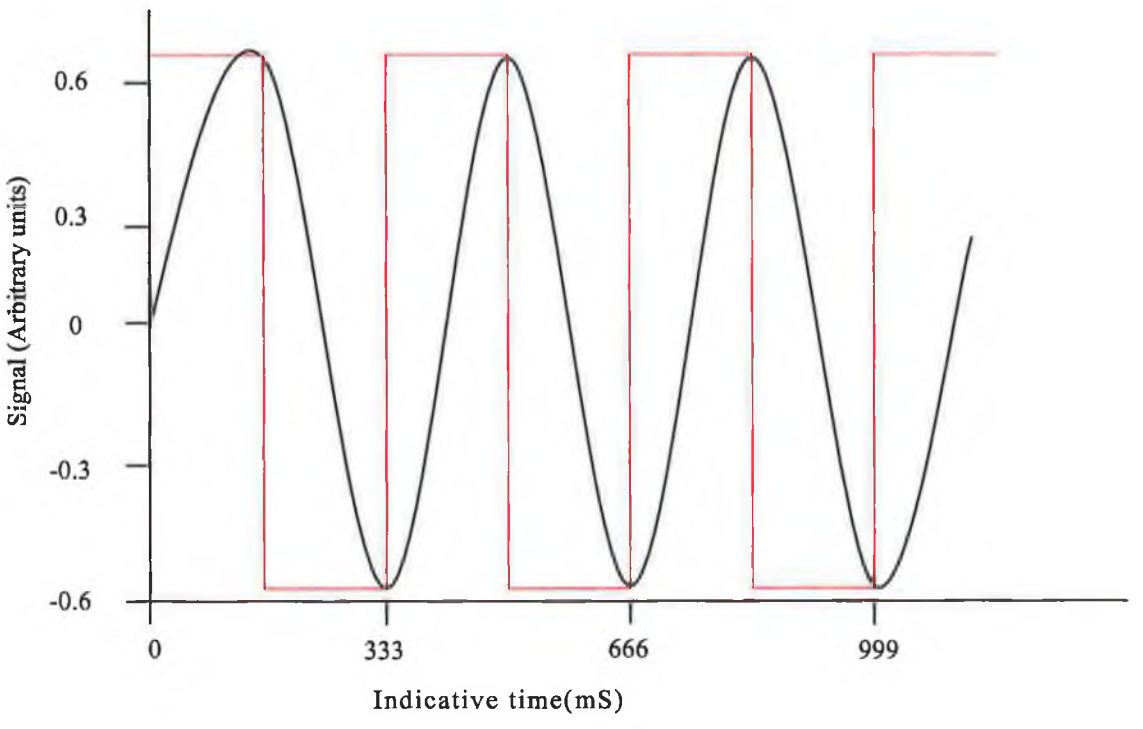

Figure 4.8 Relationship between lamp drive and pyroelectric output

By taking a peak to peak reading just at the point of toggling the lamp source reasonably accurate peak and trough measurements can be obtained. The outputs of the pyroelectric were fed into an A/D converter. The A/D converter used was a 12-bit Successive Approximation Register (SAR) converter. The MCP3204 by

Microchip was the chosen converter. This gives a resolution of 0 to 4095 in digital output format. The A/D converter was supplied with an external 2.5V reference, which meant that 1 decimal out of the A/D, equated to a 0.6mV analogue input. This high resolution was desired for accurate and linear readings. An ADC of a lower bit resolution would introduce a quantisation error to the digital output. This quantisation error is the largest potential voltage error that can occur in the conversion process. For example take a 10-bit A/D. The largest potential error that can be introduced with a 2.5V reference is 2mv. As mentioned above a 12-bit A/D results in a 0.6mV potential error. This tighter accuracy was needed for this particular application.

Now that there was a highest peak reading and a lowest trough reading, a peak to peak value could be calculated. This process was carried out on both pyroelectrics, reference and active. Due to the reduction of the active pyroelectric output in the presence of gas, the active amplitude needed to be of a magnitude greater than that of the reference pyroelectric. The output AC sinusoid is imposed on a DC pedestal of approximately 0.6V to 1V. In the presence of gas it was not desirable that the active peak to peak would dip below the reference peak to peak. This would result in the maths routine falling out, as the ratio between the two would then become greater then one. This will be shown in greater detail later when the maths software is described. It was hence decided to set the gain for the active pyroelectric output at 2V peak to peak and the reference pyroelectric to be set to 860mV peak to peak. The big gap between each signal achieved a greater signal to noise immunity and went some way to combating zero drift problems. The 2V peak to peak signal had a highest peak of approx 2.2V and this left some room for fluctuations on the signal without the A/D converter saturating above its 2.5V voltage reference. The trough read about 300mV. For the hydrocarbon version of the infrared gas detector the application of 50% lower explosive level (LEL) methane resulted in a 6% reduction in the active output signal. In the carbon dioxide version the reduction for 5% CO2 was 45%. The difference between the two due to more active molar absorption by the carbon dioxide molecules as detailed in chapter 3.

The active and reference peak to peak values were then averaged by simple means first, consisting of a 16-bit unsigned integer variable which held the sum of 16 ADC conversion for each signal. This technique did remove some noise and smoothed out the signal. However as the signals were analysed and also superimposed onto artificial noise it became clear that some initiative averaging needed to be carried out on the signal to achieve better immunity and also better averaging and smoothing. The algorithm devised will now be detailed.

In the initial solution an ADC conversion was taken just at the moment when the lamp source changed state. For the implemented algorithm a timer interrupt was generated every 161.3mSec. The decision was taken to break up the sine wave into a series of time slices. 16 slices to be exact, over a full period of the sinusoid. For each slice a timer interrupt was generated which meant that the timer overflowed every 20.1mSec. A timer tick variable was created and incremented on every timer interrupt. With this tick variable it was now known at any time where on the sinusoid the program was located. When an interrupt was generated and the timer tick was at 8 the infrared lamp was turned off. When the tick reached 16 the lamp was turned on again and the tick variable reset to zero. Figure 4.9 graphically depicts how the sinusoid is time sliced.

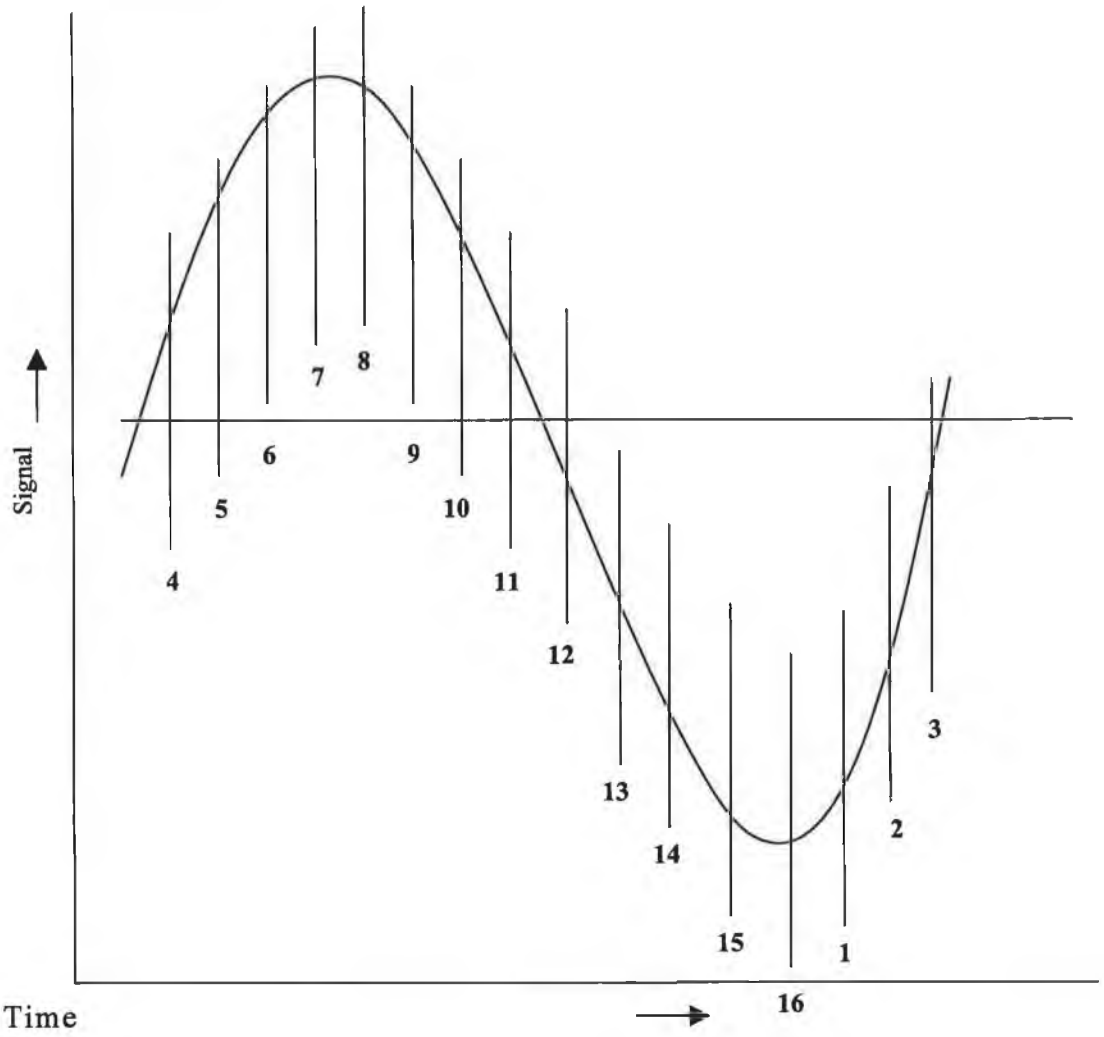

Figure 4.9 Sinusoidal Time Slicing

As can been seen the diagram the highest peak of the sinusoid resides between tick 7 and 8. The lowest point of the waveform resides between tick 15 and 16. Now there is an accurate known time when the peak and trough occurs on the sinusoid. By taking a number of readings between timer ticks 7 and 11 a highest peak reading can be obtained. By comparing each reading with the previous highest recorded reading, the absolute peak can be recorded. The time between timer ticks 3 and 6 is 60.3mSec. The total ADC conversion time is 1.2mSec. This meant that 50 conversions could take place on the reference and active signals, which gave 25 conversions to each. The same technique was used to calculate the lowest point of the signals. Between timer ticks 15 and 3 the same number of readings were taken and a lowest point recorded. When the tick

counter reaches 16 it is reset back to 1, and the next period of the waveform is tracked. Below is the pseudo code used to generate the source code.

```
while( timerTick ! = 7 )
{
        do microcontroller housekeeping;
 }

initialise rolling buffer to zero values;

do
{
        refPeak = 0; actPeak = 0;
        move rolling buffer forward 1 element;
        take active signal ADC reading and place in rolling buffer;
        take reference ADC reading and place in rolling buffer;

        for ( buffCnt = 0; buffCnt < 4; buffCnt++ )
        {
                refHiTotal += refBuffer[ buffCnt ];
                actHiTotal += actBuffer[ buffCnt ];
         }
        refHiTotal /= 4;
        actHiTotal /= 4;

        if( refHiTotal > refPeak )
                refPeak = refHiTotal;
        if( actHiTotal > actPeak )
                actPeak = actHiTotal;

 }
while( ( refHiTotal == refPeak ) || ( actHiTotal == actPeak ) && ( timerTick <
11 ) );
```

The do while iteration is entered after the seventh timer tick. This, as explained previously, is when the signal peak should be approaching it's highest. The variables storing the peak values and the rolling buffer elements are initialised to zero, as the values will obviously be greater than zero at the highest. Each signal, reference and active, are sampled and placed in the rolling buffer that has been moved one place forward. The rolling buffer elements accumulative value is calculated and averaged. The variables holding both peak values are updated only if they are lower than the peak readings just taken. The condition for exiting this do while iteration is come true either when the reference or active total's are not higher than the recorded peak value. This indicates that the sinusoid is falling. The reason for not exiting the iteration unless the live ADC readings are equal to the recorded peak is to provide a means of noise suppression. This technique will however be explained in detail in section 4.4.7. The second part of the condition to be met is when the timer tick counter is greater than 11.

The pseudo code for the trough detection is as follows.

```
while( timerTick ! = 15 )
{
        do microcontroller housekeeping;
}

initialise rolling buffer elements to 4095;

do
{
        refPeak = 4095; actPeak = 4095;
        move rolling buffer forward 1 element;
        take active signal ADC reading and place in rolling buffer;
        take reference ADC reading and place in rolling buffer;

        for ( buffCnt = 0; buffCnt < 4; buffCnt++ )
        {
                refLowTotal += refBuffer[ buffCnt ];
```

```
            actLowTotal += actBuffer[ buffCnt ];
        }
    refLowTotal /= 4;
    actLowTotal /= 4;

    if( refLowTotal < refTrough )
            refTrough = refLowTotal;
    if( actLowTotal < actTrough )
            actTrough = actLowTotal;

}
```

while((refLowTotal == refTrough) || (actLowTotal == actTrough) && ((timerTick == 15) || (timerTick < 3)));

On exiting the peak detection section the code enters another while loop until timer tick 15 is reached. In this loop, as before, housekeeping duties are attended to such as checking for button presses, kicking the watchdog timer: etc. The rolling buffer and the live ADC trough reading variable is this time initialised to 4095. This value is the full range scale of the 12-bit ADC (2^{12}). Because it is now the trough that is being sought after the recorded trough variables are updated only if the live readings are less than the previously recorded trough. As in the peak detection algorithm the exit condition for do while is made true when the recorded lowest point of the signal is equal to the live ADC readings. For the iteration to be left the timer tick counter must also be either equal to 15 or less than 3. This combination once more provides some noise suppression that will be detailed later in the following sections.

The implemented algorithm has achieved what was set out at the start. True peak-to-peak detection has been obtained with extremely accurate results, down to plus and minus 3-4mV. The maths routine is run approximately 3 times a second which calculates the gas concentration. This is more than enough to produce a quick T90 response time that is an important component of the functional requirements for the project. Detailed below is the program flow of the interrupt service routine and the peak, trough detection algorithm.

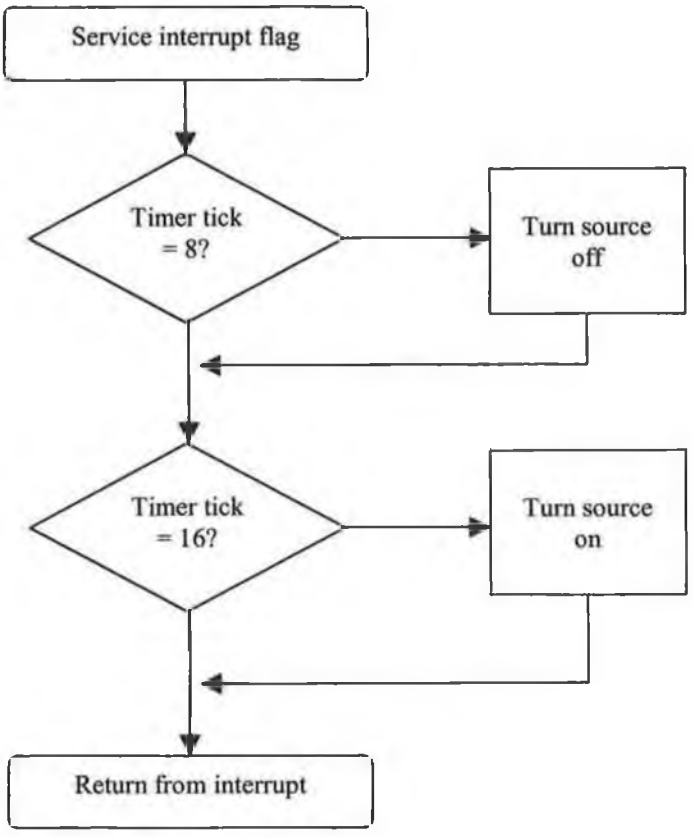

Figure 4.10 Interrupt service routine

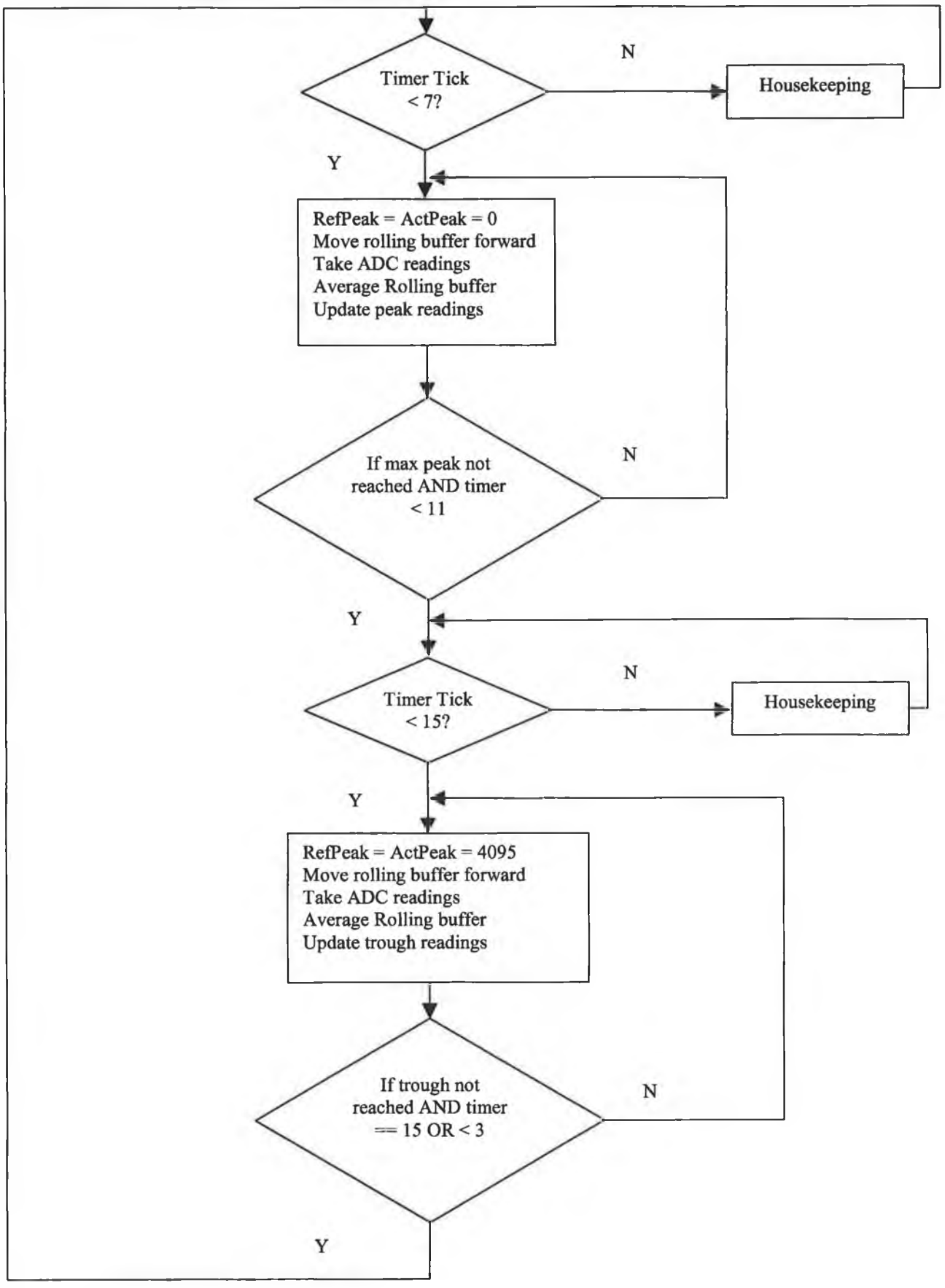

Figure 4.11 Software flowchart peak, trough detection

4.4.6 Temperature Compensation

Due the characteristics of pyroelectric detectors temperature variations pose a problem in the design of the instrument. A described in section 3.5 a pyroelectric detector consists of a number of components. The active and reference detector elements, two JFET's and two gate resistors. All these components are temperature dependent. All Monicon Technology's products have an operating temperature range of –20°C to +50°C. The infrared detector is no different. Due to high number of Monicon installations in eastern bloc countries, where temperatures as low as minus 20°C are commonplace, the detector needs to perform excellently in such environments. High temperature regions and also boiler room installations require linearity and minimal drift at the higher end of the temperature scale. So for the reasons outlined above a thermistor was incorporated into the infrared detector. The thermistor is positioned right at the pyroelectric to give an accurate reading as possible of the temperature. An NTC (Negative Temperature Coefficient) thermistor was chosen and used. An NTC thermistor's resistance decreases with increasing temperature. At ambient temperature, 22°C the thermistor has a resistance of approx 3.3KΩ. At -20°C this rises to approx 30KΩ and drops to 1KΩ at +50°C. By connecting 10KΩ series resistor connected to a 2.5V reference the temperature can be derived directly from the voltage across the thermistor by the expression:

$$\text{Temp } (^{\circ}C) = 77.595 - 126.9 * v + 73.193 * v^2 - 17.681 * v^3$$

This expression is known as the Steinhart-Hart equation and it linearizes the voltage output from the thermistor. Each thermistor is non-linear over temperature ranges. The constants in the equation are got by consulting the manufacturer's datasheet, these vary from different manufacturers and different part types. The resistance of the thermistor used in this case at ambient (25 °C) is 3KΩ.

The first means of temperature compensation however does not need the thermistor. As mentioned before the infrared detector utilises two pyroelectric detectors. A reference, whose filter's bandpass is outside that of the target gas

absorption frequency, and an active element whose filter is within the required frequency. The usable signal is the ratio of these two detector outputs and that is where the first form of temperature compensation occurs. Any fluctuations in temperature will occur at both elements and as a result will cancel each other out. This was one of the main reasons for a dual pyroelectric detector design. Many other products on the market utilise a single pyroelectric and inherently suffers from drift, instability and fluctuation. Having the two pyroelectrics on the one substrate also improves the effectiveness of this. This alone however would not prove enough to maintain the instrument's stability and integrity throughout the desired temperature range. Hence the need for temperature monitoring.

Below is listed the main contributing factors to pyroelectric fluctuations in varying temperature conditions:

- The gate leakage current of a JFET increase substantially with increases in temperature. The gate leakage of a typical JFET increases from 1pA at +25°C to well over 30pA at +60°C. This increase in leakage current results in higher detector noise.
- Any variation in temperature will reduce or decrease the forward transconductance of the JFET and as a result will either increase or decrease the pinch-off voltage of the transistor.
- The spectral transmission of the filter windows on the pyroelectrics will vary with temperature. Generally as temperature increases the bandpass filters will shift to longer wavelengths. This can introduce some non-absorbing wavelengths that can affect the maths routine. This is because the span constant, which takes into account the non-absorbing wavelengths contribution to the signal, would now be slightly incorrect.

The thermistor required for temperature is located as close as possible to the dual pyroelectric detector. This gives the most accurate reading of the temperature where it matters most. In the early software design stages the methodology was to compensate the gas concentration by a factor determined by

the difference between the temperature at which the instrument was calibrated and the current temperature of the instrument. In other words the gas concentration was offset by a factor to compensate for the non-linear deviation from the ideal response, caused by temperature variations. This involved analysing the gas response over a wide range of temperatures in a temperature cycling chamber. The instrument was first zeroed with the appropriate gas and then spanned to full scale in ambient temperature. Then the zero and full-scale responses were recorded at intervals of 10 °C increments up to 50 °C. It was then brought back to ambient and decremented to -20 °C. A temperature change of no more than 0.25 °C per second was observed. A rapid fall in temperature would result in the gate of the FET transistors being pulled to a negative voltage. This would cause the DC offset voltage to clip and the sinusoid signals would be temporarily lost. A sudden rise in temperature would cause the opposite and the DC offset voltage would be clamped once again resulting in a loss of signal. When a 10 °C increment or decrement was accomplished the temperature was kept constant for 30 minutes to allow the pyroelectrics to stabilise. At the end of the stabilisation time the gas concentration was noted at zero gas present and at full scale. By testing a number of samples, approximately 30, in such fashion two compensation figures were derived. A zero temperature compensation factor and a full-scale compensation factor. At zero and full scale, different deviations were evident from the data collected. Throughout the tested sample there appeared to be repetitive deviations at both points. Hence the compensation factor 0.0055 and 0.0025 for the zero and full scale respectively were derived. These figures were multiplied by the temperature offset (sensor temperature – calibration temperature) and added to 1. This factor was then multiplied by the ratio, for the zero temperature compensation, and multiplied by the SPAN constant in the maths routine for full-scale compensation. This technique of temperature compensation worked quite well over the full temperature range and initial testing of the instrument looked promising.

However as more batches of the pyroelectric detector were received from the manufacturer (Infratec Gmbh) it became apparent that batch to batch variations meant that the compensation technique described above would not work. Only

slight variations in production batches meant that a simple compensation factor could not be used to offset the gas concentration over varying temperature conditions. The 30 or so detectors used in the initial testing originated from the same production batch. As a result a new temperature compensation technique needed to be drawn up.

The approach adopted for solving this problem involved individually temperature profiling each complete sensor. Each completed sensor is enclosed in a stainless steel body that contains the optical cavity pyroelectrics and associated PCB and passive components. It is connected to the main PCB via an 8-way ribbon cable. This sensor, as part of its production cycle, needs to be fully tested by means of in-house automatic test equipment (ATE) at Monicon Technology. The idea was to incorporate the temperature profiling into the ATE and automatically set up the compensation parameters for each individual sensor. The technique utilised will now be described in detail.

Some non-volatile memory needed to be located on board the sensor to store the compensation parameters. A one wire 1Kb EEPROM interface from Dallas Semiconductor, the DS2431, was ideal for the situation and was incorporated in to the detector PCB. One spare pin was available on the 8-way connector to the main PCB. This was used to read and write data from the device. A jig was designed which would hold a batch of 25 sensors in the temperature cycling chamber and have all the associated electronics on board to communicate with each sensor and also with the ATE controlling software. The ATE software used in Monicon Technology is Labview by National Instruments. Before the profiling takes place each sensor is functionally tested to ensure correct operation. This is carried by a separate test jig. Throughout the profiling communication is maintained between the temperature chamber and Labview so as current temperature, etc is known to Labview. The steps taken in temperature profiling each sensor will now be detailed.

1) The test block of 25 is placed in the cycling chamber and left to stabilise at 20 °C for one hour and then the zero value is measured. This is the active peak to counts divided by the reference peak to

peak counts. There is now a reference zero (Zref). This is stored by the jig's electronics for each sensors along with it's associated temperature.

2) A known calibration gas is applied to each sensor and is then allowed to stabilise for e.g one minute. Active/Reference is measured and from this the absorbance is calculated. Absorbance = [1 – (Active/Reference) / Z_{REF}]. This value is called A_{REF} and is stored for each sensor.
3) The chamber's temperature is slowly decremented by 5 °C and the sensors are allowed to stabilise for one hour.
4) A zero gas is applied, the signals are allowed to stabilise and active/reference is measured. This is called Z_{T1} and a correction value can now be worked out using Z_{REF} / Z_{T1}. Each sensor correction is worked out using the same technique. This is now the first temperature correction factor for zero temperature dependency drift and its stored in the individual EEPROM for each sensor.
5) The same calibration as before is applied to each sensor, the signals are allowed to stabilise and active/reference is measured. This is called A_{T1} ($Absorbance_{T1}$) and a correction value can now be worked out using A_{REF} / A_{T1}. This is the span temperature dependency drift correction for 15 °C. Each sensor is worked out in turn and the correction figures stored accordingly.
6) Steps 3-5 are repeated to get Z_{T2}, A_{T2}, Z_{T3}, A_{T3}, etc over the range 20 °C to -20 °C. There now is a table of correction figures for each temperature stage. These are stored in the specific EPPROM location for each individual sensor. The firmware on the instrument knows which location corresponds to which temperature when it reads them into RAM on a power up.
7) The chamber is brought back up to 20 °C in the same fashion as it was brought down to -20 °C and on the way up the zero and span correction values are verified by the jig's electronics and firmware.
8) The whole process is then repeated between 20 °C and 50 °C. The calculated correction values are once again verified on the way back

down from 50 to 20 °C. If verification is ok then the temperature profiling is complete

When the temperature profiling is complete each individual sensors now possesses a full set of 14 correction values that are unique to that sensor's characteristics. Variations in batches no longer effect how the sensors will be temperature compensated. Extended testing of this technique yielded extremely positive results and it was felt that each sensor would perform excellently over a wide range of temperatures.

Notes:

- The timing of when the sensor readings are taken is controlled by Labview, which in turn has communication with the temperature chamber as to what its current temperature is.
- The applied gas is fed through a copper coiled tube in the chamber so the gas is at the chambers temperature when it reaches the sensor.
- Each sensor on the jig is zeroed with a suitable calibration gas before the profiling commences.
- Dedicated electronics and firmware for each sensor control the profiling procedure.

4.4.7 Twin lamp source investigation

Part of the proposed project goals, outlined at the start of the project, was to conduct an investigation on integrating two infrared lamp sources into the detector. Preliminary research into the idea looked promising and it was thought that maybe a more stable and effective design could be achieved by taking this approach. The following section details the investigations and it's findings.

The approach of using two infrared lamp sources differs from the technique described throughout this chapter. Firstly, and obviously, there are two lamps as opposed to one. Secondly a single pyroelectric is used which is optically filtered

to the target gas's bandwidth, as described previously. In the dual pyroelectric arrangement the second detector is used as a reference channel. This channel does not react to the target gas and its function is to allow for environmental factors, system aging and other undesirable factors. The idea of the second lamp is also to provide a reference for such factors, which in turn eliminates the need for a dual pyroelectric detector. Below is a diagram of the arrangement and a detailed description of its operation.

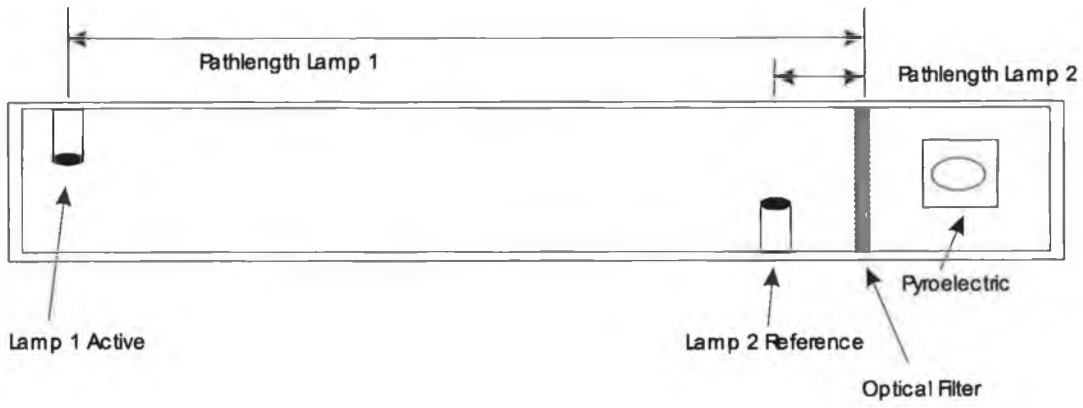

Figure 4.12 Twin Lamp Source Arrangement

The infrared radiation from lamp 1 has a much longer pathlength through the gas then the radiation from lamp 2. Hence in the presence of the target gas there will be less absorbance on the lamp 2 radiation then there will be on the lamp 1. From this we can calculate two signals, the active lamp signal and the reference lamp signal from the maths discussed in section 4.4.4.

Active lamp signal = $\mathbf{I_1 = I_0\, e^{-\in *c*Pathlength\ 1}}$

Reference lamp signal = $\mathbf{I_2 = I_0\, e^{-\in *c*Pathlength\ 2}}$

From these signals the ratio can be got, (I_1 / I_2), which in fact exhibits the same absorption characteristics as a single lamp source arrangement with a pathlength equal to Pathlength 1 – Pathlength 2. However in providing the second infrared source with a different pathlength we are in fact compensating for unwanted

factors that may affect the detector. Environmental factors, such as pressure, relative humidity etc, lamp source ageing and other undesirable effects will all have an impact on the pyroelectric output signal. The signal from the second lamp source will be affected in the same way. Because it is the ratio of the two signals that is used to determine the absorption these undesirable factors are as a result cancelled out.

This twin lamp source approach worked quite well in the lab and it was thought that this was the concept that would be utilised in the optical cavity design. However when the concept was integrated into the design of the detector problems arose, and it became evident that a return to the previous approach of dual pyroelectrics was the only solution.

When the prototype optical cavity was designed in the lab it consisted of a cylindrical hollow tube with a high reflectivity on the inner surface and the components locations the same as illustrated in figure 4.9. When the components were integrated into the Monicon compliant enclosure the reduced pathlength, (45mm), meant that the effect witnessed with the prototype optical cavity would not be replicated in the smaller cavity. The positioning of the second lamp, which could realistically only be positioned in one spot, meant that there was only a minimal difference between the active lamp signal and the reference lamp signal. In extensive laboratory tests, which involved simulated aging and deterioration of the detector, it was clear that this small differential was not enough to provide a reliable referencing point. Figure 4.13 shows the arrangement of the optical cavity with twin lamp source.

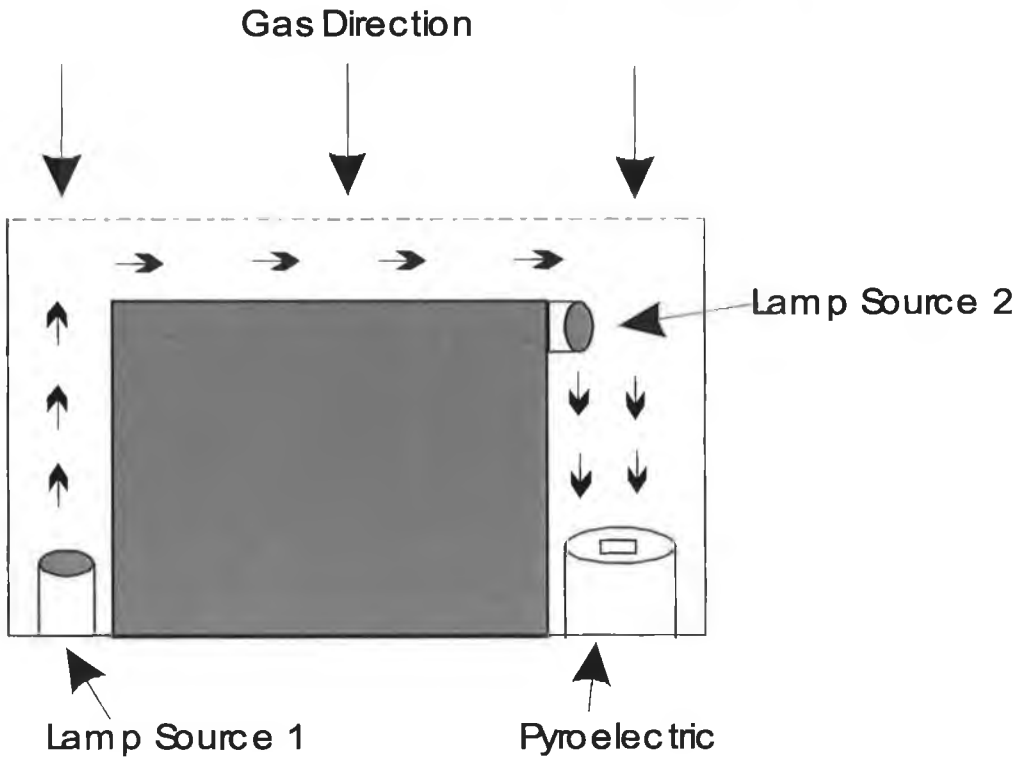

Figure 4.13 Twin lamp source cavity

The second lamp source could only be positioned in the one place due to wiring concerns. This left a pathlength of approximately 7mm. Such a pathlength was too small to encourage sufficient infrared absorption that would constitute a usable signal. This was particularly true for the hydrocarbon gases that do not absorb infrared as well as other gases, such as carbon dioxide. So because of the dimensional restrictions imposed on the optical cavity the twin lamp source approach to detecting infrared gas absorption was shelved and the dual pyroelectric design methodology was adopted for the detector. Coincidently it was discovered afterwards that Texas Instruments had recently taken out a patent against a certain aspect of the idea that ruled out the possibility of developing a similar detector in any case.

4.4.8 Noise Suppression

The suppression of externally induced noise in the instrument was one of the main requirements drawn up at the start of the infrared gas detector project. Noisy environments exist in many on-site installations Monicon supply to. Walkie-talkies, wireless equipment, mobile phones etc all contribute to fill a

site or plant room with potentially damaging interference, which can result in false alarms, spurious response patterns and other negative effects. Therefore the design of the instrument needed to incorporate ways to reduce these effects to a manageable level.

The noise suppression techniques implemented on the infrared detector mixed software techniques along with hardware techniques. In the following section both the software and hardware solutions utilised will be presented in detail.

Hardware noise suppression

The pyroelectric detector and optical cavity is mounted on a PCB and assembled in a stainless steel enclosure, as mentioned previously. A 8-way ribbon cable connects this board to the main control PCB. Due to the potted stainless steel enclosure, which would be earthed in the industrial field, interference would more than likely not be coupled from the pyroelectric detector signal lines back into the main control board. In order to prevent noise being coupled into the pyroelectric PCB from the main control board a low pass filter was incorporated into the pyroelectric PCB.

The low pass filter compromised of an inductor and capacitor (LC). The idea of the low pass filter is to let through the low frequency signals associated with the pyroelectric, ie: 3Hz sinusoid, and block the higher frequencies which could introduce noise into the system.

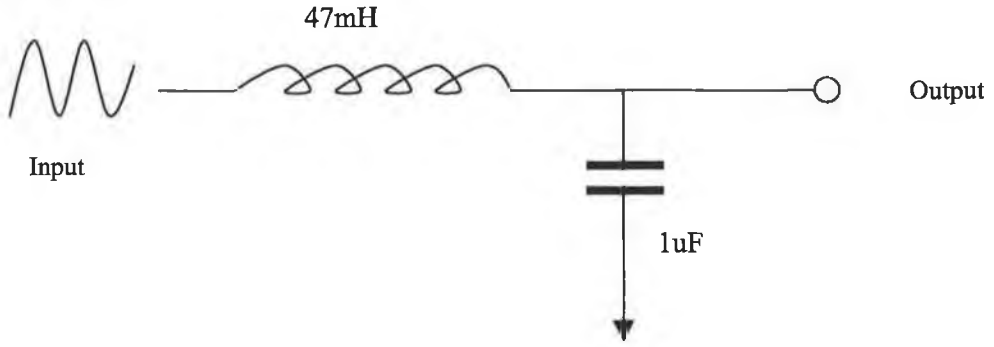

Figure 4.14 Low pass LC filter

Figure 4.14 shows a low pass LC filter. It has an order of two because it contains two reactive components, an inductor and a capacitor. The desired cut off frequency for the filter can be calculated by the following equation.

$$f_o = \frac{1}{2\pi \sqrt{LC}}$$

The value of the components used in the were 47mH and 1uF for the inductor and capacitor respectively. Slotting these values into the above equation gives a cut off frequency of approximately 734Hz.

$$f_o = \frac{1}{2\pi \sqrt{(47 * 10^{-3}) * (1 * 10^{-6})}}$$

$$f_o = 734.13\text{Hz}$$

This low pass filter proves to be relatively effective in blocking high frequency noise up to a realistic power level. Three separate filters were deployed on the pyroelectric PCB. One for each pyroelectric, reference and active channel, and also a filter for the +5V supply rail to the pyroelectric. A noisy supply voltage would also carry through to the output of the JFET's. Surface mount components were used, with 0603 package size to reduce the amount of real estate used on the 30mm PCB.

Software noise suppression

The software algorithm implemented to combat noise interference used a form of digital filtering to achieve its goals. As detailed in section 4.4.5 Peak detection techniques, the peak to peak digitised value for the reference and active signals are calculated from the algorithm described. These two values now needed to undergo software filtering to try and reduce the effects that noise might have on the signals.

The concept of the software filtering was to create, in a sense, a software damper, which would alter itself in real time to certain changes in the analysed signals and the calculated data. As mentioned previously the peak to peak digital value is smoothed by a 16-fold rolling average. So the peak to peak value of both signals is really the sum of the 16 previously recorded values. After each calculation this total value is divided by 16. This value is then subtracted from the 16-way average and the new reading added in to the rolling average. So to calculate the gas concentration these two readings, active counts and reference counts, are plugged into the maths formula. In order to create the software damper some more variables need to be calculated.

$\sum$ ActTotal = summation of the active signal counts

$\sum$ RefTotal = summation of the reference signal counts

$$\text{ActMean} = [\sum \text{ ActTotal} / 16]$$

$$\text{RefMean} = [\sum \text{ RefTotal} / 16]$$

$\sum$ Act = $\sum$ Act + [A_n – ActMean], where A_n is the live active peak to peak reading

$\sum$ Ref = $\sum$ Ref + [R_n – RefMean], where R_n is the live active peak to peak reading

damper = adaptive damping variable for suppressing noise.

All these variables are updated at the end of a period of the waveforms, in other words when the timer tick counter reaches 16.

The variables $\sum$ Act, $\sum$ Ref hold the change in the active and reference signal counts respectively. If the active or reference signals increase or decrease in amplitude, let it be from a response to the target gas or else sporadic noise, then the two variables will keep track of it. Positive for a decrease in amplitude and negative for a increase in signal amplitude. When a full period of a waveform has been analysed and recorded the peak to peak 16-fold values are calculated by the expressions:

$$Act_{ptop} = Act_{ptop} * ((damper - 1) / damper) + \sum Act$$

$$Ref_{ptop} = Ref_{ptop} * ((damper - 1) / damper) + \sum Ref$$

Act_{ptop} , Ref_{ptop} hold the previous peak to peak values. By analysing $\sum$ Act and $\sum$ Ref we can determine what to set the damper variable to in order compensate for an increase or decrease in signal readings. Taking an example will help to explain the concept better.

For a 2V peak to peak active pyroelectric signal the ADC reading will be 3270 decimal approximately. Setting up the damper variable with a default value of lets say 8 will leave the reading at 2860 decimal. The same will apply to the reference signal reading, peak to peak 850mV and dampened to 744mV. The software filtering algorithm is optimised to filter up to ±50mV of noise on the sinusoid signals. For a negative change in $\sum$ Act or $\sum$ Ref the damper variable is increased. A decrease in 10 decimal over a full period in, for example, the active signal counts will increase the damper by one. $\sum$ Act is now equal to -100. The previous peak to peak reading is multiplied by 0.888 and added to this is the change in the live reading compared to the previous reading. Working this through the filtering equation leaves the peak to peak active value at 2442. So by increasing the damper it is in effect smoothing the signal

4.4.9 Zero and span drift compensation

Zero and span drift is an inherent problem in all gas detectors. Regardless of the sensing technology used, let it be infrared, thermo-catalytic, semiconductor sensing etc, there is always drift at the zero base line and also at full scale range. Detector drift can be minimised through some compensation techniques but never fully eliminated. Regular calibration and maintenance procedures are recommended to further inhibit this phenomena. Explained below are the techniques investigated and implemented in the infrared detector to try and reduce drift.

The Non Dispersive Infrared (NDIR) technique for detecting gas is probably one of the most stable techniques with regard to drift. As mentioned previously when the instrument is zeroed by means of the user menu it stores the raw ADC peak to peak counts in non-volatile memory. This is the base line with which the live reference and active peak to peak counts are compared against, the ratio being used in the maths routine. Zero drift occurs when in the absence of the target gas the live readings deviate from the stored zero values. This can happen for a few reasons. As the infrared source lamp ages the intensity of the radiation can decrease. As already discussed the pyroelectric output sinusoid's amplitude depends of the amount of incident radiation falling on its surface. Hence a dip in the lamps radiation will have a proportional decreases in the signal output. Once more the reason for incorporating a dual pyroelectric detector into the design is justified. Any change in incident radiation will be experienced by both pyroelectrics. It is the ratio of the active signal against the reference signal so the same decrease will occur at each output. The ratio will not change, even though the amplitude of both are changing. The choice of a dual pyroelectric on the same substrate and right beside each other also means that the decrease in incident radiation will be the same on each surface. Some other detector designs use two single pyroelectric spaced apart that will experience different rates of change for each surface. So the first means of drift compensation is achieved by the choice of a dual pyroelectric component. As lamp intensity drops off the ratio remains the same due to the referencing detector.

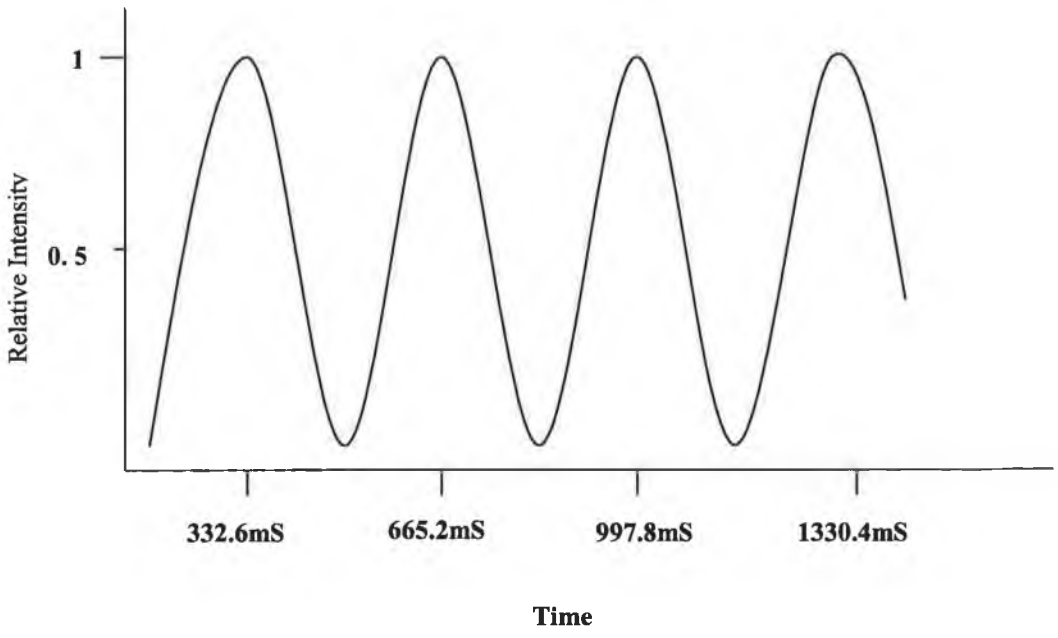

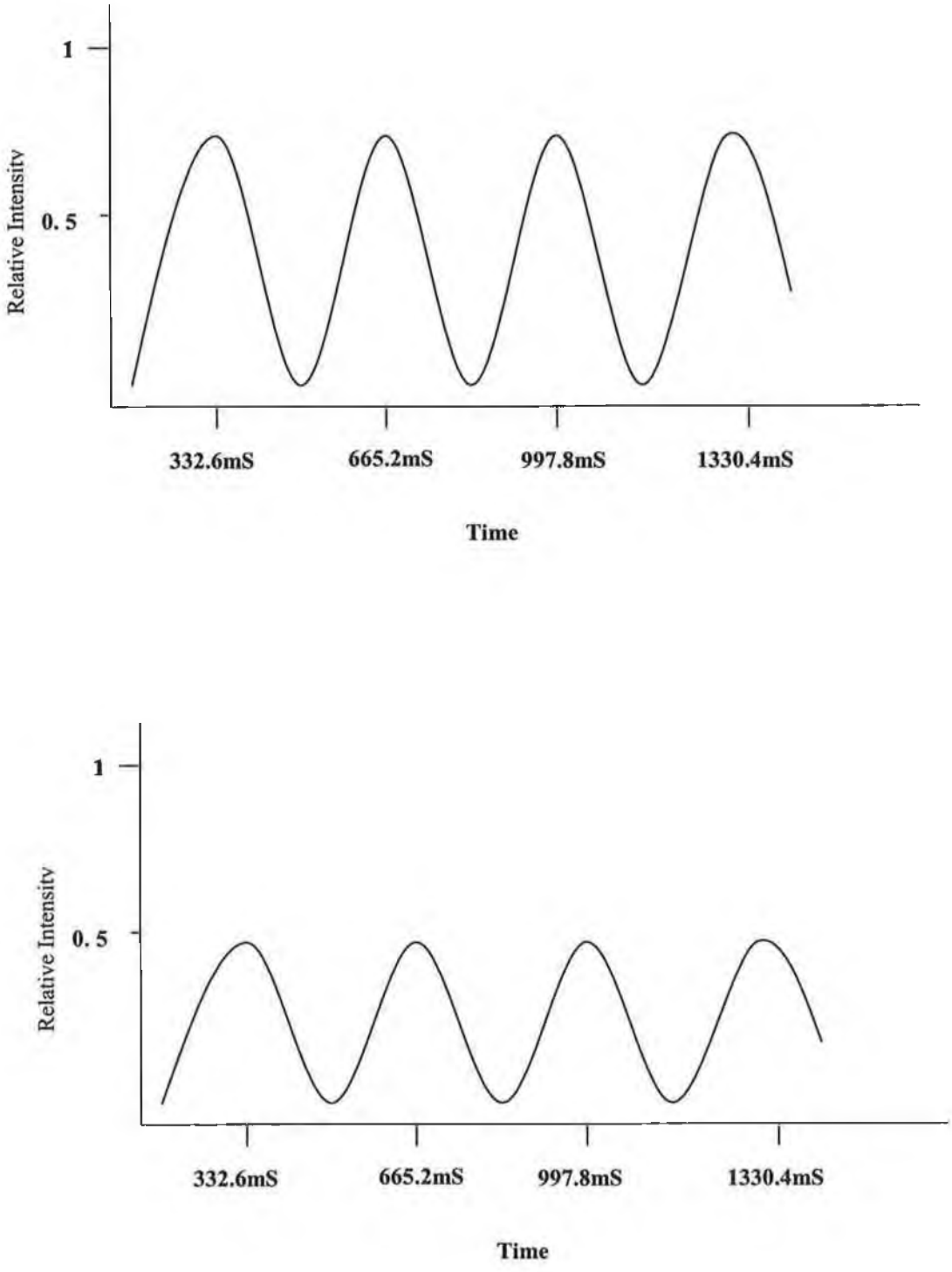

Figure 4.15 Pyroelectric output for varying radiation intensities

Another contributing factor to the cause of zero and full scale drift is degradation of the optical cavity's interior. Corrosion on the interior surface can result from harsh corrosive environments, ageing of the instrument amongst other factors. The degradation of this reflective medium, in which the infrared radiation bounces and reflects en-route to the pyroelectric detectors, can result in a reduction of incident radiation reaching the detector surface. Like the lamp ageing situation detailed previously this in turn could result in a reduction in the output signal from any one the pyroelectrics. Also, if formed, corrosive elements on the cavity's interior surface will change the transmission path of the infrared. Although these are only very slight differences the effect can be noticeable. A small reduction in incident light reaching the detector will have small difference on the low level output sinusoid. This low level signal (6 – 7mV) will have that small difference amplified resulting in a noticeable shift from it's original zero base level. It should be also noted that the hydrocarbon detector output sinusoid reduces by a factor of 12% approximately for 100% LEL methane. It follows that a 1% reduction in the active pyroelectric's output signal will result in a drift of 8.3% LEL. Which pyroelectric is effected and by how much is totally unpredictable in a situation like this, so the detector drift can be arbitrary. To reduce the effects described the optical cavity is hence gold plated. This has already being described in section, 4.4.3 Optical cavity design. The idea once again being to halt the cavity's degradation and maintain the integrity of the infrared transmission pathlength.

Both of the drift compensation design solutions described have had a highly positive effect on the instrument's performance. The drift characteristics are quite impressive and although regular calibration is still recommended it is thought that the goals were attained in trying to minimise zero and span drift as much as possible.

4.4.10 Predictive Response

In some gas monitoring applications the response rate (T90) of the detector is critical for rapid detection of a target gas. The idea of introducing a predictive response algorithm into the firmware is to extrapolate a high level gas response reading by analyzing low gas level response rates.

As described in previous sections as the target gas is introduced into the optical cavity the sinusoidal peak to peak output of the active pyroelectric detector decreases in amplitude. This decrease in amplitude is proportional to the gas concentration of the target gas present. By closely analyzing the initial early response rates of the sinusoid amplitude, caused by the presence of a target gas, it was envisaged that the gas concentration would be predicted ahead of the detector's natural reaction to the gas. This in turn would decrease the T90 of the instrument making it a more responsive detector. The next section describes and details how this technique was implemented.

As described in chapter 3 the sinusoid output of the pyroelectric detector decrease when the target gas to be monitored is present. This is because the gases molecules absorb the infrared radiation, which in turn results in less incident radiation reaching the pyroelectric. By using a relatively simple algorithm this decrease in amplitude can be recorded over a set period of time for a range of target gas concentrations. As part of the calibration procedure the instruments predictive response data was recorded and stored in non-volatile memory. This data consisted of the decrease in amplitude of the active pyroelectric detector for each of the gas ranges involved in the response profiling. For the IR80 instrument the ranges of CO_2 used were: 1%, 2%, 3%, 4% and 5%. In the case of the S500-IR the ranges of CH_4 used were: 10% LEL, 20% LEL, 30% LEL, 40% LEL and 50% LEL. The predictive response calibration routine is only available on entry to the engineer mode, details of which are explained in the subsequent section. The diagram below shows the menu layout of the predictive response calibration routine. The set button on the instrument scrolls through the menu while the cal button saves the relevant data to the on-board EEPROM.

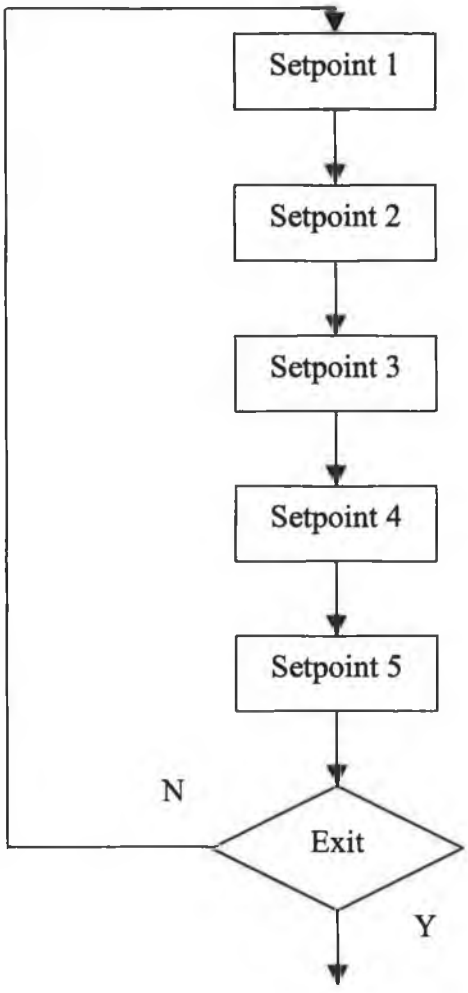

Figure 4.16 Predictive response calibration menu layout

In a typical predictive response calibration procedure the first set point gas concentration would be applied with the menu displaying SETPOINT 1. So for the IR80, 1% CO_2 would be applied to the detector. In order to synchronize the application of the gas with the starting of the microcontroller on-board timer some control external control circuitry was required. This circuitry consisted of relay controlled valve (similar to the one used in the temperature profiling procedure) a pushbutton and a microcontroller with its associated components for correct functionality. When the pushbutton is activated the relay is opened, exposing the detector to the target gas. When the decrease in amplitude has reached a certain level, 1% decrease in the IR80 and 0.5% in the S500-IR, the timer is turned on. A interval of fifteen seconds is generated with the timer. At the end of this interval the change in the active sinusoid's amplitude is noted in

decimal format. This exercise is repeated for each of the 5 calibration set points. On exit of the routine the amplitude differentials are written to EEPROM so that they are available after a power-down power-up sequence. The tables below shows the results of a sample depicting typical decreases in amplitude, over a 15 second interval, due to varying concentrations of target gases for both the IR80 and S500-IR.

IR80 (CO_2 5%)

Target Gas Concentration	Signal Decrease	% Decrease
1%	0.12V	6%
2%	0.36V	18%
3%	0.54V	27%
4%	0.72V	36%
5%	0.9V	45%

Table 4.1 IR80 predictive response calibration data

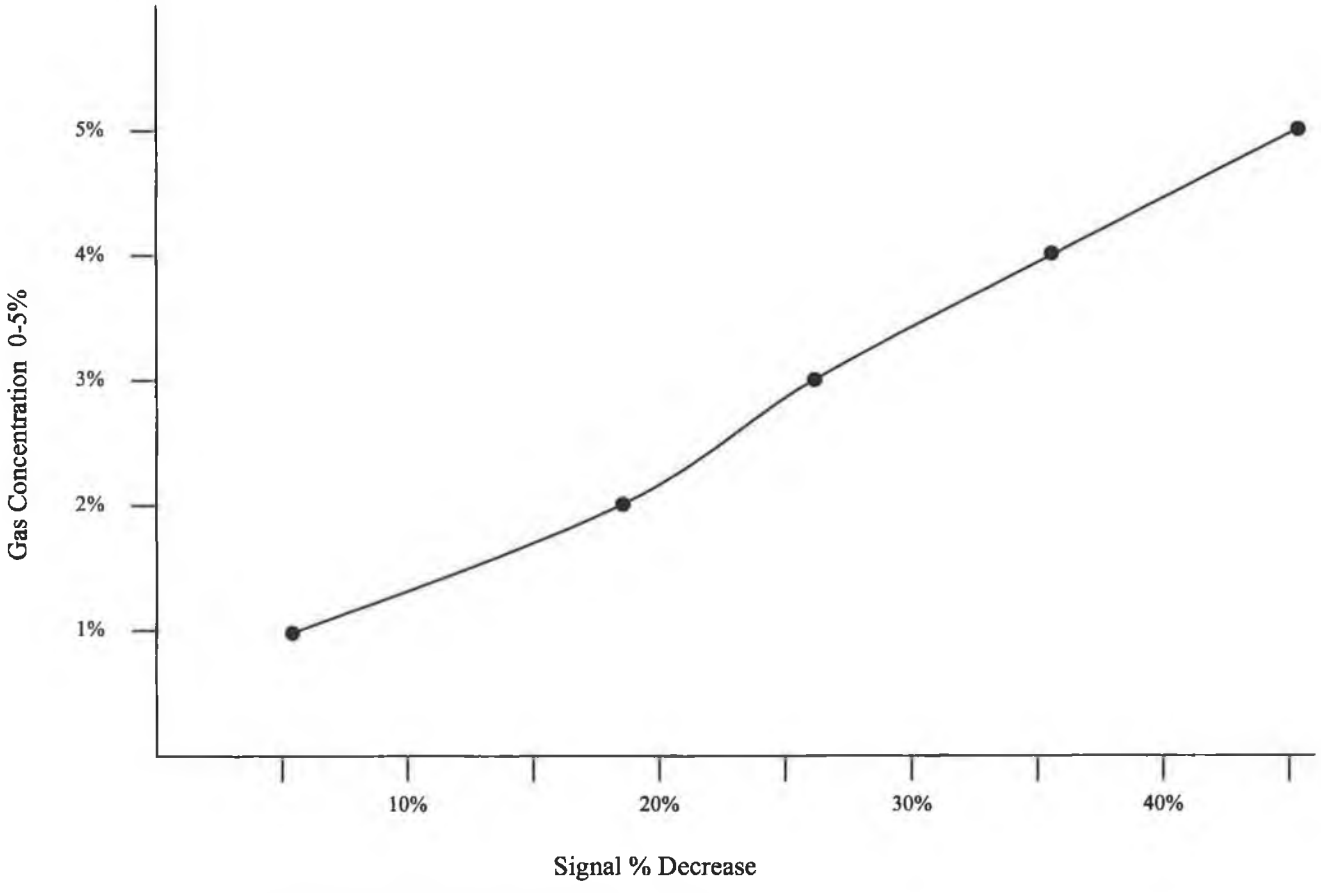

Figure 4.17 IR80 predictive response calibration graph

S500-IR (CH_4 50% LEL)

Target Gas Concentration	Signal Decrease	% Decrease
10% LEL	0.018V	0.9%
20% LEL	0.034V	1.7%
30% LEL	0.066V	3.3%
40% LEL	0.098V	4.9%
50% LEL	0.122V	6.1%

Table 4.2 S500-IR predictive response calibration data

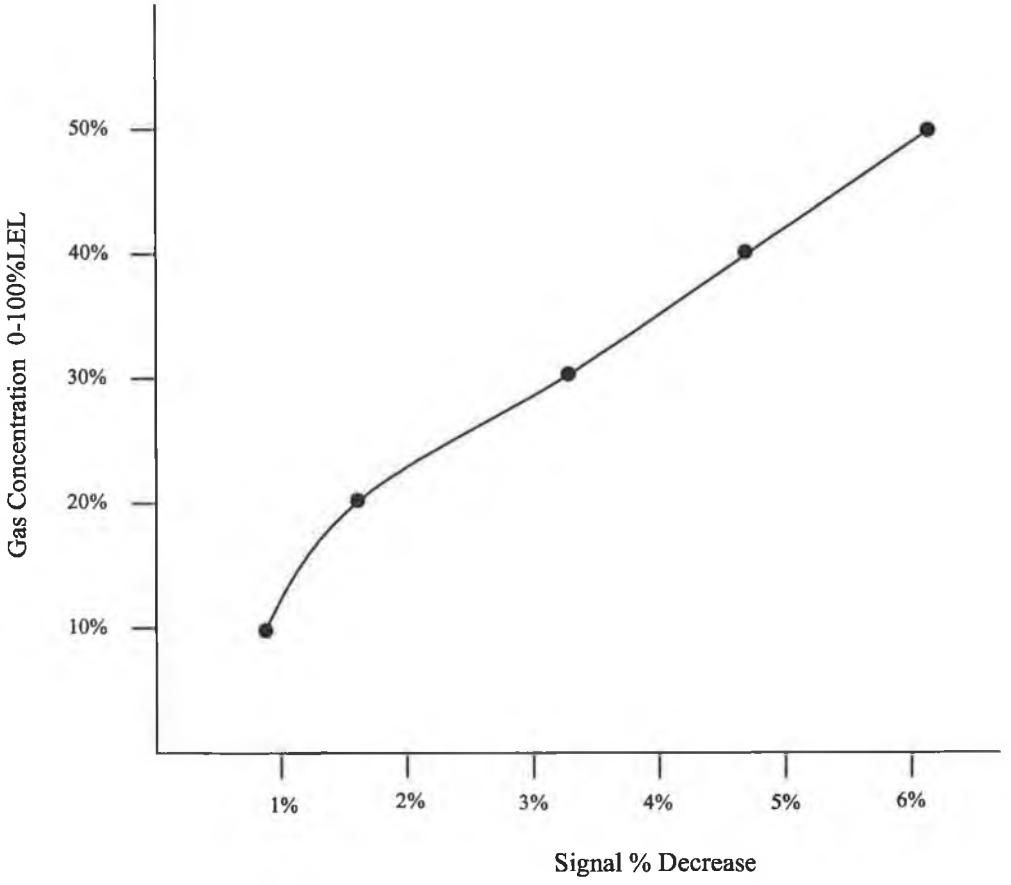

Figure 4.18 S500-IR predictive response calibration graph

Stored in memory now was the reduction in signal for a range of target gas concentrations. In normal operation the timer is set running when the threshold amplitude decrease is reached, there being different thresholds for each instrument. At the end of the fifteen second interval, and with the instrument detecting and displaying gas concentration as normal during this interval, the decrease is compared with the predictive response calibration figures. The decrease that is the closet match to the pre-recorded readings is taken as the gas concentration. This concentration now becomes the predicted gas concentration and a rapid ramp towards this figure is implemented in the firmware. The live un-predicted gas response is still monitored however and is continually compared to the predicted response in order to verify correct execution of the algorithm. When the un-predicted response has stabilized it resumes command again and the predictive response is discarded as its function is complete. When the same threshold that started the timer is reached it indicates that the target gas is no longer present and the instrument response status flag is set to zero as a consequence.

Without the predictive response algorithm the T90 of both instrument are approximately 30 seconds. The implemented algorithm decreases its response time by up to 10 seconds, which is a significant decrease. Figure 4.16 shows the flow diagram of the predictive response routine.

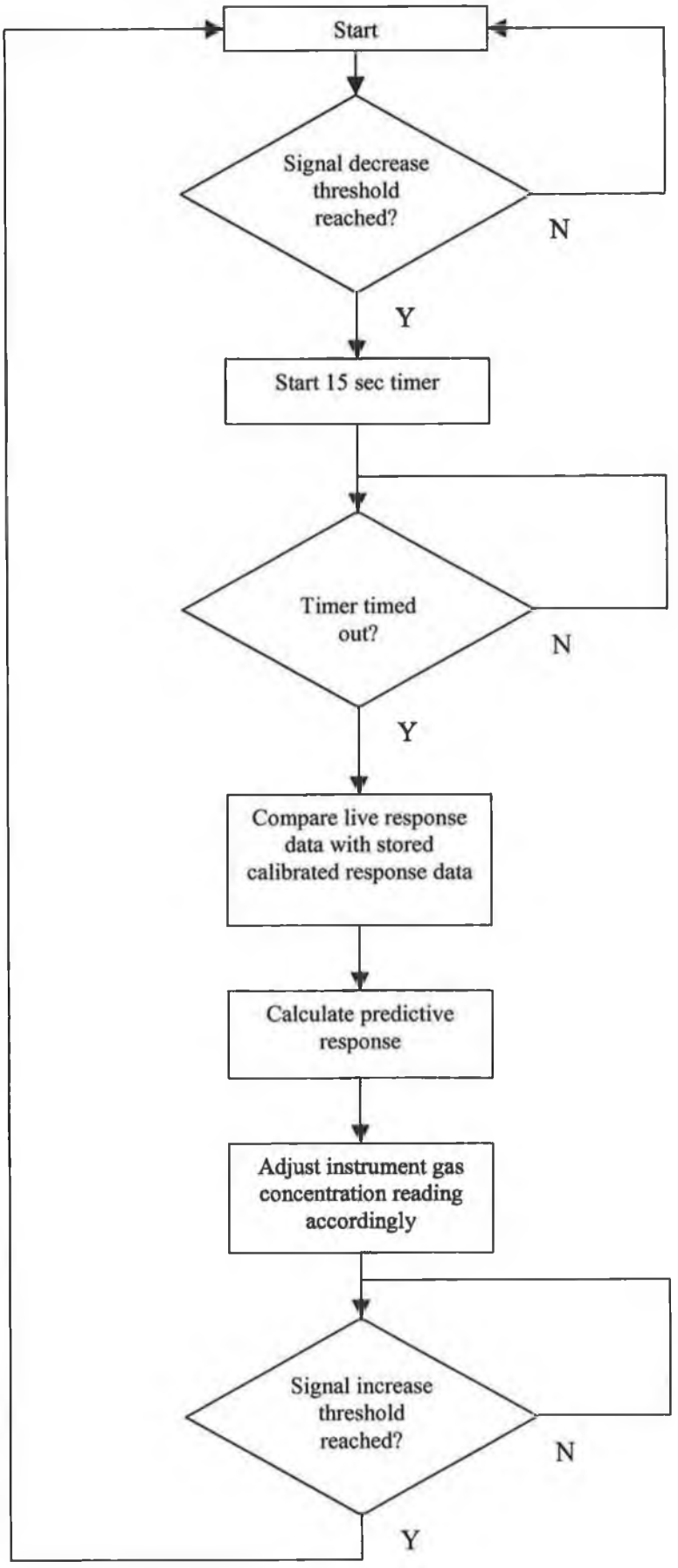

Figure 4.19 Predictive response algorithm flowchart

4.5 Serial Communications

As outlined in the project requirements the infrared gas detector was to have serial communication capability. Most instrumentation installations require that there is communications link between a master station and a Remote Terminal Unit (RTU). This is generally for data logging purposes and also live readings of the RTU's status back to a control room. The communications link can be implemented in several ways, which include MODBUS over serial line (RS-485 physical interface), HART field communications protocol, TCP/IP over Ethernet, Profibus protocol and Fieldbus protocol. All the above protocols were researched and evaluated as a possible method to implement the serial communications. In the end it was decided that MODBUS over RS-485 physical interface would be the most appropriate for the project. The following section gives a brief description of each protocol researched and details the implementation of the MODBUS over RS-485 in the infrared gas detector.

4.5.1 HART Field Communication Protocol

HART (Highway Addressable Remote Transducer) is a popular digital communication protocol designed for industrial process measurement applications. HART uses a low level modulated sinusoid signal superimposed on a standard 4-20mA current loop. The integrity of the analogue current signal is not affected because the HART signal is so small and made up of sine waves. This means that the average value is zero. Compatabilty with existing systems is still maintained while allowing simultaneous digital communication for device configuration, status checking, diagnostics and so forth. Figure 4.17 below depicts how the HART signal is superimposed on the current signal [Tomasi 1998].

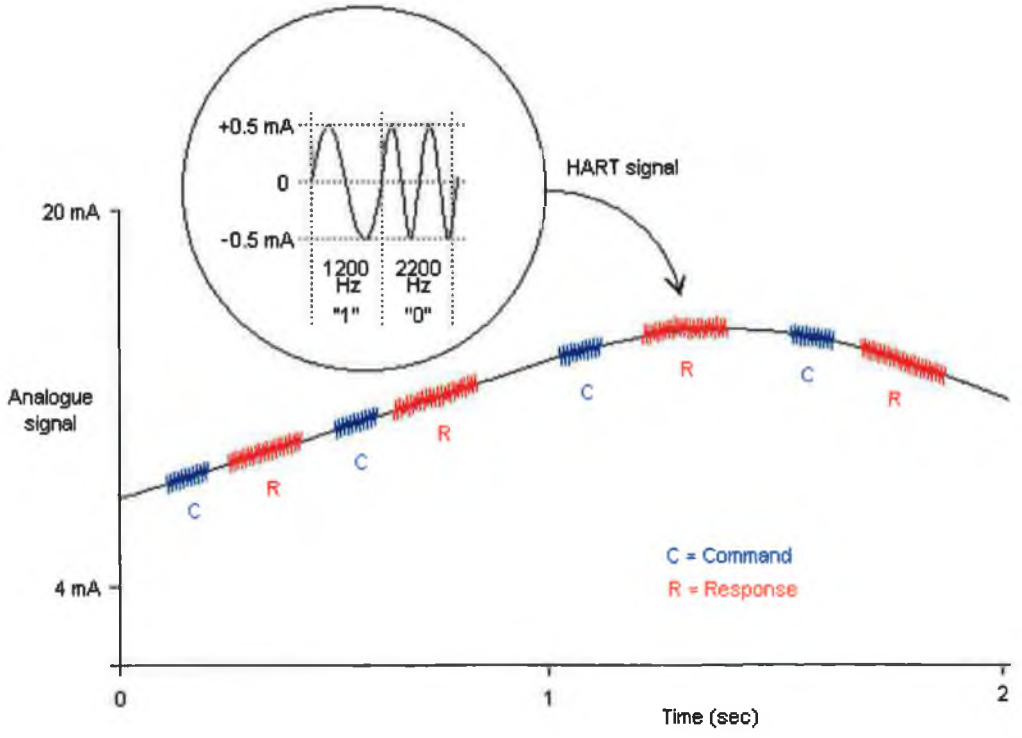

Figure 4.20 HART signal superimposed on 4-20mA signal

The structure of a HART massage is shown below.

PREAMBLE	START	ADDR	COMM	BCNT	[STATUS]	[DATA]	CHK

Figure 4.21 HART message structure

Preamble - Between 5 and 20 bytes of 0xFF (all 1's). Helps the receiver to synchronize the character stream.

Start – Consists of 1 byte and may have several values indicating the type of message. Master to slave, slave to master, burst message from the slave, also the address format: short frame or long frame.

Addr – Includes both the master address (a single bit: 1 for a primary master, 0 for a secondary master) and the slave address. In the short frame format, the slave address is 4 bits containing the polling address (0 to 15). In the long frame format, it is 38 bits containing a unique identifier for that particular device. (One bit is also used to indicate if a slave is in burst mode).

Comm - The command register contains the HART command for the message. Universal commands are in the range 0-30, common practice commands are in the range 32-126 and device specific commands are from 128-253.

Bcnt - The byte count register, which is 1 byte long, contains the number of bytes to follow in the status and data bytes. The receiver uses this to know when the message is complete.

Status - The status field, also known as the response code, is two bytes. It is only present in the response message from a slave. It contains information about communication errors in the outgoing message, the status of the received command, and the status of the device itself.

Data - This field may or may not present, depending on the particular command. A maximum length of 25 bytes is recommended.

Chk - Finally, the checksum byte contains an exclusive-or or longitudinal parity of all previous bytes, from the start character onwards. Together with the parity bit attached to each byte, this is used to detect communication errors.

One of the limitation of using the HART protocol is that it only supports up to 32 devices on the one loop. This was one of the deciding factors in omitting it from the project.

4.5.2 TCP/IP over Ethernet

TCP/IP is a four-layer protocol. It is made up of the Link layer, Network layer, Transport Layer and the Application layer.

Application layer	FTP, SMTP, SNMP
Transport layer	TCP, UDP
Network layer	IP
Link layer	IEEE802.x, PPP, SLIP

Table 4.3 The 4 layers of TCP/IP and their associated protocols

These four levels are part of the 7-layer OSI communication model. Figure 4.18 shows this model.

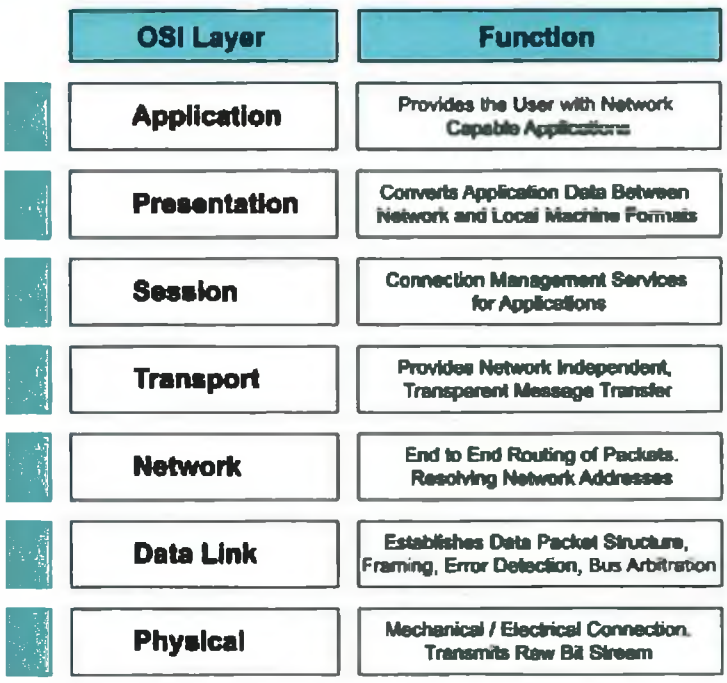

Figure 4.22 The OSI communication model [Stevens 1994]

The link layer is responsible for presenting an interface for an error-free transmission. Ethernet is the most common type of network for supporting TCP/IP. The Ethernet protocol is designed for carrying blocks of data called frames. A frame consists of a header containing 48-bit hardware destination and source address, a 2-byte length field and some control fields. Then the data follows which is a minimum of 38 bytes long. A 32-bit cyclic redundancy check (CRC) completes the frame. The network layer encompasses the Internet domain knowledge. It contains the routing protocols, and it understands the Internet addressing scheme. The IP addressing mechanism must be converted into physical (MAC) addresses before the data can be transmitted by the link and physical layers. The transport layer implements reliable sequenced packet delivery known as connection-oriented transfer. This layer incorporates retrying and sequencing necessary to correct for lost information at the lower layers. The

transport for TCP/IP actually provides two protocols: TCP for reliable or connection-oriented transmission, and UDP for unreliable, or connectionless transmission. The application layer includes virtually all applications of TCP/IP networking, including network file systems, web server or browser, or client server transaction protocols [Hall 2000].

4.5.3 Profibus Protocol

The profibus protocol was created in Germany in 1989 by a consortium of factory automation suppliers. Originally developed in order to enable discrete processing it has expanded into process automation and enterprise wide applications. Profibus comprises of several industrial bus protocol specifications some of include Profibus-DP, Profibus-PA and Profibus-FMS.

Profibus-DP is a device level bus that supports both analog and discrete signals. Profibus-DP has widespread usage for such items as remote I/O systems, motor control centers, and variable speed drives. Profibus-DP communicates at speeds from 9.6 Kbps to 12 Mbps over distances from 100 to 1,200 meters.

Profibus-PA is a full-function fieldbus that is generally used for process level instrumentation. Profibus-PA communicates at 31.25 Kbps and has a maximum distance of 1,900 meters per segment. Profibus-PA is designed to support Intrinsically Safe applications.

Profibus-FMS is a control bus generally used for communication between Data Control Systems and a PLC [Hall 2000].

Profibus, like the HART protocol, only supports up 32 devices per segment (62 with repeaters).

4.5.4 Fieldbus Protocol

The fieldbus protocol is an all digital, serial, two-way communications protocol running at 31.25kbits/s. It is mainly used to interconnect field equipment such as sensors, actuators and controllers. Fieldbus is Local Area Network (LAN) for instruments used in both process and manufacturing automation with built in

capability to distribute the control application across the network. Each field device has low cost computing power installed in it, making each device a smart device. Each device is able to execute simple functions on it's own such as diagnostic, control, and maintenance functions as well as providing bi-directional communication capabilities.

Fieldbus retains the desirable features of the 4-20mA analog systems such as:

- A standardized physical interface to the wire
- Bus-powered devices on a single wire pair
- Intrinsic safety options

In addition fieldbus offers:

- Increased capabilities due to full digital communications
- Reduced wiring and wiring terminations due to multiple devices on one wire
- Connection to a high speed Ethernet backbone for larger systems.

Fieldbus uses standard "Function Blocks" to implement the control strategy. Function blocks are standardized automation functions. Many control system functions such as analog output (AO); analog input (AI) and PID control may be performed by the field device through the use of functions blocks. Fieldbus signals are encoded using the Manchester Biphase-L technique. The signal is called "synchronous serial" because the clock information is embedded in the serial data stream. Data is combined with the clock signal to create the fieldbus signal. The receiver of the fieldbus signal interprets a positive transition in the middle of a bit time as a logical "0" and negative transition as a logical "1" [Mahalik 1997].

4.5.5 The Modbus Protocol

The Modbus protocol is a messaging structure developed by Modicon, now Schneider Electric, in 1979 [Modbus 2002]. It is used to establish master-slave/client-server communication between intelligent devices. When using Modbus over serial line (RS-485 physical interface), which is the case for this

project, then only the physical, data link and application layers of the 7-layer OSI model are used. The Modbus serial line protocol is a master-slave protocol. Only one master (at the same time) time is connected to the bus and from 1 to a maximum of 247 nodes are connected to the same serial bus. The master always initiates a Modbus communication. The slave nodes will never transmit data without receiving a request from the master node. The slave nodes never communicates with each other. The master nodes can issue a Modbus request to the slave nodes in two modes. In unicast mode, where the master addresses a individual slave, or in broadcast mode where all slaves are addressed.

A Modbus frame consists of an address field, a function code, the data to be sent and CRC field.

Address field	Function code	Data	CRC

Figure 4.23 Modbus frame

The address field contains the slave address (1 byte). The function code indicates to the recipient what kind of action to perform (1 byte). The data field can contain anything up to 252 bytes. Error checking is provided by means of a CRC calculation on the message contents and is made up of two bytes, CRC high and CRC low.

The serial transmission mode used for the IR80/S500-IR is RTU mode. When devices communicate using the RTU (Remote Terminal Unit) mode each 8-bit byte in a message contains two 4-bit hexadecimal characters. The main advantage of this mode is its greater character density allows better data throughput than the other mode (ASCII) for the same baud rate. Each message must be transmitted however in a continuous stream of characters. Each byte in RTU mode is made up of 11 bits. 1 start bit, 8 data bits, 1 bit for parity completion and a stop bit [Modicon 1996].
The next section details the serial communications protocol for the IR80 and the S500-IR.

4.5.6 Implementing MODBUS on the IR80/S500-IR

There are two Modbus function codes implemented. Function code 03 (Read Holding Registers) is used to read the status from a slave unit. Function code 06 (Preset Single Register) is used to write a command to the slave unit. When the master unit wishes to query a particular slave about its holding registers it sends a read query message. Table 4.4 below show the Modbus read query message.

Byte	MODBUS	Range	Referenced to IR80/S500-IR
1st	Slave Address	0-247 (Dec)	IR80/S500-IR ID (Address)
2nd	Function Code	03	Read Holding Registers
3rd	Starting Address Hi	00	Not Used
4th	Starting Address Lo	00-FF (Hex)	IR80/S500-IR Commands
5th	No. of registers Hi	00	Not Used
6th	No. of Registers Lo	01	No. of 16-bit Registers
7th	CRC Hi	00-FF (Hex)	CRC Hi Byte
8th	CRC Lo	00-FF (Hex)	CRC Lo Byte

Table 4.4 Modbus Read Query Message

The read response message to such a query is detailed below.

Byte	MODBUS	Range	Referenced to IR80/S500-IR
1st	Slave Address	0-247 (Dec)	IR80/S500-IR ID (Address)
2nd	Function Code	03	Read Holding Registers
3rd	Byte Count	02	No. of Data Bytes
4th	Data Hi	00-FF (Hex)	IR80/S500-IR Hi-Byte Status Data
5th	Data Lo	00-FF (Hex)	IR80/S500-IR Lo-Byte Status Data
6th	CRC Hi	00-FF (Hex)	CRC Hi Byte
7th	CRC Lo	00-FF (Hex)	CRC Lo Byte

Table 4.5 Modbus Read Response Message

Tables 4.6 and 4.7 below show the structure when a write command is being executed.

Byte	MODBUS	Range	Referenced to IR80/S500-IR
1st	Slave Address	0-247 (Dec)	IR80/S500-IR ID (Address)
2nd	Function Code	06	Preset Single Registers
3rd	Register Address Hi	00	Not Used
4th	Register Address Lo	00-FF (Hex)	IR80/S500-IR Commands
5th	Preset Data Hi	00-FF (Hex)	IR80/S500-IR Hi-Byte Command Data
6th	Preset Data Lo	00-FF (Hex)	IR80/S500-IR Lo-Byte Command Data
7th	CRC Hi	00-FF (Hex)	CRC Hi Byte
8th	CRC Lo	00-FF (Hex)	CRC Lo Byte

Table 4.6 Modbus Write Query Message

Byte	MODBUS	Range	Referenced to IR80/S500-IR
1st	Slave Address	0-247 (Dec)	IR80/S500-IR ID (Address)
2nd	Function Code	06	Preset Single Registers
3rd	Register Address Hi	00	Not Used
4th	Register Address Lo	00-FF (Hex)	IR80/S500-IR Commands
5th	Preset Data Hi	00-FF (Hex)	IR80/S500-IR Hi-Byte Command Data
6th	Preset Data Lo	00-FF (Hex)	IR80/S500-IR Lo-Byte Command Data
7th	CRC Hi	00-FF (Hex)	CRC Hi Byte
8th	CRC Lo	00-FF (Hex)	CRC Lo Byte

Table 4.7 Modbus Write Response Message

Exception Responses and Exception Codes

In a normal communications query and response the master sends a query to the IR80 or S500-IR and the unit receives the query with no communications error and handles the query normally within the master device's allowable

time-out. The slave unit then returns a normal response to the master. An abnormal communication produces one of four possible events.

1. If the IR80/S500-IR does not receive the query due to a communication error then no response is returned from the IR80/S500-IR. The master device will eventually process a time-out condition for the query.
2. If the IR80/S500-IR receives the query but detects a communication error (CRC, etc) then no response is returned from the IR80/S500-IR and a time-out is generated.
3. If the IR80/S500-IR receives the query without a communication error but cannot process the query within the masters time-out setting then no response is returned and the master will eventually process a time-out condition for the query. In order to prevent this from happening the maximum response time for the IR80/S500-IR is 200mS. Therefore the master's time-out setting should be greater than 200mS.
4. If the IR80/S500-IR receives the query without any communication error but cannot process it due to reading or writing to a non-existent IR80/S500-IR command register then the IR80/S500-IR will return an exception response message informing the master of the error.

The exception response message has two fields that differentiate it from a normal response:

Byte	MODBUS	Range	Referenced to IR80/S500-IR
1st	Slave Address	0-247 (Dec)	IR80/S500-IR ID (Address)
2nd	Function Code	83 or 86	MSB is Set with Function Code
3rd	Exception Code	01 to 06 (Hex)	Appropriate Exception Code (See Below)
4th	CRC Hi	00-FF (Hex)	CRC Hi Byte
5th	CRC Lo	00-FF (Hex)	CRC Lo Byte

Table 4.8 Exception Response Message

In an exception response the IR80/S500-IR returns an exception code in the data field. This exception code describes the condition that caused the exception. Below is the list of exception codes supported by the IR80 and the S500-IR.

Code	Name	Description
01	Illegal Function	The function code received in the query is not an allowable action for the IR80/S500-IR
02	Illegal Data Address	The data address received in the query is not an allowable address for the IR80/S500-IR.
03	Illegal Data Value	A value contained in the query data field is not an allowable value for the IR80/S500-IR.
04	Slave Device Failure	An unrecoverable error occurred while the IR80/S500-IR was attempting to perform the requested action.
05	Acknowledge	The IR80/S500-IR has accepted the request but it will take a long length of time to process it. This code is returned to the master to prevent it from timing out.
06	Device Busy	The IR80/S500-IR is performing a long duration program operation. The master should retransmit later when the slave is free.

Table 4.9 IR80/S500-IR Exception Codes

IR80/S500-IR Command Register Locations

Parameter	Function	Type	Scale	Access	Register Address	Master I/O Address
Analog	0-20mA current output	Value	16-bit	R	0000	40001
Status/Errors	Indicates errors	Bit		R	0001	40002
Type unit	Indicates the unit			R	0002	40003
Software Rev	Indicates the software revision	ASCII	2-char	R	0003	40004
Address	Unit address	Value		R/W	0004	40005
Span Adjust	Adjusted percent of span figure	Value	16-bit	R/W	0005	40006
Baud rate	Indicates present baud rate (2400, 4800, 9600)	Value	(0-4)	R/W	0006	40007
Total receive errors	Total number of receive errors	Value	8-bit	R	0007	40008
Function code error	Total number of function code errors	Value	8-bit	R	0008	40009
No. of register errors	Total number of register errors	Value	8-bit	R	0009	40010
RXD CRC Hi errors	Total number of RXD CRC Hi errors	Value	8-bit	R	000A	40011
RXD CRC Lo errors	Total number of RXD CRC Lo errors	Value	8-bit	R	000B	40012
Framing errors	Total number of framing errors	Value	8-bit	R	000C	40013
Clear comm errors	Clear all comm errors	Bit	1-bit	W	000D	40014

Table 4.10 IR80/S500-IR Command Register Locations

IR80/S500-IR Command Register Details

Analog: A read returns a value, which is proportional to the 0-20mA output current. The current is based on a 16-bit value

Status/Errors: A read returns the errors that are occurring at the present time and are indicated by the bit position in the return byte.

Function	Bit Position	Access
EEPROM	5	Read
Lamp failure	4	Read
Thermistor failure	3	Read
Supply voltage too low	2	Read
Excessive negative drift	1	Read

Table 4.11 Status/Error

Type Unit: A read returns the decimal value 80 for the IR80 and decimal value 500 for the S500-IR.

Software Rev: A read returns the software revision number of the instrument in 2 ASCII characters.

Address: A read returns the address of the instrument. A write changes the address to the requested address. The range of the address is 0-247.

Span Adjust: A read returns the span adjust figure which offset the span constant in the gas calculation maths routine. A write changes the span adjust to the required figure. The range of this figure is 0-20.

Baud Rate: A read returns the baud rate of the instrument. A write changes the baud rate to the requested value. After the baud rate is changed communications will cease as the master unit has a different baud rate from the slave. Changing the master's baud rate to the slave new baud rate will restart communication once more.

Baud Rate	Low Data Byte	Access
9600	02	Read/Write
4800	01	Read/Write
2400	00	Read/Write

Table 4.12 Baud Rate

If the baud rate is not in range an illegal data value (03) is returned.

Total Receive Errors: A read indicates the total amount of Modbus communication receive errors that occurred in the slave device. The maximum count is 255, the counter will roll over to zero and begin counting again if it exceeds 255. The errors that can occur are listed below.

Function Code Error: A read indicates the total amount of function code errors that occurred in the slave device. The maximum count is 255, the counter will roll over to zero and begin counting again if it exceeds 255.

Number of Register Errors: A read indicates the total amount of register errors that occurred in the slave device. The maximum count is 255, the counter will roll over to zero and begin counting again if it exceeds 255.

RXD CRC Hi Errors: A read indicates the total amount of RXD CRC Hi errors that occurred in the slave device. The maximum count is 255, the counter will roll over to zero and begin counting again if it exceeds 255.

RXD CRC Lo Errors: A read indicates the total amount of RXD CRC Lo errors that occurred in the slave device. The maximum count is 255, the counter will roll over to zero and begin counting again if it exceeds 255.

Framing Errors: A read indicates the total amount of framing errors that occurred in the slave device. The maximum count is 255, the counter will roll over to zero and begin counting again if it exceeds 255.

Clear Comm Errors: A read or write resets all the Modbus communication error counters to zero.

4.6 Summary

This chapter presented the implementation of the infrared gas detector. At the start of the chapter the functional and non-functional requirements are listed. This list contained the special requirements that should be implemented in the instrument design. The problems associated with temperature fluctuations were addressed and eliminated. Noise suppression techniques, both hardware and software, were implemented in order to reduce false alarms and spurious response patterns. The various algorithms implemented in the firmware are described and detailed. Algorithms for predictive response, peak to peak detection and noise reduction are all explained with the aid of flow diagrams and detailed diagrams. The

electronic hardware design is detailed and explained. The methodologies used to design the gas sensing optical cavity is also explained in depth. Zero and span drift compensation techniques that are incorporated in to the instrument design are listed. Research conducted into the viability of using a twin lamp source arrangement in the optical cavity is described. Finally the research conducted into serial communications protocols is presented. Modbus over RS-485 physical interface was the chosen protocol for the project and the implementation of the Modbus is described in detail. The next chapter presents the testing and validation that was carried out on the completed instrument.

Chapter 5

Testing and validation

5.1 Introduction

5.2 Lab Tests

5.3 Expert Feedback

5.1 Introduction

This chapter summarizes the testing and validation used for the IR80/S500-IR Infrared gas detectors. The testing is broken into two parts: lab tests and feedback from experts in the gas detection industry. These included Monicon Technology distributors, existing customers using Monicon's instruments in the field along with experts in the specific field of infrared gas detection. The lab analysis tests the functional aspects of the solution. Results are given in numerical and descriptive form along with the test procedures used to generate them.

5.2 Lab Tests

In order to test and validate the IR80/S500-IR Infrared gas detector a suite of tests procedures were used as described in this chapter.

5.2.1 Instrument Repeatability

The repeatability of a gas detection instrument is how repeatable the indicated gas concentration is compared to the applied gas concentration. This is quite an important figure when accurate measurements need to be achieved on a regular basis, e.g. gas concentration process control in breweries, etc. The test setup for repeatability consisted of a relay controlled flow meter connected to the target

gas to be monitored and a cylinder of nitrogen, the zero gas. The control board for the relay was constructed in Monicon and was driven by control software written in Labview, which was also coded in Monicon. Labview is a software package by National Instruments, which is extensively used, in industrial test and control situations. The program consisted of a simple loop that opened and closed the relays that controlled the gas flow. The instruments on test where exposed to target gas every 20 minutes for a 2 week period. Gas was exposed to the sensors for 1 minute; the gas concentration reading on the instruments was read off the serial port and stored in the Labview program. The sensors were then purged with the zero gas nitrogen. For the IR80 infrared gas detector the ten sensors on test were exposed to 5% carbon dioxide while the ten S500-IR infrared gas detectors on test were exposed to 50% LEL methane. The figures collated at the end of the test period resulted in a repeatability figure of 1%, which is more then acceptable in the gas detection industry. The results for repeatability testing are listed below in table 5.1.

IR80 highest reading	5.1%	S500 highest reading	50% LEL
IR80 lowest reading	5.0%	S500 lowest reading	49% LEL
IR80 repeatability %	±1%	S500 repeatability %	±1%

Table 5.1 IR80/S500 repeatability results

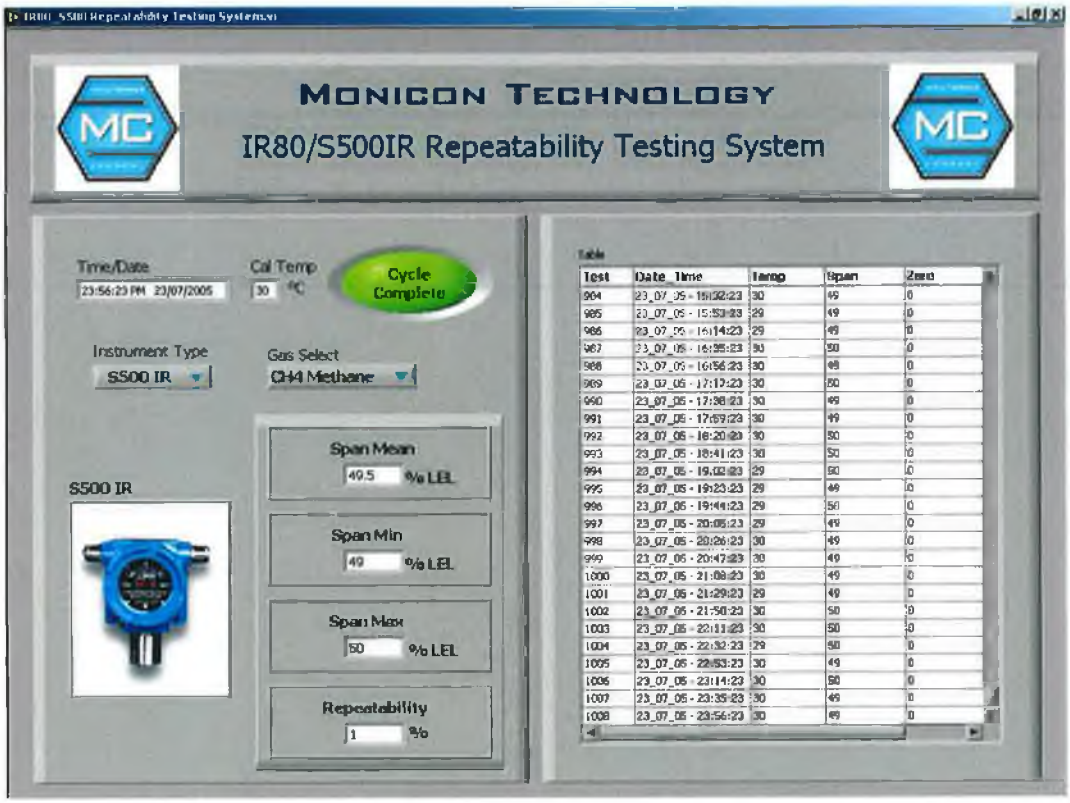

Figure 5.1 Labview test program for instrument repeatability

5.2.2 Temperature Compensation Verification

The problems, solution and implementation of temperature compensation are detailed in section 4.4.6. The verification of the solution was carried out over a two-week testing period inside a temperature cycling chamber. A test program was once again written using Labview that communicated with the instruments on test along with the temperature cycling chamber. The test chamber temperature cycled from 50°C to -20°C and back over a 20-hour time frame. The relay control board was utilised once again to expose the detectors to the target gas and the zero gas. Increments and decrements of 5°C were observed in the temperature chamber. The Labview program read the zero and span gas concentration readings of the instruments at each temperature stage and logged the information in a report. Ten S500-IR's and ten IR80's were placed in the chamber and at the end of the two weeks 100% temperature compensation success was noted for each detector tested.

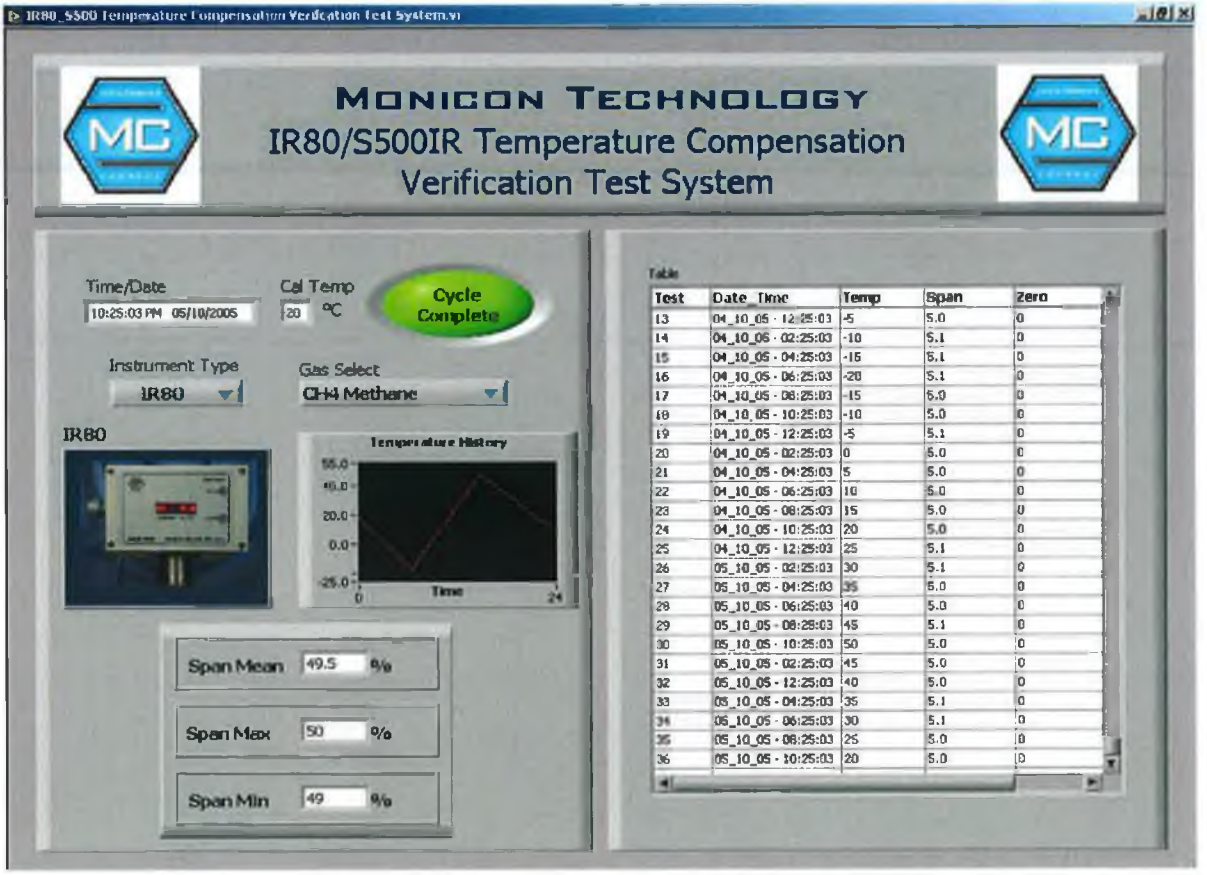

Figure 5.2 Labview test program for temperature compensation verification

5.2.3 Noise Compression Verification

The techniques used to implement noise compression, both hardware and software solutions, are explained in chapter 4, section 4.4.8. In order to test the implemented techniques and also in order to comply with the standards EN 50081-1: 1992 and EN 50082-2: 1992 a suite of tests were conducted on the IR80 and the S500-IR infrared detectors in order to evaluate their Electromagnetic Compatibility (EMC) emissions and immunity. These tests were conducted by an EMC test-house. The following section describes and details the tests completed and the results.

5.2.4 Radiated Field Immunity

Standard: EN 50082-1: 1992

This test was carried out in a shielded room in accordance with the standard IEC 801-3. This standard relates to the testing of equipment immunity to radio frequency interference (RFI). The field strength of the test was 3V/m (volts per metre) and the frequency sweep was 27MHz to 500MHz.

Test Equipment:

Marconi 2022 RF Generator (10kHz to 1GHz).
Amplifier Research 30W1000M7 Power amplifier. (27MHz to 500MHz).
Holaday HI-4400 Broadband measurement system with
Holday HI-4421 Isotropic electric field probe (10kHz to 1GHz).
Skyband T601 Discone antenna.
Custom software to control and level the field.
Schaffner Burst Generator NSG 255.
RF absorbing foam to dampen response of screened room.
Closed circuit TV to monitor the equipment under test during the test.

The field was applied as follows:
From 27MHz to 100MHZ in 5% frequency steps,
from 100MHz to 200MHZ in 2% frequency steps and
from 200MHz to 500MHZ in 1% frequency steps.

Both horizontal and vertical polarizations and the 4 right-angled orientations were used over the frequency range and the dwell time on each frequency was 3 seconds. The parameter monitored was the display on each instrument. For this test the equipment under test needed to remain operating as intended. No degradation of performance or loss of function is allowed below a performance level specified by the manufacturer (Monicon), when the instrument is used as intended.

Test Voltage (V/m)	Result	Effects Observed
3	Pass	No malfunctions observed

Table 5.2 Radiated field immunity results

Comments: Display variation tolerance ±5 %. No display variation observed during the test.

5.2.5 Fast Transient Immunity

Standard: EN 50082-1: 1992

This test was once again carried out in a shielded room in accordance with the relevant standard IEC 801-3. The purpose of this test in to evaluate the instruments ability to recover from fast transients that appear on the AC supply line and also the signal lines from the sensor to the ADC. In other words it's a functional test of the microprocessor's watchdog timer. The AT89C51RD2 has a built in watchdog timer which is controlled by writing to a specific register periodically in the firmware. The instrument needs to be able to continue to operate as intended after the test and no degradation of performance or loss of function is allowed below a performance level specified by the manufacturer (Monicon), when the instrument is used as intended.

Line Description	Test Voltage (kV)	Result	Effects Observed
AC Supply	± 1	Pass	See comments
Sensor Lines	± 1	Pass	No malfunctions observed

Table 5.3 Fast transient immunity results

Parameters monitored: Display on instruments

Comments: There was some functional disruption observed during the tests. The IR80 and S500-IR resumed normal operation immediately after the test.

5.2.6 Cost Comparison

The IR80 CO_2 monitor costs €405 to manufacture. Compared to the original Monicon Infrared CO_2 monitor (IR100) that was purchased from an outside source and sold as a Monicon product, the IR80 costs €495 less to manufacture. This means that the instrument can be sold at a more competitive price, which in turn can lead to greater sales of the instrument.

The same can also be said for the hydrocarbon detector, the S500-IR. The S500-IR costs €620 to manufacture. This compares to €1015 for the hydrocarbon version of the IR100. The ability to quote the instruments at a lower cost than previously allowed was one of the initial goals of the project.

5.3 Expert Feedback

After the lab tests were done, some independent form of feedback was required to validate the infrared gas detector. Initial feedback came in the form of a product launch and demonstration in the Monicon head office in Galway. Installation engineers and sales mangers from a number of Monicon's distributors worldwide attended. The installation engineers who are responsible for the configuring, commissioning and maintenance of all Monicon products made the following comments:

- Both of the infrared gas detectors allowed for easy set-up, configuration and maintenance.
- The calibration interval for each instrument could now be stretched to 6 months as opposed to every 3 months for other products, due to the low zero drift and span drift characteristics of the detectors.
- The diagnostic capabilities of the instrument are of great benefit to the installation engineer. Full read out of calibration parameters, live readings of active and reference signal counts along with instrument set-up constants are available over the RS-485 physical interface. This data can be retrieved by a communications module, design and supplied by Monicon.

- The innovative design ideas and firmware implemented in the infrared gas detector greatly enhance the instrument as a whole.

The sales teams made the following observations:

- The internal temperature compensation will make the instruments attractive to applications where extremes of temperatures are experienced.
- The relatively low list price of the product would make it extremely competitive when in competition with other gas detector manufactures for a particular job.
- Instrument repeatability and drift characteristics of the instrument as good if not better than current competitors alternatives on the market.
- The instrument is housed in an aesthetically pleasing enclosure and the PCB layout and routing is designed in a neat fashion, both of which can be influencing factors in impressing a potential customer at first glance.

As well as the product launch and demonstration both instruments were field tested by Monicon's Irish distributor, Irish Superior. The instruments were placed on a six-month test in two pharmaceutical plants in Ringaskeedy, Co Cork. The instruments were connected to a SCADA system and the gas concentration readings logged continuously. The results from these tests were very positive. There was minimal zero or span drift exhibited on either detector. The detectors gave no spurious readings or false alarms over the six-month period that can be attributed to the techniques deployed, both hardware and software, in reducing the effects of background noise. Overall the companies that conducted the field tests were happy with the tested instruments and as a result both agreed to install the infrared detector throughout their plants.

Chapter 6

Conclusions and Further Development

6.1 Thesis Summary

This thesis researched the development, application and implementation of an infrared gas detector. Innotative software algorithms were developed to implement the various design features laid out in the project requirements. The hardware was designed in a fashion that maximized the performance of the instrument and also took in account Design For Manufacture (DFM) considerations. Chapter 2 looked at alternative methods of detecting the presence of specific gases. The advantages and disadvantages of each technology were discussed and outlined. Chapter 3 examined infrared gas monitoring as a whole. Infrared spectroscopy, the study of how molecules absorb infrared radiation, was detailed and explained giving an insight to the chemistry involved in infrared gas monitoring. Information was presented on the Beer-Lambert law that relates the amount of light absorbed to the concentration of the substance absorbing in a quantitative manner. This law was incorporated into the firmware to calculate the gas concentrations. Deviations from this law can occur and the methods deployed to counteract these deviations were outlined. These methods included linearization techniques in the firmware. The pyroelectric detector is a device used to detect changes in incident radiation and it is used in the project to detect the absorption of infrared radiation by specific gases. The construction and functional characteristics of the pyroelectric detector were examined in detail. Chapter 3 concludes with a list of advantages that infrared gas monitoring hold over other gas monitoring technologies. Chapter 4 presented

the development and implementation of the infrared gas detector. Firstly the requirements were derived, mainly from shortcomings exhibited in infrared gas detectors currently on the market, secondly the technologies to be used were detailed and finally a technical description of the design and implementation of the infrared gas detector was presented. The electronics used in the instrument and details of the optical cavity design were explained in depth. The algorithm deployed for accurate and reliable peak-to-peak detection was detailed. Temperature compensation was required in the instrument in order to compensate for the negative effects that temperature fluctuations have on the pyroelectric detector. The implementation of this temperature compensation, which included the use of a thermistor positioned adjacent to the dual pyroelectric, is described. Careful design of the detector and optical cavity ensured that the problems of zero drift and span drift were reduced to a manageable level. In order for the instrument to be immune from the effects of background noise both hardware and software methods were used to reduce these effects. A predictive response algorithm was also implemented for situations were a fast and accurate response was required. Finally the research conducted into serial communications protocols is presented. Modbus over RS-485 physical interface was the chosen protocol for the project and the implementation of the Modbus is described in detail. Chapter 5 detailed the testing and validation of the IR80 CO_2 monitor and the S500-IR hydrocarbon monitor. The methods used to test the system were given along with results from the lab and feedback from instrumentation experts.

6.2 Conclusions

From the testing and validation of the IR80 CO_2 monitor and the S500-IR hydrocarbon monitor, the following conclusions can be drawn:

- The temperature compensation implemented on the infrared gas detector has resulted in an instrument that is extremely stable, repeatable and reliable across a range of temperature from -20°C to

+50°C. Figures of approximately ± 100ppm for the IR80 and ± 1%LEL for the S500-IR were achieved.

- Careful and precise design of the optical cavity has ensured that the repeatability of the instrument is well within the industry norm for such an instrument.
- The noise suppression techniques implemented in the project significantly reduce the negative effects that background noise can create. A factor of four times improvement in signal to noise ratio was obtained. Tests conducted in the field as well as the lab tests that were carried out verified this.
- Dual pyroelectric detectors are most certainly the best approach from a design point of view. The effect of having a referencing signal to filter out unwanted disturbances on the detector along with the two pyroelectrics contained on the one substrate combine to create a extremely stable signal output.
- A predictive response can be obtained in a relatively simple fashion at calibration time. The demand for this option in the firmware is somewhat limited but could be a deciding factor in the sale of the instrument for T90 critical applications.
- The accuracy and consistency of the sinusoid peak-to-peak ADC counts obtained are very satisfactory. This was an important factor outlined at the start of the project. The integrity of the instrument as a whole depended on the availability of highly accurate ADC readings.
- Expert feedback gathered indicated that the target of developing and designing an infrared gas detector that exhibited excellent performance characteristics along with intuitive electronic and software engineering concepts was fully achieved.

6.3 Further Developments

The IR80 CO_2 monitor and the S500-IR hydrocarbon monitor could further be enhanced with the following developments:

- The gain of the op-amp circuitry, which provides amplification to the low level pyroelectric sinusoidal outputs, is controlled by two 25-turn potentiometers. One potentiometer for each pyroelectric, reference and active. By introducing digital potentiometers the human intervention required for set-up could be further reduced. The ADC readings could be monitored and the digital pots automatically tweaked by the firmware until the desired amplitude is reached. The digital pots, in most cases, receive a 8-bit binary code that translates to a resistance within the range of the digital pot. Each binary code hence has a unique resistance.
- An infrared detector that would provide a pellistor style output could be developed using the existing design used in this project. A pellistor as described in chapter 2 has typical output voltages in the order of mV, which increases in the presence of a combustible gas. One disadvantage of pellistor-based detectors is that certain substances can easily poison them. This does not happen with infrared. By miniaturizing the electronics and including a high resolution digital to analogue converter (DAC), the processed gas concentration could be outputted in mV identical to a pellistor. This type of detector would be extremely popular where a plug in replacement is desired for existing pellistor-based installations.
- Halocarbons, e.g. Freon, can be detected using the NDIR method. However in order to acquire a usable signal a longer pathlength for infrared absorption is required, due to the poor molar absorption characteristics of these gases .By redesigning the optical cavity such a detector could be developed using the same hardware and software.

References

[Allen 1968] P.S Allen "Infrared Radiation" 1968.

[Almond 1996] D. P Almond, P.M Patel "Photo-thermal science and techniques, Physics and its applications (10)" 1996
ISBN: 0 412 57880 8

[Atkins 1995] P.W Atkins "Physical Chemistry – 5th Edition" 1995
ISBN: 0 19 855730 2.

[Becker 1968] Ralph S. Becker, A.B.F Duncan, F.A Matsen, D.R Scott, W.West "Chemical applications of spectroscopy, Part 1" 1968

[Berry 1968] James Berry "Exploring Crystals " 1969

[Cima 1993] Sensors" D Cima "Introduction to IR pyroelectric detectors,

1993.

[Davis 2000] Christopher C. Davis "Lasers and Electro-Optics, Fundamentals and Engineering 2000
ISBN: 0 521 48403 0

[Deitel 1999] H.M Deitel, P.J. Deitel, "C How to Program" 1999, Prentice Hall

[Douglas 1994] Douglas A. Skoog, Donald M. West, F. James Holler "Analytical chemistry, An introduction – 6th edition" 1994
ISBN: 0 03 098982 5

[Dyer 1965] John R.Dyer " Applications of absorption spectroscopy of organic compounds" 1965

[Ewing 1975] Galen W.Ewing "Instrumental methods of chemical analysis – 4th Edition" 1975
ISBN: 0 07 019853 5

[Fifield 1975] F.W Fifield, D. Kealy "Principles and practice of analytical chemistry" 1975
ISBN: 0 7002 0257 9.

[Firth 1973] J.G Firth, Alan Jones, T.A Jones "The Principles of the Detection of Flammable Atmospheres by Catalytic Devices"; Department of Trade and Industry, Safety in Mines Research Establishment, Sheffield S3 7HQ, England
1973.

[Friess 1961] S.L Friess, E.S Lewis, A. Weissberger "Technique of organic chemistry Volume VIII, Rates and mechanisms of reactions Part 1 - 2nd edition" 1961

[Glasser 1977] L.S Dent Glasser "Crystallography and its applications" 1977
ISBN: 0 442 30135 9

[Hall 2000] Eric A. Hall, "Internet Core Protocols, The Definitive Guide", 2000, O' Reilly & Associates.

[Hammond 1990] C. Hammond "Introduction to crystallography, Royal microscopical society, Microscopy handbooks (19)" 1990 ISBN: 0 19 856423 6

[Hart 1995] Hart, Craine, Hart "Organic chemistry A short course, 9th edition" 1995 ISBN: 0 395 70838 9

[Hendrickson 1970] Hendrickson, Cram, Hammond "Organic chemistry – 3rd edition " 1970

[Higson 2003] Seamus Higson "Analytical chemistry" 2003 ISBN: 0 19 8502893

[Hollas 1996] J. Michael Hollas "Modern spectroscopy – 3rd edition" 1996 ISBN: 0 471 96523 5

[Kemp 1975] William Kemp "Organic spectroscopy" 1975 ISBN: 333 18153 0

[Liu 1978] S.T Liu, D. Long "Pyroelectric detectors and materials Proc. IEEE" 1978

[Maas 1972] J.H van der Maas "Basic infrared spectroscopy – 2nd Edition" 1972 ISBN: 0 85501 029 0

[Mahalik 1997] N.P Mahalik, P.R Moore "Fieldbus Technology based Distributed Control in Process Industries: A case study with Lonworks Technology" 1997 ISSN: 0957 6061

[Mahalik 1997] N.P Mahalik "Fieldbus Technology: Industrial Network Standards for Real Time Distributed Control" 1997

[Malvino 1999] Albert Paul Malvino "Electronic Principles – 6th edition" 1999
ISBN: 0 07 115604 6

[Mayo 1994] Dana W.Mayo, Ronald M.Pike, Peter K.Trumper "Microscale organic laboratory, with multistep and multiscale synthesis – 3rd edition" 1994
ISBN: 0 471 57405 4

[Modbus 2002] "Modbus Messaging Implementation Guide V1.0", 2002, http://www.modbus.org

[Modbus1 2002] "Modbus Messaging on TCP/IP Implementation Guide", 2002, http://www.modbus.org

[Modicon 1996] "Modicon Modbus Protocol Reference Guide", 1996, Modicon, Inc., Industrial Automation Systems, One High Street, North Andover, Massachusetts USA.

[Moore 1972] Walter J Moore "Physical Chemistry - 5th Edition 1972
ISBN: 0 582 44234 6

[Mosley 1987] PT Mosley, BC Tofield "Solid state gas sensors" 1987
ISBN: 0 85274 514 1

[Nakamoto 1986] Kazuo Nakamoto "Infrared and Raman Spectra of inorganic and coordination compounds – 4th Edition" 1986
ISBN: 0 471 01066 9

[Olsen 1975] Eugene D.Olsen "Modern optical methods of analysis" 1975
ISBN: 0 07 047697 7

[Pallas-Areny 2001] Ramon Pallas-Areny, John G. Webster "Sensors and signal conditioning – 2nd edition" 2001
ISBN: 0 471 33232 1

[Pescok 1968] Pescok & Shields "Modern methods of chemical analysis" 1968

[Plambeck 1982] James.A Plambeck "Electro-analytical chemistry, Basic principles and applications" 1982
ISBN: 0 471 04608 6

[Price 1974] W.J Price "Analytical atomic absorption spectrometry' 1974
ISBN: 0 85501 045 2

[Putley 1970] E.H Putley "Semiconductor and semi-metals, The pyroelectric detector' 1970

[Riley 1987] T. Riley, C. Tomilson "Principles of electro-analytical methods" 1987
ISBN: 0 471 91330 8

[Rouessac 1998] Francis Rouessac and Annick Rouessac "Chemical analysis, Modern instrumentation methods and techniques- 4th edition" 1998
ISBN: 0 471 98137 0

[Rubeska 1971] I. Rubeska, B. Moldan – English translation edited by P.T Woods "Atomic absorption spectrophotometry " 1971
ISBN: 0592 05044 0

[Saltzamn 1975] R.S Saltzamn, L.Zinn, R.Sims "Analysis instrumentation, Volume 13 – Proceedings of the 21st annual ISA analysis instrumentation symposium, May 6-8 1975, Philadelphia"

[Shriver 1999] D.F Shriver, P.W Atkins "Inorganic chemistry – 3rd edition" 1999
ISBN: 0 19 850331 8

[Skoog 1992] Skoog, Holler, Nieman "Principles of instrumental analysis- 5th Edition" 1992
ISBN: 0 03 002078 6

[Stanley 1984] William Stanley "Operational amplifiers with linear integrated circuits" 1984
ISBN: 0 675 20090 3

[Stevens 1994] Stevens, W. Richard "TCP/IP Illustrated, Vol. 1, The Protocols" 1994

[Strobel 1975] Howard A.Strobel "Chemical instrumentation, a systematic approach to instrumental analysis – 2nd edition"
ISBN: 0 201 07301 3

[Stroud 1993] K.A Stroud "Engineering Mathematics - 3rd Edition" 1993
ISBN: 0 333 44887 1

[Stuart 1996] Barbara Stuart, Bill George and Peter McIntyre "Modern Infrared Spectroscopy" 1996
ISBN: 0 471 95917 0

[Tabor 1993] D Tabor "Gases, liquids and solids, and other states of matter" 1993
ISBN: 0 521 40488 6

[Tomasi 1998] Wayne Tomasi "Electronics Communications Systems" 2002, Prentice Hall.

[Verdin 1973] Anthony Verdin "Gas analysis instrumentation" 1973
ISBN: 333 12614 9

[Vogel 1968] Arthur I. Vogel "A text-book of quantative inorganic analysis including elementary instrumental analysis – 3rd edition" 1968

[Willard 1988] Hobart H.Willard, Lynne L.Merrit Jr, John A.Dean, Frank A.Settle Jr "Instrumental methods of analysis – 7th edition" 1988
ISBN: 0 534 08142 8

[Wilson 1989] J. Wilson, J.F.B Hawkes "Optoelectronics, An introduction - 2nd Edition" 1989
ISBN: 0 13 638495 1

Appendix A1

A1.1 Photographs

IR80 PCB

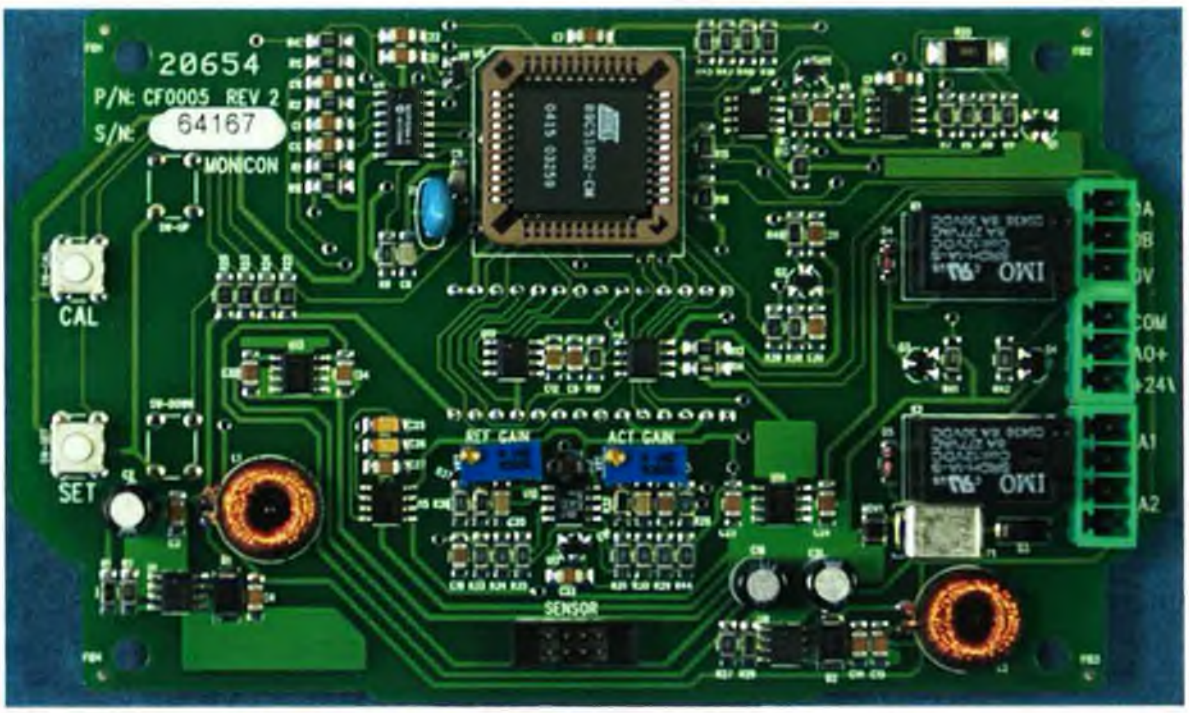

IR80 Enclosure

S500-IR Analogue PCB

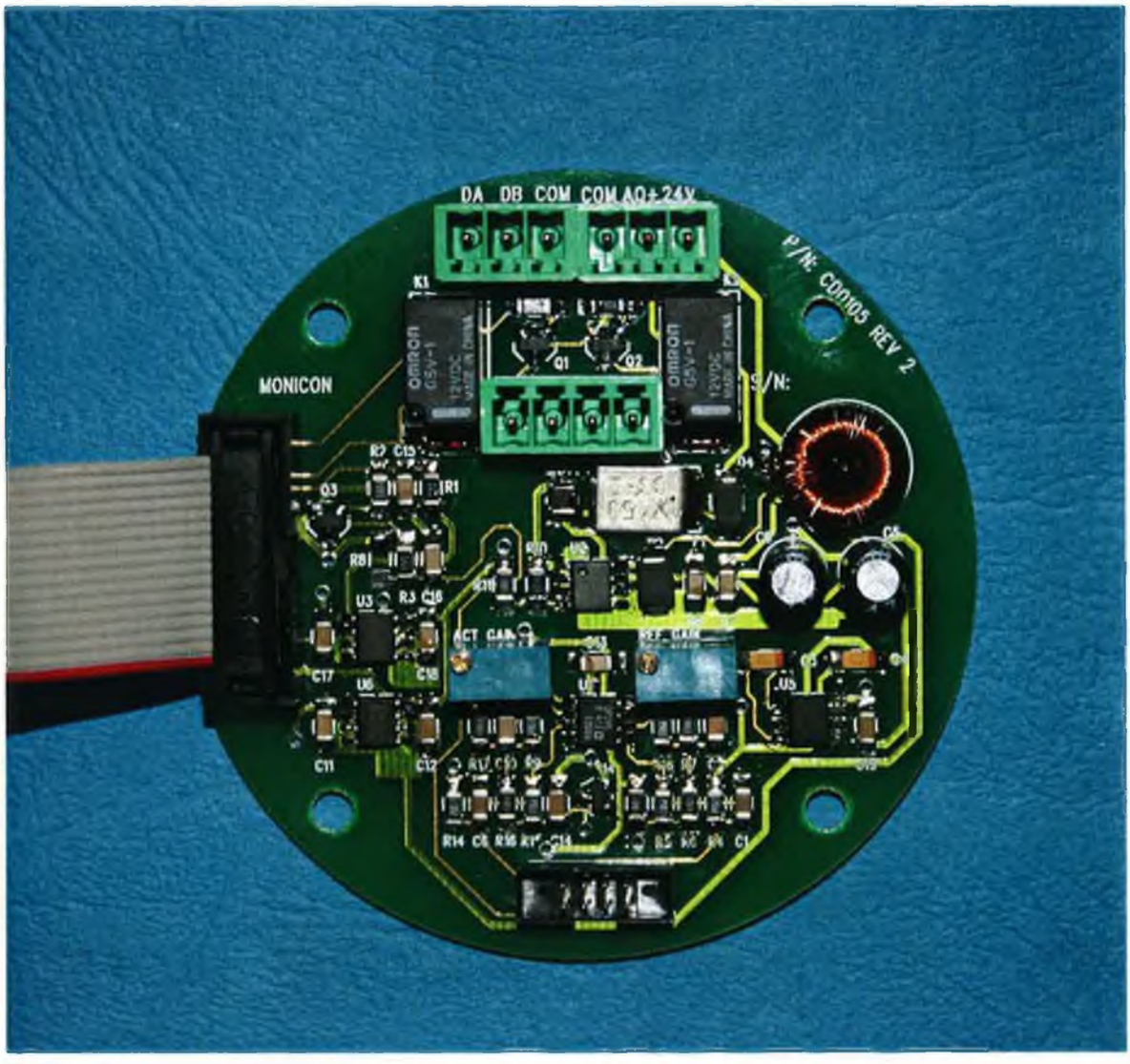

S500-IR Digital PCB

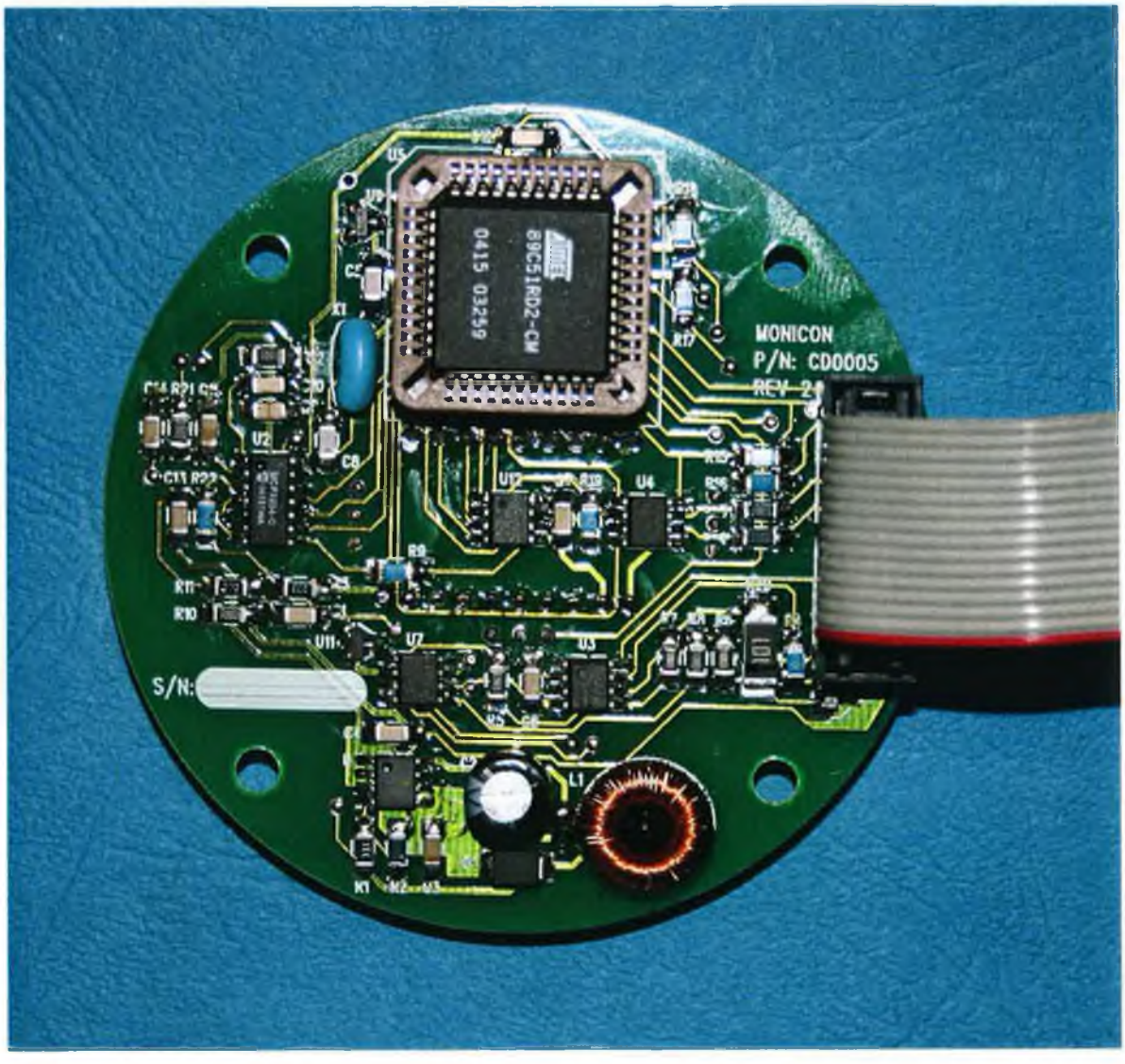

S500-IR Enclosure